NAVAL SHIP RESEARCH AND DEVELOPMENT CENTER
Washington, D.C. 20007

NAVAL SHIP RESEARCH AND DEVELOPMENT LABORATORY
ANNAPOLIS, MARYLAND 21402

GAS-TURBINE SHIP-PROPULSION DYNAMICS

By
C. J. Rubis and A. J. Moken

ELECTRICAL LABORATORY

RESEARCH AND DEVELOPMENT REPORT

January 1969

Report 2846

GAS-TURBINE SHIP-PROPULSION DYNAMICS

By
C. J. Rubis and A. J. Moken

January 1969 ELECLAB 213/68 Report 2846

ABSTRACT

This report is the first-phase analysis of the ship- and propulsion-plant dynamics for a vessel of the destroyer escort type.

A combined gas turbine base and gas turbine boost single-screw propulsion plant of over 45,000 horsepower consisting of two FT4A-2 gas-turbine engines driving a reversing reduction gear with a water brake for dynamic braking was investigated. The analysis was conducted with an all digital simulation on an IBM System 360 computer.

Quantitative results for all the major ship- and propulsion-plant parameters are given for the ship in a calm sea with no turning motions during acceleration, coast down, dynamic braking, and reversing under open-loop fuel-scheduled operation. These results are given for both the base- and base-plus-boost plant operating modes.

ADMINISTRATIVE INFORMATION

This report concludes the first phase of the Independent Exploratory Development task, "Gas Turbine Propulsion Plant Control." The task area is Z-F013 01 01, Task 11275, Assignment 62-139.

TABLE OF CONTENTS

DEFINITIONS AND TERMINOLOGY

A_E	- Expanded area - actual surface area of all blades of the propeller neglecting the hub (ft^2)
A_o	- Disk area = $\pi D^2/4$ (ft^2)
D	- Propeller diameter (ft)
E	- Rotational kinetic energy (ft-lb)
EAR	- Expanded area ratio (A_E/A_o) (dimensionless)
g	- Acceleration due to gravity (32.2 ft/sec^2)
H_o	- Propeller pitch - distance the propeller advances while making 1 revolution without slip (ft)
H_o/D	- Propeller pitch ratio (dimensionless)
I	- Polar moment of inertia of drive train (usually referred to propeller speed unless otherwise indicated) ($lb\text{-}ft\text{-}sec^2$)
k_g	- Reduction gear ratio (dimensionless)
K_Q, K'_Q, C_Q	- Propeller torque coefficients (dimensionless)
K_T, K'_T, C_T	- Propeller thrust coefficients (dimensionless)
k_1, k_2, k_3	- Reduction gear intermediate ratios (dimensionless)
m	- Ship mass (w/g) (slugs)
n	- Propeller angular speed (defined as positive for steady-state forward ship motion) (rps)
N	- Propeller shaft speed (rpm)
N_{SLIP}	- Reversing clutch slip speed (rpm)
N_3	- Engine free turbine speed (rpm)
p	- Clutch air pressure (lb/in^2)
P_C	- Clutch absorbed power (ft-lb/sec)
P_d	- Delivered horsepower to propeller (ft-lb/sec)
P_E, EHP	- Effective horsepower (ft-lb/sec)

P_{ENG} - Engine horsepower (ft-lb/sec)

Q - Propeller torque (lb-ft)

Q_b - Water brake torque (at propeller speed) (lb-ft)

Q_C - Clutch torque (lb-ft)

Q_d - Engine torque developed on propeller shaft (lb-ft)

Q_E - Engine free turbine torque (lb-ft)

Q_f - Reduction gear and bearing friction torque (lb-ft)

R_T - Total ship resistance (lb)

S - Distance traveled or head reach (ft)

SFC - Engine specific fuel consumption (lb/hp-hr)

SHP - Shaft horsepower (ft-lb/sec)

t - Thrust deduction fraction (dimensionless) or time (sec)

T - Propeller open water thrust (lb)

T_p - Propeller net thrust (lb)

V - Ship speed (fps)

V_p - Propeller speed of advance (defined as positive for steady-state forward ship motion) (fps)

w - Wake fraction (dimensionless)

W - Ship weight (lb)

W_f - Engine fuel flow rate (lb/hr)

η_D - Quasi-propulsive coefficient (dimensionless)

η_G - Reduction gear efficiency (dimensionless)

η_P - Propulsive coefficient (dimensionless)

λ - Propeller advance coefficient (dimensionless)

λ' - Propeller inverse advance coefficient (dimensionless)

μ - Propeller first modified advance coefficient (dimensionless)

ρ - Mass density of water (64/32.2) (slugs per ft^3)

σ - Propeller second modified advance coefficient (dimensionless)

ω - Angular speed (radians/sec)

NAVAL SHIP RESEARCH AND DEVELOPMENT LABORATORY

GAS-TURBINE SHIP-PROPULSION DYNAMICS

By
C. J. Rubis and A. J. Moken

INTRODUCTION

Gas turbines for ship propulsion are becoming increasingly attractive because of the high power density (typically 2 hp per lb)* and the extremely fast response time (about 2 minutes from cold start to full power, or about 5 seconds from idling to full power).

Foreign navies such as the British, Danish, and Swedish are using gas-turbine propulsion either with all gas turbines or in combination with diesel or steam. The principal ship types using gas turbines are destroyers, patrol boats, and frigates.

In the United States, an all-gas-turbine merchant ship, the ADM WM. M. CALLAGHAN, was launched in October 1967, and has joined the Military Sea Transport Service (MSTS).

Combined diesel or gas-turbine (CODOG) cutters have been put in service with the Coast Guard, and the U. S. Navy is now building the PG-84 class gunboats with CODOG propulsion systems.

Gas-turbine propulsion for destroyer escorts and surface effect ships is also under study by the U. S. Navy.

The gas turbine for marine propulsion is usually an aircraft-type jet engine (used as a gas generator) driving a free turbine which is then coupled via reduction gears or electric drive to the propeller.

Ship-propulsion plants are generally operated in open-loop control. Since ship speed is very closely linearly proportional to shaft rpm, the controlled variable is shaft rpm; follow-up shaft speed control is generally not used. In steam-driven ships, for example, both merchant marine and naval, an ordered shaft rpm is requested by the bridge; the engine room throttleman maintains this rpm manually by opening and closing a steam valve. Thus, in a sense the feedback loop is closed around the throttleman, who in most cases does not provide accurate control of shaft rpm.

*Abbreviations used in this text are from the GPO Style Manual, 1967, unless otherwise noted.

As more automation is designed into ships, direct bridge throttle control is becoming almost a standard practice even for large vessels. Consequently, an increased measure of automatic response is necessary, and this leads to follow-up shaft speed or power-governed systems.

In order to achieve high speeds (up to 40 knots for destroyer escort vessels or up to 100 knots for surface effect ships) the horsepower requirements are very large - in the vicinity of 150,000 shaft horsepower. With the largest presently available gas turbines, this would require up to six turbines. This power may be distributed among two or more shafts, and it is required to maintain stable load sharing among the prime movers, to provide for differential power requirements on the shafts as the ship maneuvers, and to cope with random sea effects on the propulsion system.

The effect of sea disturbances on directional stability and seakeeping of ships has been under investigation for many years, but the subject of sea state disturbances affecting the propulsion train has not received any significant attention. This is probably due to the historical development of manually controlled open-loop propulsion systems under constant human supervision.

Additional fundamental knowledge is needed because of increased emphasis on automation; high-performance, fast-responding prime movers such as gas turbines; and the possibility of multiple engines or combined plants and more sophisticated propulsion systems.

The ship and propulsion system dynamics program, of which this report is the first phase, will investigate for various ship types the dynamic response and control system optimization for ship-propulsion systems with various propulsion plants. These studies will seek broad principles (i.e., closed-loop, open-loop, or mixed systems, etc) for both power- and speed-governed systems used on propulsion systems for ships maneuvering in a significant seaway. Such information as maximum and minimum expected operating limits in the prime mover, shaft torques and thrusts, ship response in ahead and reverse maneuvers, cycling of the engines in a seaway, stability problems in load sharing, system or engine stability, etc will ultimately be determined.

The justification for this work is the necessity for additional research and design theory for the development of automated, high-performance, ship-propulsion control systems.

BACKGROUND

This activity has been conducting system studies on automated ship-propulsion systems and integrated ship control since the inception of the

SEA HAWK Project in 1963. A study completed in 1967,[42] investigated the use of an automated combined gas-turbine base and gas-turbine boost (COGAG) electric propulsion plant aboard a vessel of the destroyer escort type. This propulsion plant consisted of a regenerative gas-turbine base plant with electric drive and a geared simple-cycle boost plant.

During the preparation of "Automated COGAG Propulsion Plant Study,"[42] an analysis of the relative complexity of various types of automated propulsion plants, including gas turbine, diesel, and steam, was begun and then continued under another task during Fiscal Year 1967. This study[41] was published in December 1967.

In preparation for ship-propulsion dynamics studies to follow, an investigation of "Representation of Propeller Thrust and Torque Characteristics for Simulations"[2] was completed in April 1968.

This report is the first phase of ship-propulsion dynamics investigations and was initiated under an Independent Exploratory Development Program entitled, "Gas Turbine Propulsion Plant Control."

SCOPE

This report presents the first-phase analysis of the ship and propulsion plant dynamics for a vessel of the destroyer escort type. To keep the work unclassified, however, exact data for a particular ship were not used; instead a "typical DE study ship" was formulated with realistic derived data.

The analysis was carried out with an all-digital simulation on an IBM System 360 digital computer.

A COGAG propulsion plant driving a reversing reduction gear was used in this study with a total installed capacity in excess of 45,000 shaft horsepower.

This report provides quantitative results for all the major ship and propulsion plant parameters for the ship in a calm sea with no turning motions during acceleration, dynamic braking, and reversing under open-loop fuel scheduled operation. These results are given for both base and base-plus-boost plant operating modes. Most of the results of this study obtained with a reversing gear are applicable to gas-turbine propulsion plants in general.

[42]Superscripts refer to similarly numbered entries in Appendix C.

SHIP CHARACTERISTICS

The "study ship" used in this analysis uses powering-speed characteristics derived in such a way as to present typical performance and to provide a consistent set of data over the entire speed range of interest.

The following characteristics apply to the destroyer escort study ship:

Length between perpendiculars (ft)	420
Maximum beam (ft)	46
Depth, amidships (ft)	30
Full load displacement (long tons)	about 4000
Propeller	one; conventional fixed pitch
Propulsion plant	COGAG reversing reduction gear about 43,600 SHP
Corresponding ship speed, full load, at 43,600 SHP (knots)	31 .

The derivation of the major ship characteristics of concern in this study was begun by assuming a profile of typical shaft horsepower versus ship speed. The curve of ship resistance versus speed was then calculated to match the steady-state propeller thrust characteristic over the entire speed range, and the propeller torque had to simultaneously match the ship power-speed profile. Propeller data were taken from Baker and Patterson[2] who reduced the data originally published by Miniovich[33] for 18 propeller types to a form more readily adapted to simulations. All the propeller types studied by Miniovich were three-bladed; consequently, the propeller data used in this study are for a three-bladed propeller. However, for the same propeller diameter, pitch ratio, and expanded area ratio, the thrust and torque characteristics of three-bladed propellers match fairly well those of propellers with more than three blades.

To derive a consistent set of characteristics between the ship, propeller, and propulsion plant required a process of iteration involving more than 15 parameters. The major parameters which were varied to obtain a "fit" were: expanded area ratio, pitch and diameter of the propeller, engine characteristics, reduction gear ratio, ship shaft horsepower versus speed profile, wake fraction, and thrust deduction factor.

Results of this process to define a study ship for subsequent dynamic analysis are as follows:

Base turbine rating (normal) (hp)	20,000
Boost turbine rating (hp)	25,000
Reduction gear ratio, k_g	14.3589
Propeller diameter, D (ft)	15.0
No. of propeller blades	3
Propeller pitch ratio, H_o/D	1.05
Propeller expanded area ratio, EAR	0.8

TOTAL SHIP MASS

The total ship mass is composed of the full load displacement plus the added mass due to entrained water. From SNAME[18] the recommended entrained water mass to be used for ship dynamics studies is 8% of the full load displacement. Thus, the ship weight, W, including entrained water is

$$W = (1.08)\ (4000 \text{ tons})\ (2240 \text{ lb/ton}) = 9.68 \times 10^6 \text{ lb} ,$$

and the ship mass is

$$m = \frac{W}{g} = \frac{9.68 \times 10^6}{32.2} = 3.006 \times 10^5 \text{ slugs} .$$

Other data on the study ship are shown in Figures 1 through 3.

SHAFT HORSEPOWER VERSUS SHIP SPEED

Shaft horsepower (SHP) is defined by SNAME[11] as "the net power supplied by the propelling unit to the propulsion shafting after passing through all speed-reducing and other transmission devices and after power for all attached auxiliaries has been taken off. In multi-shaft vessels the total power on all shafts should be denoted by total shaft horsepower and the power of each shaft by shaft horsepower per shaft."

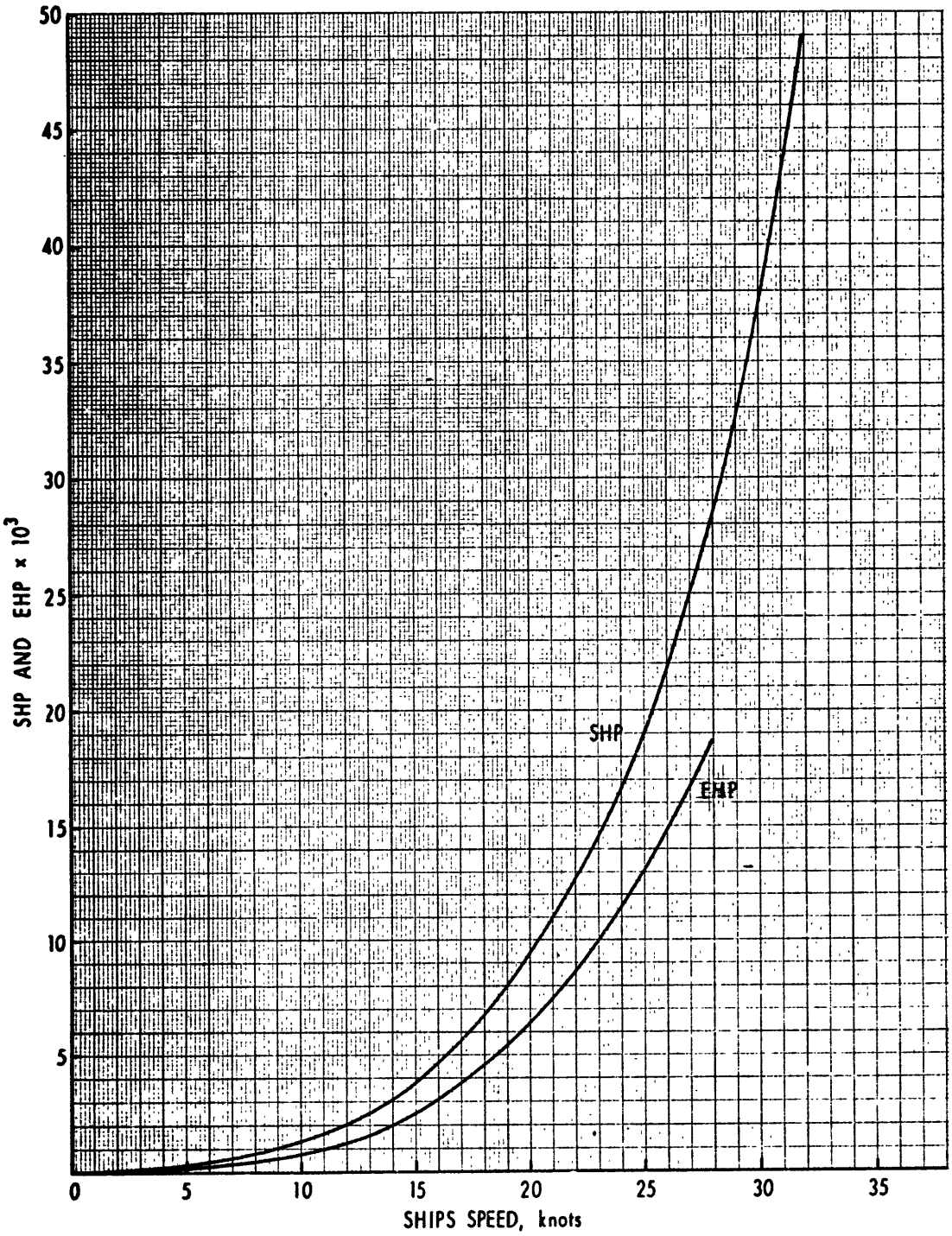

Figure 1 - Assumed Typical Shaft and Effective Horsepower Versus Ship Speed

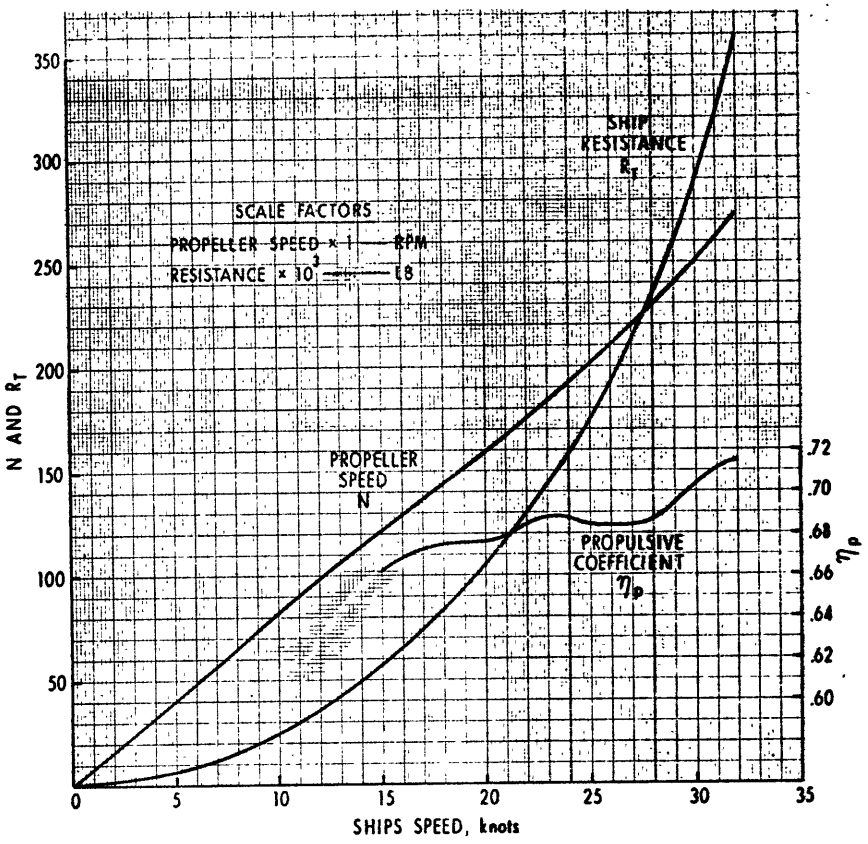

Figure 2 - Propeller Speed, Ship Total Resistance, and Propulsive Coefficient Versus Ship Speed

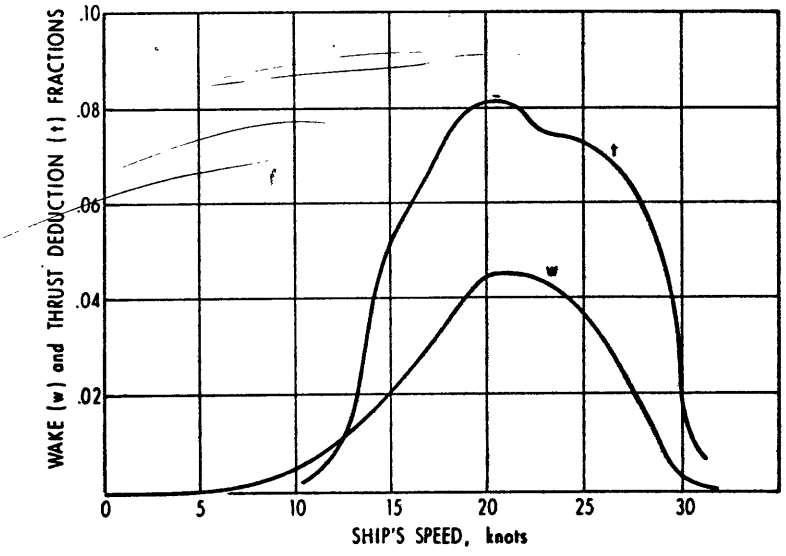

Figure 3 - Wake and Thrust-Deduction Fractions Versus Ship Speed

Figure 1 shows the shaft horsepower versus ship speed with shaft horsepower defined above. This curve has a velocity exponent of 3 in the low speed range (10 to 15 knots) and increases to a velocity exponent of about 4 at 30 knots. The engine horsepower, P_{ENG}, is larger than the shaft horsepower by the amount of the reduction gear losses; both are discussed later in this report.

SHIP RESISTANCE VERSUS SHIP SPEED

A curve of the calculated total ship resistance (R_T) versus speed is shown in Figure 2. This curve is the clean hull resistance at a full load displacement of 4000 tons.

The velocity exponent varies from 2 in the speed range of 10 to 15 knots to about 3.4 at 30 knots.

SHAFT SPEED VERSUS SHIP SPEED

Figure 2 shows the derived angular speed of the propeller shaft as a function of ship speed. This curve is essentially linear with speed and has a slope of 8 rpm per knot at 20 knots.

WAKE DEDUCTION FRACTION

The difference between the ship speed, V, and the speed of advance of the propeller, V_p, is called the wake speed. The wake fraction, w, expresses the wake speed as a fraction of the ship speed, so that

$$w = \frac{V - V_p}{V} \quad \text{(wake fraction)};$$

thus,

$$V_p = V(1 - w) \quad \text{(propeller speed of advance)}.$$

The wake is due to three principal causes:[39]

> "(a) The frictional drag of the hull causes a following current which increases in velocity and volume toward the stern, and produces there a wake having a considerable forward velocity relative to the surrounding water.
>
> "(b) The streamline flow past the hull causes an increased pressure around the stern, where the streamlines are closing in. This means that in this region the relative velocity

of water past the hull will be less than the ship's speed and will appear as a forward or positive wake augmenting that due to friction.

"(c) The ship forms a wave pattern on the surface of the water, and the water particles in the crests have a forward velocity due to their orbital motion, while in the troughs the orbital velocity is sternward. This orbital velocity will give rise to a wake component which will be positive or negative according to whether there is a crest or a trough of the wave system in the vicinity of the propeller.

"The total wake is made up of these three components, and in the great majority of cases is positive. Exceptions arise in very high-speed craft such as destroyers and high-speed motor boats. At a speed of 34 knots, the wave length of the system created by the ship will be some 640 ft., so that a destroyer 340 ft. in length would have a trough in the vicinity of the propellers, and the wave wake will be negative. With such a fine hull the potential or streamline wake would be small, and with large-diameter propellers much of the disk will be outside the frictional wake. Under these conditions, the total wake over the propeller may be zero or slightly negative.

"In a twin-screw ship the average wake over the propeller disk will, as a rule, be less than in a single screw ship of the same fullness, because of the different propeller location, but there will be a considerable concentration immediately behind the ends of the bossings or behind the struts in the case of open shafts."

B. V. Korvin-Kroukowsky provides additional theory on wake and thrust deduction fractions.[27,28,29] The following discussion of wake fraction is his:[28]

"When a ship moves through still water with velocity V, it creates various perturbation velocities; the sum, u, of the components of these velocities in the direction of travel, at the location of the propeller, is most significant in defining the design of the propeller and the final efficiency of propulsion. The ratio u/v is known as 'wake fraction': and is usually designated by Ψ or w. The relative axial speed of the propeller with respect to the water is therefore V(1-w). The magnitude of u or w can be determined on a ship model by various means, for instance, by a pitot tube survey of the propeller disc area with the propeller removed. The value

so obtained is termed 'nominal wake,' and is evidently a property of hull form, dependent on speed V. It has been shown by Horn,[25] Frezenius,[14] Helmbold,[23] and Dickmann[6-8] that the perturbation velocity u can be considered as composed of three boundary components: u_r - due to formation of boundary layer and turbulent wake, u_p - due to the potential flow around the body, (treated as submerged), and u_w due to the formation of surface waves. Correspondingly the wake fraction w is subdivided into

$$w = w_r + w_p + w_w$$

The above expression can be considered to a first approximation, to have each cause acting independently, or, to a second approximation, to have each term include the interference effect of the others. For instance, in the first approximation, w_p can refer to a bare hull, and in the second to a hull with displacement thickness of the boundary layer added. This subdivision is important in any theoretical investigation since the terms obey different laws, absorb different amounts of energy, and their effects extend differently through the ambient space.

"With the propeller in operation all perturbation velocities are disturbed; furthermore, experimental measurement in the propeller plane is no longer possible. For design purposes, a new concept of 'effective wake' is introduced. This is defined as the ratio $\frac{V-V_o}{V}$, where V_o is the velocity of translation of a propeller through undisturbed water, for which the thrust or torque are found to be identical with that of the same propeller working in its normal position on a ship advancing with velocity V.

"In connection with the above definitions, it should be noted that 'effective wake' is determined as mean for the entire propeller disk. On the other hand, the nominal wake can be measured by pitot tubes, giving the distribution of wake over the propeller disk area, the integration of which gives the mean wake."

In this report a steady-state wake fraction was used in the analysis (Figure 3) and is a function of velocity. These data were taken from SNAME[30] and represent model data for a destroyer escort, single-screw vessel.

However, for a true dynamic description of the ship in a transient maneuver, a transient wake factor must be included. Sharp[1] discusses this problem as follows:

> "If wake and ship both stopped simultaneously, a constant wake coefficient could reasonably be assumed. But when the ship is first stopped the wake will have a residual velocity and the wake coefficient should become infinite. Furthermore, during the transient there must have been a point where wake velocity and ship's velocity were equal, resulting in a wake coefficient of 1.0. Thus the small wake coefficient appropriate for steady motion must be inappropriate in transients. During a stopping transient the vessel decelerates faster than the surrounding water; the wake coefficient must increase, starting from its steady state value and reaching infinity when the vessel is dead in the water. It appears reasonable that the range in which the wake coefficient exceeds one and goes to infinity is a small part of the total transient, and is not of major importance. To consider wake effects properly the variation of the wake coefficient during transients would have to be known. The crudest assumption would be the steady state value as a constant wake coefficient during the transient. A more refined model would gradually increase it from its steady state value to 1.0 at the end of the transient."

Due to the lack of transient wake information, a steady-state, velocity-dependent, wake fraction was used in the simulation. It is expected that during rapid transients such as those encountered in acceleration, dynamic braking, and reversing, the computer propeller torques and thrusts will not be exact. However, the worst part of the transient is over in a matter of several seconds, and the rest of the dynamic simulation is fairly well described.

THRUST DEDUCTION FRACTION

The thrust deduction fraction is described as follows:[39]

> "When a hull is towed, there is an area of high pressure over the stern which has a resultant forward component reducing the total resistance. With a self-propelled hull, however, the pressure over some of this area is reduced by the action of the propeller in accelerating the water flowing into it, the forward component is reduced, the resistance is increased and so also the thrust necessary to propel the model or ship.

"It is found in model work, where the necessary measurements can be made, that if the resistance of a hull when towed is R_T the thrust necessary to propel the model at the same speed V is greater than R_T and the increase is called the augment of resistance. It is expressed as the ratio of the increase in thrust to the resistance, so that

$$\alpha = \frac{T-R_T}{R_T} = \frac{T}{R_T} - 1$$

$$\text{or } T = (1 + \alpha) R_T$$

α is called the resistance augment fraction and $(1 + \alpha)$ the resistance augment factor.

"Although viewing the problem from the resistance point of view is the more logical one, the common practice is to look upon this increase in resistance as a deduction from the thrust available at the propeller, so that although the screw provides a thrust of T tons, say, only R_T tons are available to overcome resistance. This 'loss of thrust' $(T-R_T)$, expressed as a fraction of the thrust T is called the thrust-deduction fraction, t, where

$$t = \frac{T-R_T}{T} = 1 - \frac{R_T}{T}$$

$$\text{or } R_T = (1-t)T$$

The expression (1-t) is the thrust-deduction factor."

After correction for the thrust-deduction factor, the net propeller thrust is

$$T_p = T (1 - t) .$$

In the analysis the thrust-deduction fraction, t, was taken from SNAME[20] and is shown in Figure 3. It should be noted that as with the wake fraction a true description of the thrust deduction fraction, t, would have to include the transient effects when the ship is accelerating or decelerating.

PROPULSIVE COEFFICIENT

The effective horsepower, P_E, for a propeller delivering a thrust as it advances through the water driving the ship at a speed, V, is

$$P_E = \frac{R_T V}{550} = EHP \qquad \text{(effective horsepower)} .$$

This effective horsepower is also often defined as the "towrope" horsepower or the power transmitted through a towrope assuming the vessel to be towed at a given speed.[44]

The power delivered to the propeller, P_d, is the shaft horsepower, as previously defined, less the power lost in the stern tube bearings and any shaft bearings.

The ratio of useful power obtained to propel the ship to the power delivered by the propulsion plant to the propeller is termed the "quasi-propulsive coefficient." Thus, the quasi-propulsive coefficient, η_D, is given by

$$\eta_D = \frac{P_E}{P_d} = \frac{\text{effective horsepower (EHP)}}{\text{delivered horsepower}} .$$

The ratio of effective horsepower to shaft horsepower is commonly called the propulsive coefficient, η_P. Thus,

$$\eta_P = \frac{EHP}{SHP} = \frac{R_T \text{ (lb) } V \text{ (knots)}}{326 \text{ SHP}} \qquad \text{(propulsive coefficient)} .$$

The difference between the two coefficients is small and is due to the shaft transmission efficiency, η_s, where

$$\eta_s = \frac{P_D}{SHP} .$$

η_s is typically 0.97 to 0.98.

The propulsive coefficient, η_P, is used in this report, Figure 2, only in synthesizing the standard ship.

The propeller torque and thrust characteristics used in this report are based on the work of Miniovich,[33] as modified by Baker and Patterson.[2] From this work a second modified advance coefficient was used to represent the thrust and torque coefficients. The data in this form was used in a linear interpolation between propeller pitch ratios of 1.0 and 1.2 to obtain a consistent set of characteristics between the study ship and a suitable propeller.

The following discussion on the second modified advance coefficient method is from Baker and Patterson:[2]

> "Applicable data, covering the entire region of propeller operation, is scarce, and most of the available data is suited to isolated situations. Mathematical representation of the data is complicated by the fact that the thrust and torque are functions of both the propeller speed of advance through the water and the shaft speed.
>
> "Some methods, such as families of curves, are sufficient for hand calculation, but are unsuited for computer applications. Others such as polynomials involving the two independent variables, are cumbersome. The calculation of polynomials is time consuming with digital computers; and in analog computers, these methods are hard to program, require excessive equipment, and produce poor results.
>
> "A solution to the problem of obtaining realistic propeller data was found in the work of Miniovich,[33] who presents thrust and torque information over the entire region of propeller operation for 18 different propellers. The method of representation employed by Miniovich is one used by naval architects in ship design. Thrust and torque coefficients are represented as functions of the advance coefficient in some regions of operation and are represented as functions of the inverse advance coefficient in others.
>
> "While this method is suited to the work of the naval architect, it is not suited to simulation. Some researchers[1,40] have solved this problem by using a modified advanced coefficient to describe modified thrust and torque coefficients.
>
> "This study considers the advance coefficient and modified advance coefficient methods of representing propeller characteristics. The notion of a

second modified advance coefficient, which has some desirable advantages in computer simulation programs, is introduced, and inherent relationships among the three methods are discussed.

"It is shown that the first and second modified advance coefficients are bounded, whereas the advance and inverse advance coefficients are unbounded. Furthermore, the first and second modified advance coefficients are each capable of representing the entire region of propeller operation by one double-valued function for thrust and another for torque. Double-valued functions of both the advance coefficient and the inverse advance coefficient are required to completely represent thrust characteristics. Another such set is required for the torque.

"The thrust, T, and torque, Q, of a screw propeller are functions of the propeller speed of advance through the water, V_p, and the propeller shaft speed, n, for a given hull-propeller configuration. To present these functions mathematically, naval architects describe thrust and torque coefficients, K_T and K_Q, respectively, as functions of the advance coefficient, λ. These coefficients are normally defined in the literature[4, 33, 35, 43] as

$$K_T = \frac{T}{\rho D^4 n^2} ,$$

$$K_Q = \frac{Q}{\rho D^5 n^2} ,$$

$$\lambda = \frac{V_p}{nD} ,$$

where D is propeller diameter, and ρ is the water mass density. As n approaches zero, the advance coefficient approaches infinity and cannot be used to describe propeller characteristics. It is necessary, therefore, to define a second set of coefficients as follows:

$$K'_T = \frac{K_T}{\lambda^2} = \frac{T}{\rho D^3 V_p^2},$$

$$K'_Q = \frac{K_Q}{\lambda^2} = \frac{Q}{\rho D^3 V_p^2},$$

$$\lambda' = \frac{1}{\lambda} = \frac{nD}{V_p},$$

where K'_T, K'_Q, and λ' are the inverse thrust, torque, and advance coefficients, respectively.

"Thus, to describe the complete propeller thrust and torque characteristics, propeller data must be presented in two different forms. Further information on this method may be found in references 18, 21, 34, and 46.

"Figures 4 through 7 provide an example of data obtained by the advance coefficient method of representation. The propeller, 1 of 18 considered, has a pitch ratio of 1.0 and an expanded area ratio of 0.8."

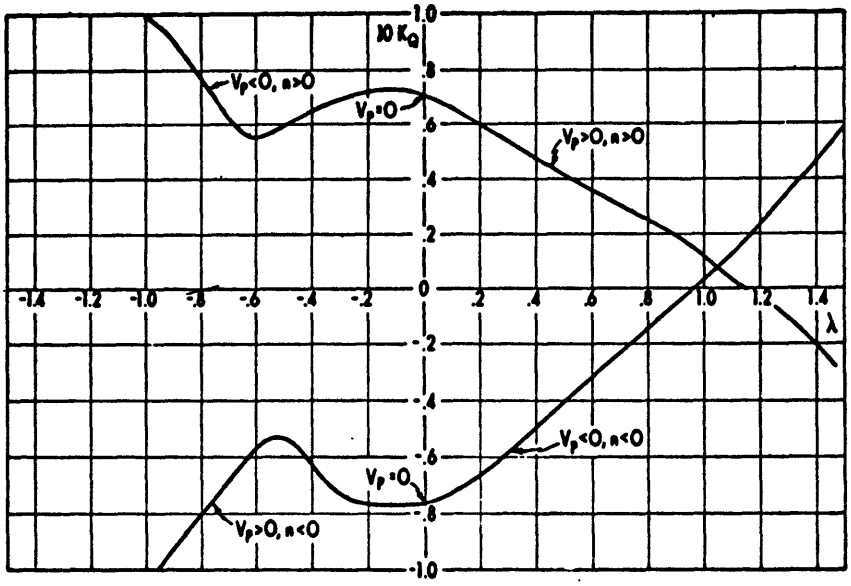

EAR = 0.8 H_o/D = 1.0
Three Blades

Figure 4 - Torque Coefficient (K_Q) Versus Advance Coefficient (λ)

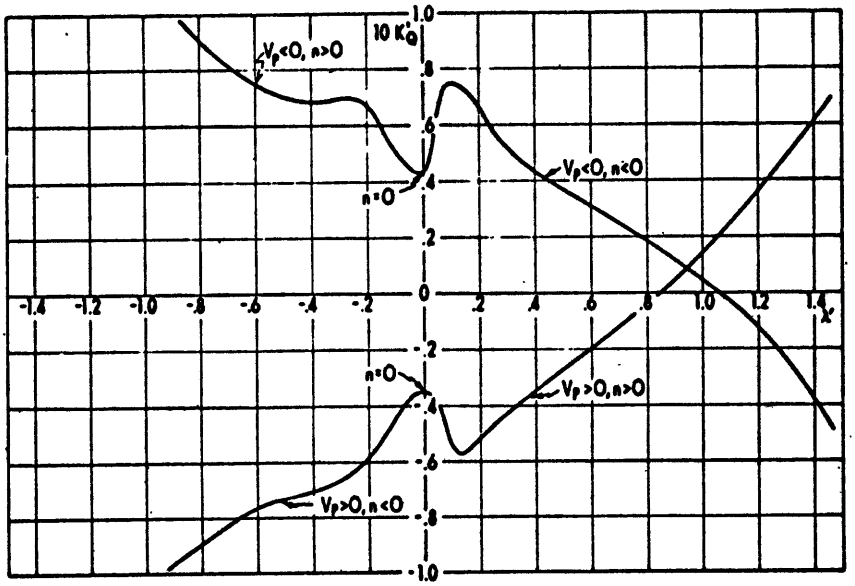

EAR = 0.8 H_o/D = 1.0
Three Blades

Figure 5 - Torque Coefficient (K'_Q)
Versus Inverse Advance Coefficient (λ')

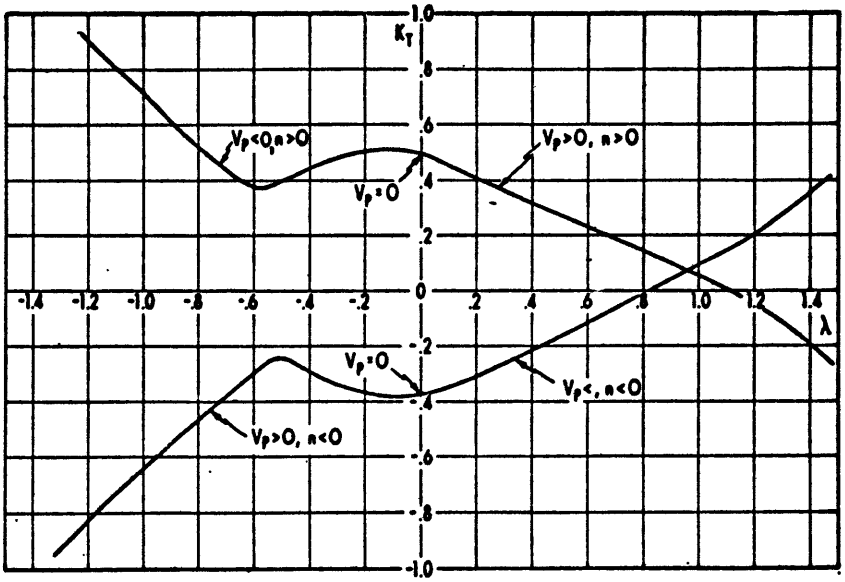

EAR = 0.8 H_o/D = 1.0
Three Blades

Figure 6 - Thrust Coefficient (K_T)
Versus Advance Coefficient (λ)

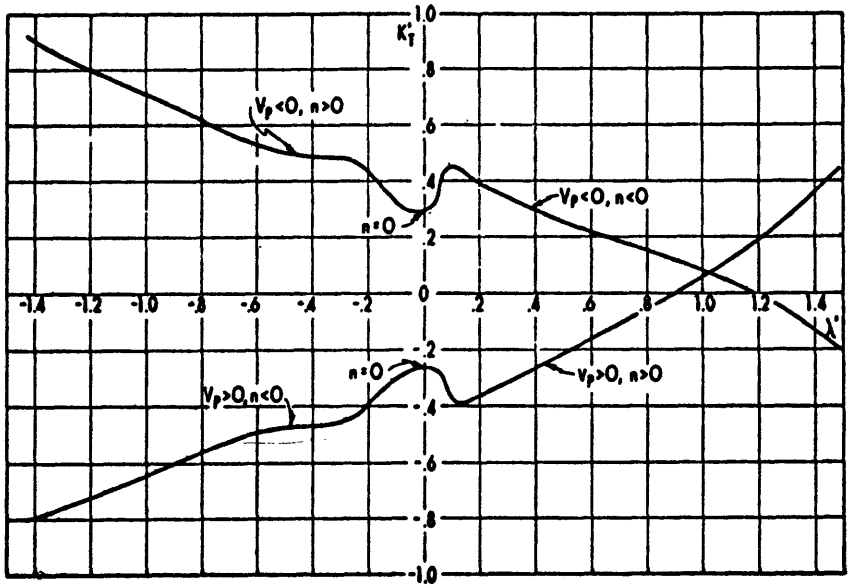

EAR = 0.8 H_o/D = 1.0
Three Blades

Figure 7 - Thrust Coefficient (K_T')
Versus Inverse Advance Coefficient (λ')

"For simulation purposes, the advance coefficient method of representing propeller characteristics has two major disadvantages: (1) the coefficients, λ, λ', K_T, K_T', K_Q, K_Q' are all unbounded, a situation which requires special consideration in a simulation, particularly an analog simulation; and (2) eight curves are required to fully describe the operating characteristics of a single propeller.

"In some simulations,[1,40] the problems encountered with the advance coefficient method have been circumvented by expressing modified thrust and torque coefficients as functions of a modified advance coefficient. We shall call this coefficient the first modified advance coefficient, μ. It can be defined as

$$\mu = \frac{V_p}{\sqrt{V_p^2 + n^2 D^2}} .$$

"The undesirable aspects[2] of the first modified advance coefficient can be circumvented by using a new coefficient. We shall call this new coefficient the

second modified advance coefficient, σ, and define it as follows:

$$\sigma = \frac{nD}{\sqrt{V_p^2 + n^2 D^2}} \quad "$$

All the analysis in this report is in terms of the second modified advance coefficient, σ.

The modified thrust and torque coefficients in terms of the second modified advance coefficient are now

$$C_T = \frac{T}{\rho D^2 (V_p^2 + n^2 D^2)}$$

$$C_Q = \frac{Q}{\rho D^3 (V_p^2 + n^2 D^2)} \quad .$$

C_T and C_Q coefficients may be related to K_T and K'_T, K_Q and K'_Q, using

$$C_T = \lambda^2 \sigma^2 K'_T = \sigma^2 K_T$$

$$C_Q = \lambda^2 \sigma^2 K'_Q = \sigma^2 K_Q \quad .$$

Plots of the C_T and C_Q coefficients in terms of σ are shown in Figures 8 and 9. The data on these figures taken from reference 2 were used in the simulation discussed later in the report.

Finally, it should be recognized that the experimental propeller data obtained[33] do not include the effects of cavitation. Thus, "The effect of cavitation was not considered in determining the hydrodynamic characteristics of propellers from experimental data with models in a test tank. Cavitation may arise during reversing of fast ships, with highly maneuverable power plants, even in cases where the screw propellers do not cavitate during the steady state run prior to reversing."[33]

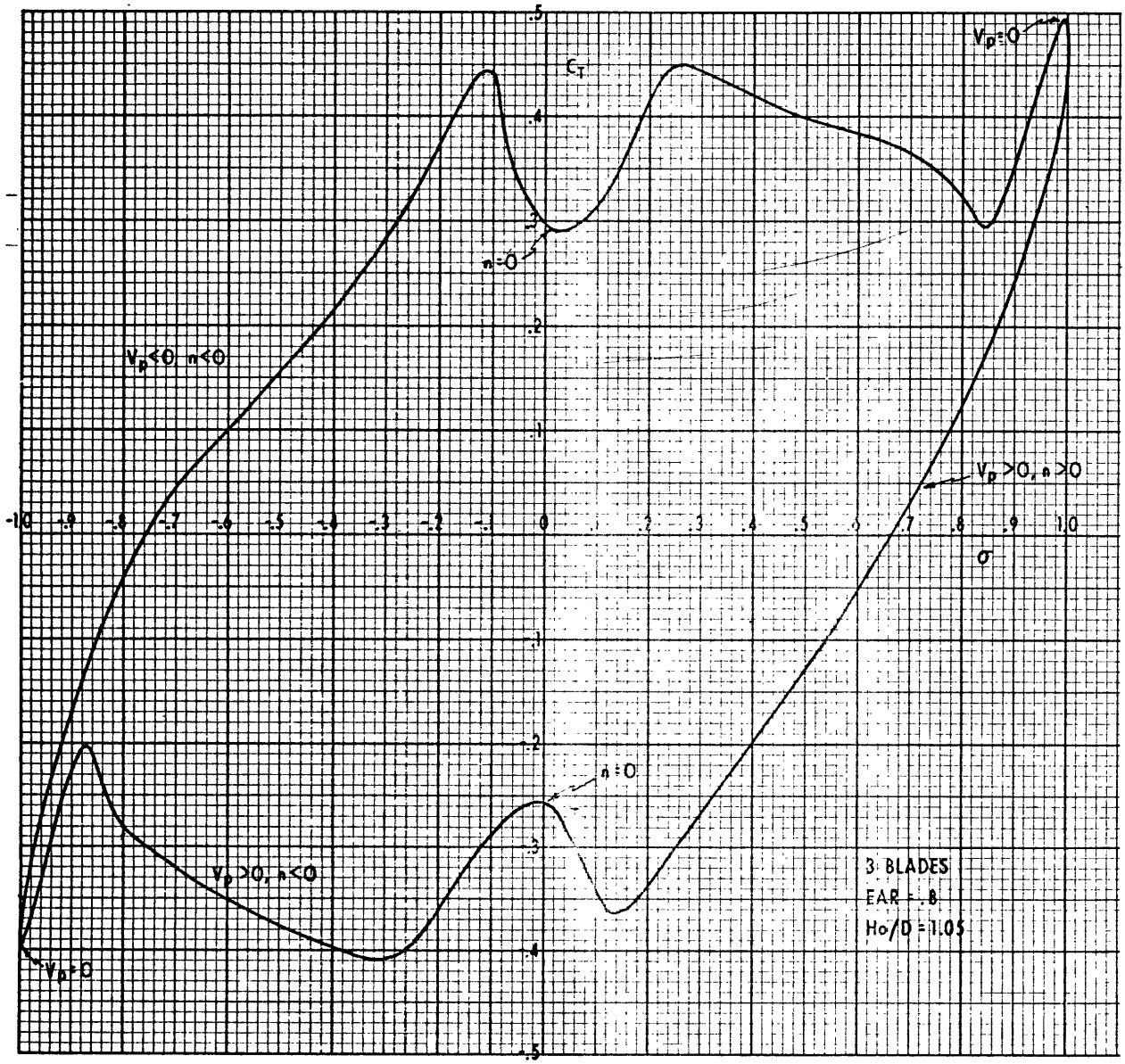

Figure 8
Thrust Coefficient Versus Second Modified Advance Coefficient

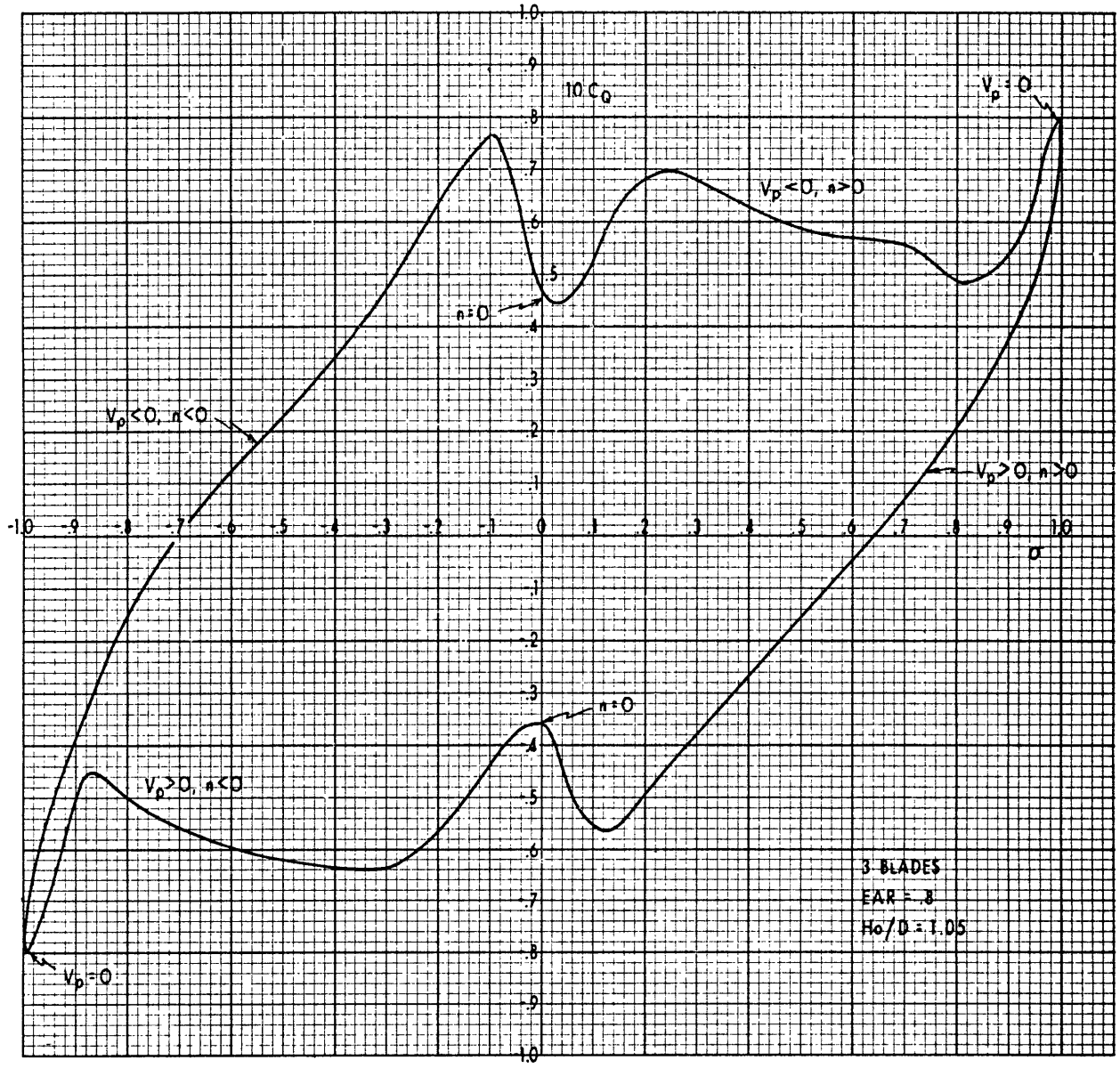

Figure 9
Torque Coefficient Versus Second Modified Advance Coefficient

ENGINE CONTROL

The propulsion system used in this study is a COGAG reversing gear system with an added feature of dynamic braking by the use of a water brake. The combined plant consists of two FT4A-2 gas-turbine engines driving a single screw. Two versions of a COGAG reversing gear system were studied, both with and without a water brake.

Automation and control aspects for this type of plant have been discussed in detail previously.[41, 42]

It should be noted that a gas-turbine plant with a reversing reduction gear is the type of propulsion plant installed on the merchant ship, WM. M. CALLAGHAN.

The primary control and sensing elements for the engine used in this study are shown in Figure 10. A brief discussion of the control of the overall propulsion system is given, and both versions of the combined plant throttle control system are shown in Figures 11 and 12.

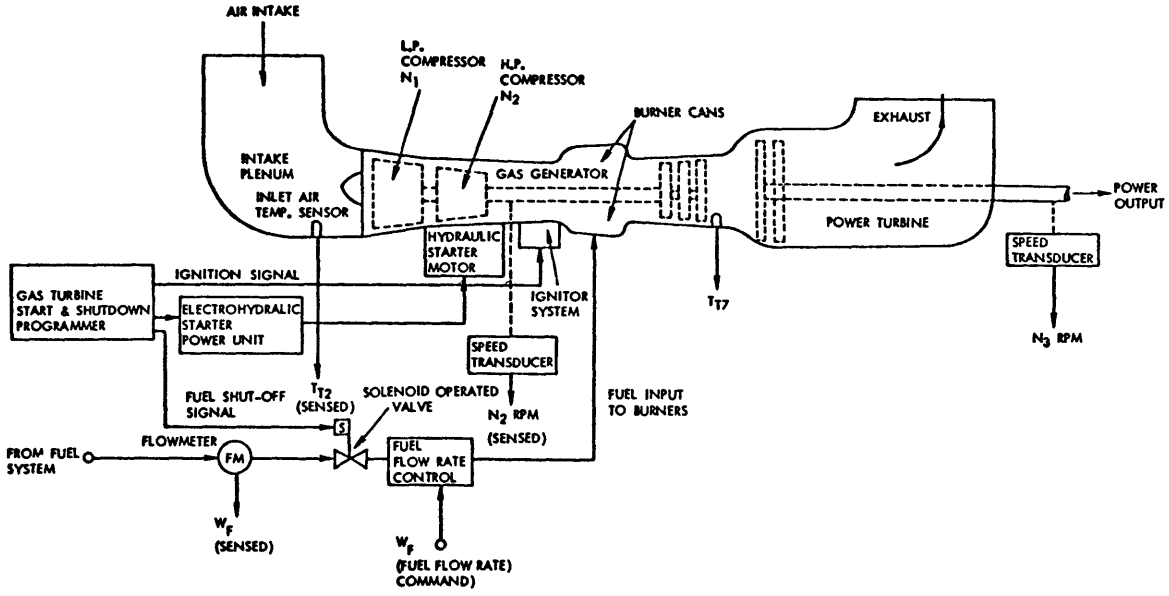

Figure 10
Gas-Turbine Control and Sensing Elements
(for Pratt & Whitney Aircraft FT4A-2 Engine)

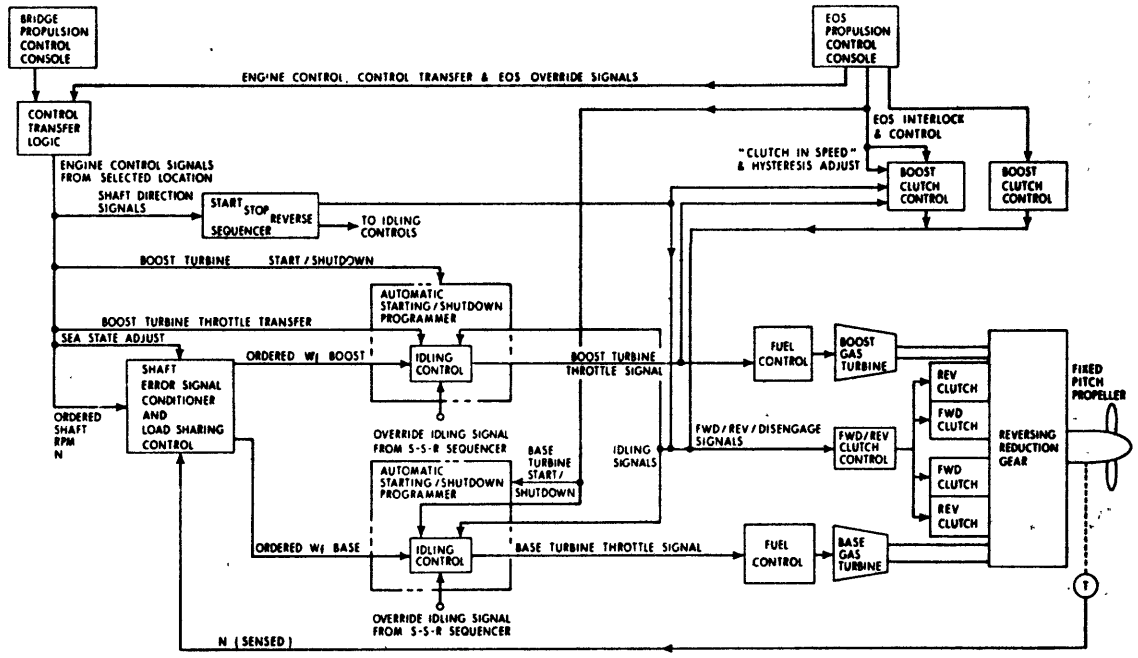

Figure 11 - Combined Plant Throttle Control System COGAG (with Reversing Gear)

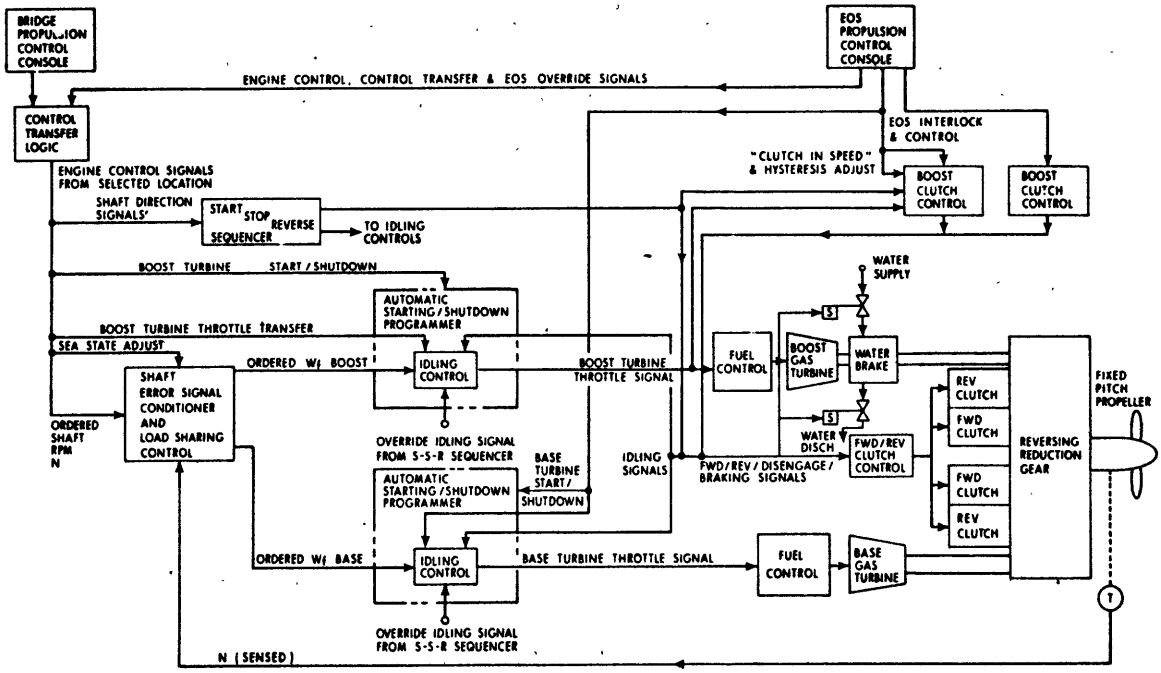

Figure 12 - Combined Plant Throttle Control System COGAG (with Reversing Gear and Water Brake)

In normal operation, the conning station (bridge) exercises direct control over shaft speed and direction. Speed and direction control systems are fully automated.

The primary control station for the propulsion plant is the engineering operating station (EOS). This station is provided with all centralized controls and monitoring and override facilities for all automatic controls. Under normal conditions, the EOS monitors the system operation with the conning station in control. However, it has the capability to assume full control at any time that circumstances require.

All automatic control systems which are critical to plant operation are paralleled by local or remote manual systems for casualty and damage resistance. The transition from normal to alternate or emergency control modes can be accomplished without disruption of plant operation.

The EOS contains an extensive array of status displays, alarms, and interlocks to facilitate optimized operation, to assist in casualty and damage control, and to diagnose improper or unsafe situations.

The ship shaft rpm is the basic controlled parameter for the propulsion plant. Shaft rpm is ordered either at the bridge or the EOS, and the propulsion control system issues turbine commands in either a closed-loop feedback or fuel scheduled control system to achieve the desired rpm.

In this first-phase study, only the open-loop commanded fuel flow rate (W_f) control mode was investigated. Comparison of power- and speed-governing systems with open- and closed-loop control via the shaft error signal conditioner and load-sharing control will be investigated in later studies.

The bridge is given control by the EOS, which always exercises an override capability on the bridge.

Shaft speed orders which involve starting, stopping, dynamic braking, or reversing the direction of the shaft cannot be executed by the gas-turbine throttles alone since this involves control of the various clutches and water brake valve controls. These control signals are provided by the "start-stop-reverse sequencer."

The automatic start/shut-down programmer accepts a start signal from the EOS, the turbine room, or the bridge (for the boost turbine) and begins a programmed starting sequence subject to interlocks, together with turbine and auxiliary system status signals through a programmed sequence of starting operations. Failure of the turbine to respond to a particular operation within a predetermined interval or set of conditions interrupts the sequence and an alarm is given. After successful start, the

turbine throttle is transferred to the idling control, and the turbine receives an idling fuel-rate signal until another signal is sent to the idling control to transfer from idling to an ordered throttle signal.

At this point, either the EOS or the bridge shaft speed control becomes "active," and the turbine receives its throttle signal via the bridge shaft speed or EOS shaft speed command. The ordered shaft rpm (N) is an output to the shaft error-signal conditioner which compares ordered and sensed shaft speed and issues the throttle signals to both engines. The error-signal conditioner contains all of the circuits necessary to match the desired shaft speed to the required throttle signals, to provide for adjustment in loop response via the sea-state adjust, and to provide for open-loop shaft control when desired (such as in high sea-state conditions). Shaft direction is interpreted and reversing is accomplished by the start-stop-reverse sequencer.

Operation to the maximum cruising speed of about 25 knots is possible on the base turbine which is normally limited to 20,000 hp at about 2900 rpm. For speeds in excess of the base power limit, the base-turbine power is normally fixed at 20,000 hp by a limit on the fuel flow rate. An indication is given at the EOS and bridge that the boost turbine, if not idling, must be started. The boost turbine is started by its automatic start-shut-down programmer when a signal from the EOS setup control or from the bridge setup control, subject to an EOS override through the EOS interlock, is initiated. After a successful start, the boost-turbine throttle is transferred to the idling control. Transfer to ordered boost-turbine rpm is accomplished at the EOS or at the bridge subject to a transfer OK from the EOS. The boost-turbine throttle signal is provided by the shaft error-signal conditioner in response to ordered shaft speed. Boost-turbine assistance provides the additional power required to satisfy the required rpm in the speed range from cruising to full speed. A maximum speed of about 31 knots is then achieved with the combined plant delivering 45,000 engine horsepower with both engines operating at 3800 rpm.

DYNAMIC BRAKING

A water brake coupled directly to the free turbine shaft and running normally in air or vacuum was investigated as a means of dynamically braking the main propulsion shaft of the ship in a short period of time, thereby decreasing the dissipated power in the clutch. Another purpose in the use of the water brake is to extend the speed range of the gas turbine by providing a load on the engine at idling speeds, thereby allowing slower ship speeds than would be possible with the gas turbine alone.

Conventional past methods of reversing the propeller thrust in ships with unidirectional prime movers, such as gas turbines and some type of diesel engines, include: electric drive, controllable-reversible-pitch propellers (CRP's), and reversing gears.

A reversing reduction gear offers an attractive method of reversing the shaft direction except for the requirement of large clutches which must dissipate a substantial amount of energy, especially in a crash-back maneuver. With a reversing reduction gear, the transmission system eliminates some of the disadvantages of the CRP or electric drive systems.

A water brake, investigated as a means to overcome the disadvantages of large clutches and possible clutch "burnout" during the reverse clutching deceleration phase of ships equipped with a reversing reduction gear, decreases the shaft speed rapidly, after which the reverse clutch is engaged to complete shaft reversal.

Thus, with a water brake, the clutch energy dissipation rating can be decreased considerably.

The reversing reduction gear (Appendix A) is of the "Falk" type similar to that used on the MSTS ship, WM. M. CALLAGHAN. Forward and reverse clutches are used with one or more individual clutches in parallel for the forward or reverse direction. The gearing is so arranged that the forward and reverse clutches drive separate gears which mesh with the main reduction or "bull" gear. Both clutches cannot normally be engaged simultaneously due to the controls which adjust clutch engaging and disengaging rates. Large friction clutch faces are used in both clutches and when going from full ahead to a full astern condition or vice versa, a large amount of heat is generated in the clutch being engaged.

The water brake can be attached directly to the output shaft of the boost gas turbine and absorbs a relatively small amount of power when turning in air. For fast deceleration, the solenoid valves to the water brake are opened and the water brake cavity is rapidly filled with water. This causes an immediate large absorption of power by the water brake and brings the shaft speed down quickly. When appropriate, the forward clutch is disengaged and the reverse clutch is engaged, thus rapidly reversing shaft rotation.

If only the base engine is on the line, the boost-turbine clutch is engaged for dynamic braking and the water brake cavity is filled. If both turbines are on the line, dynamic braking is accomplished by idling both turbines and filling the boost-turbine water brake cavity.

To reduce the power absorbed by the water brake in normal operation with an empty cavity, a vacuum can be drawn on the water brake cavity.

The water for the water brake can be supplied from the ship's fire main or storage tank, and the heated water is discharged overboard.

The primary advantage of this method is that it opens the possibility of using reversing reduction gears for larger high-powered ships with a great degree of safety against clutch burnout, with only a minimum of additional controls.

An additional feature previously mentioned is that it is possible to extend the low-speed range for the prime mover. With a gas turbine, for example, the minimum idling speed may cause the ship to proceed at a faster speed than may be desired. By partially filling the water brake, an extremely low idling shaft speed can be achieved, thus extending the speed range available with gas-turbine propulsion.

The water brake used in this study is the "Zöllner-Wasserbremse 12u2u50," manufactured by Zöllner & Co. Kiel-Gaarden, Zur Fähre 1. This is a high-speed water brake, and for this study two such brakes in tandem were used. The specifications for the tandem brake 2 x (12u2u50) are as follows:

Maximum speed (rpm)	4,000
Maximum horsepower	35,000
Approximate mounting dimensions	2.5 ft in diameter x 14 ft long

This water brake is in operation at NAVSECPHILADIV on the first model of the gas-turbine test installation.

Figure 13 shows the horsepower rating versus brake speed, N_3 (assuming direct coupling to the gas turbine) for the water brake. These data were used in the computer simulation of this study.

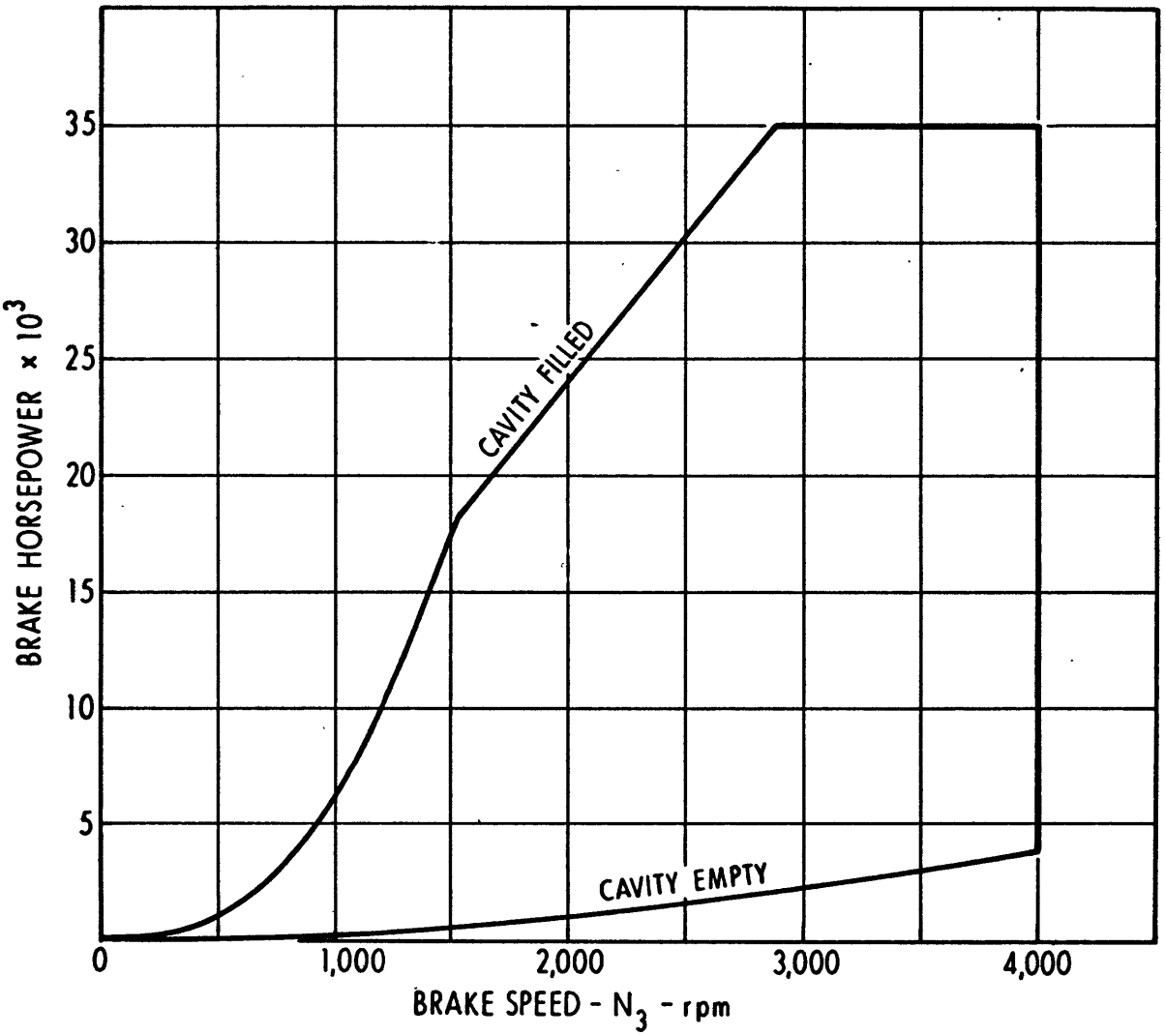

Note: Data obtained from "Description and Operating Instructions of Zöllner Water Brake Model 2xl2u2u50."

Figure 13

Water Brake Horsepower Versus Speed

ENGINES

The gas-turbine base and boost engines picked for this study are Pratt & Whitney Aircraft Type FT4A-2. A description of this engine has been previously published[42] and is also, of course, available in the FT4 Gas Turbine Engine Installation Handbook,[15] published by Pratt & Whitney Aircraft. The FT4A-2 is a version of the FT4 engine designed for marine service which involves primarily the use of materials capable of resisting corrosion in a marine environment.

For the purposes of this study, only a brief description of this engine is given: The FT4A-2 gas turbine shown in Figure 10 consists of a twin-spool, axial-flow, compressor-type engine used as a gas generator (J75), aerodynamically coupled to a free turbine. This engine is rated at 25,000 to 30,000 bhp at a free turbine (N_3) speed of 3600 rpm for Navy boost applications and a rating of 21,500 bhp at 3600 rpm for base applications. In this study the ratings used were 25,000 and 20,000 bhp for the boost and base applications, respectively.

The mass polar moments of inertia of the rotating parts of the FT4 marine engines as published[15] are:

	$LB\text{-}FT^2$
Low-pressure compressor - turbine unit	586
High-pressure compressor - turbine unit	489
Free turbine rotor	5009 .

In this study only the free turbine rotor moment of inertia is used in the analysis. The dynamic response of the gas generator which involves the moments of inertia of the low- and high-pressure turbine units is treated in the lumped pseudo-steady-state response of the gas generator discussed later.

The engine horsepower, P_{ENG}, as a function of the engine speed, N_3, and the engine specific fuel consumption, SFC, is taken from the manufacturer's curves[15] as shown in Figures 14 and 15. It should be noted that the conditions specified are for a standard barometric pressure at sea level of 29.92 in. Hg or 14.7 psia, with no inlet or exhaust duct pressure losses, and at an engine inlet temperature of 80° F. All of these conditions were assumed in the study.

The propeller steady-state load characteristic is shown on these two curves for both the base and boost engines.

FT4A-2 Gas Turbine Engine; Estimated Horsepower and
Specific Fuel Consumption Sea Level - 14.7 PSIA
No Inlet or Exhaust Duct Pressure Losses
Liquid Fuel; LHV - 18,500 Btu/Lb

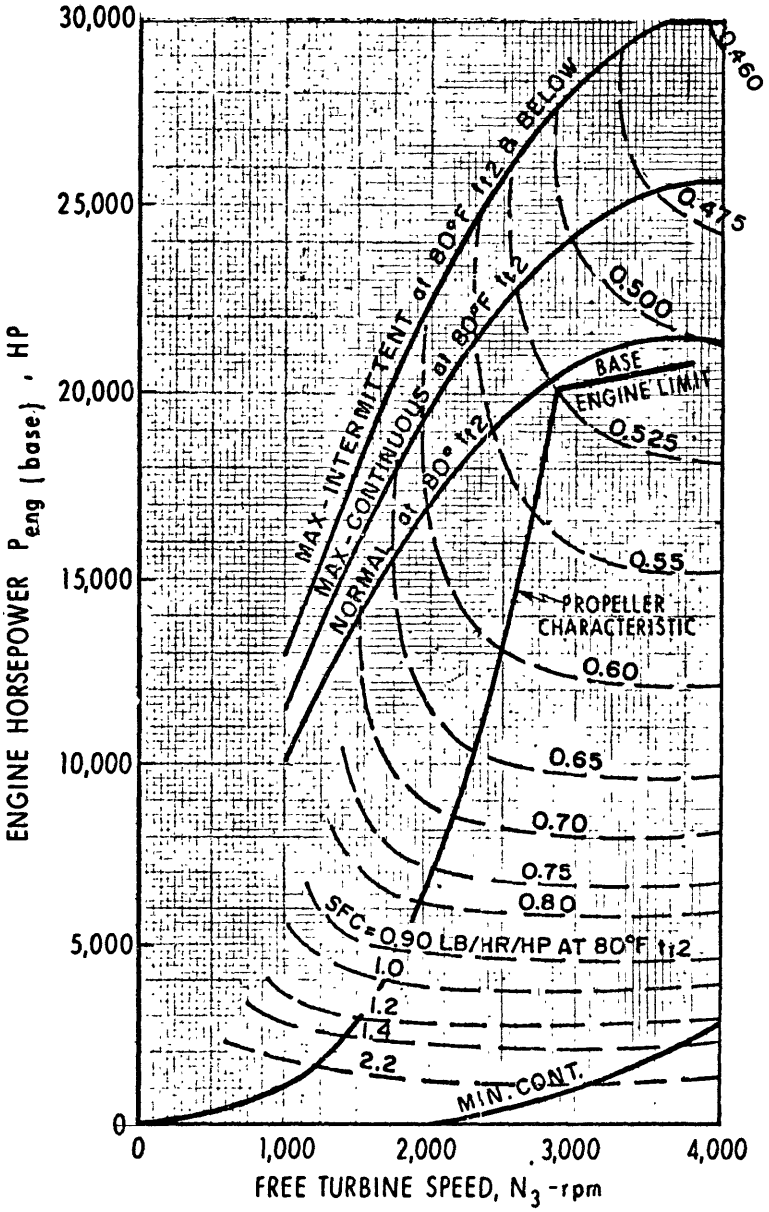

Note: Reproduced from reference 15.

Figure 14
Base Gas Turbine Engine Power
Versus Engine Speed

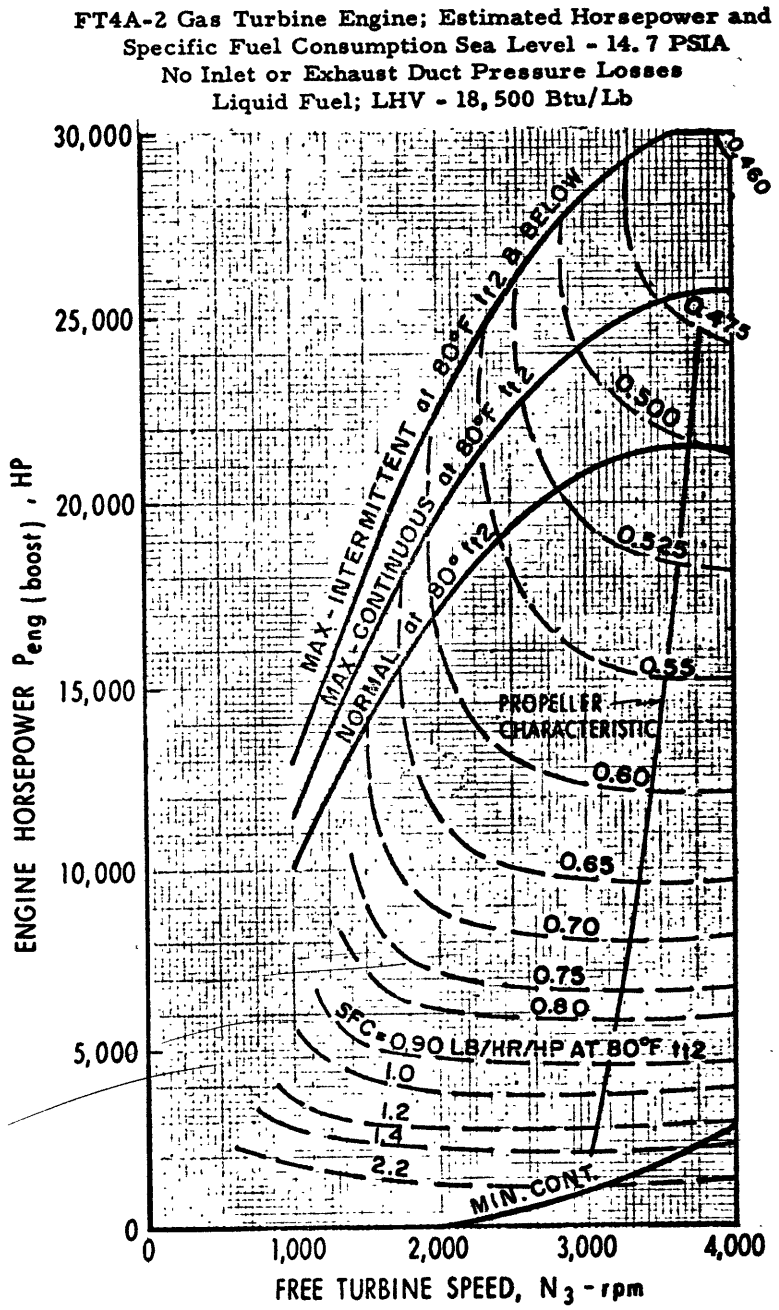

Note: Reproduced from reference 15.

Figure 15
Boost Gas Turbine Engine Power
Versus Engine Speed

In the base only mode, the base engine is normally limited to 20,000 hp at 2900 rpm. In the combined mode, the total engine power is the sum of the base and boost engine power which reaches about 38,000 hp at 3600 rpm or about 45,000 hp at 3800 rpm. The speed corresponding to this horsepower is 31 knots.

The engine horsepower for either engine is related to the engine torque and speed as follows:

$$P_{ENG} = \frac{2\pi N_3 Q_E}{33,000} = \frac{N_3 Q_E}{5252} \quad \text{(horsepower)} ;$$

where N_3 is the free turbine speed (rpm) of either the base or boost engine, and Q_E is the free turbine torque (ft-lb) of either the base or boost engine.

The power delivered to the shaft (SHP) is reduced by the amount of the losses in the reduction gear. Figure 16 shows a plot of the reduction gear efficiency as a function of the percent of full power speed.

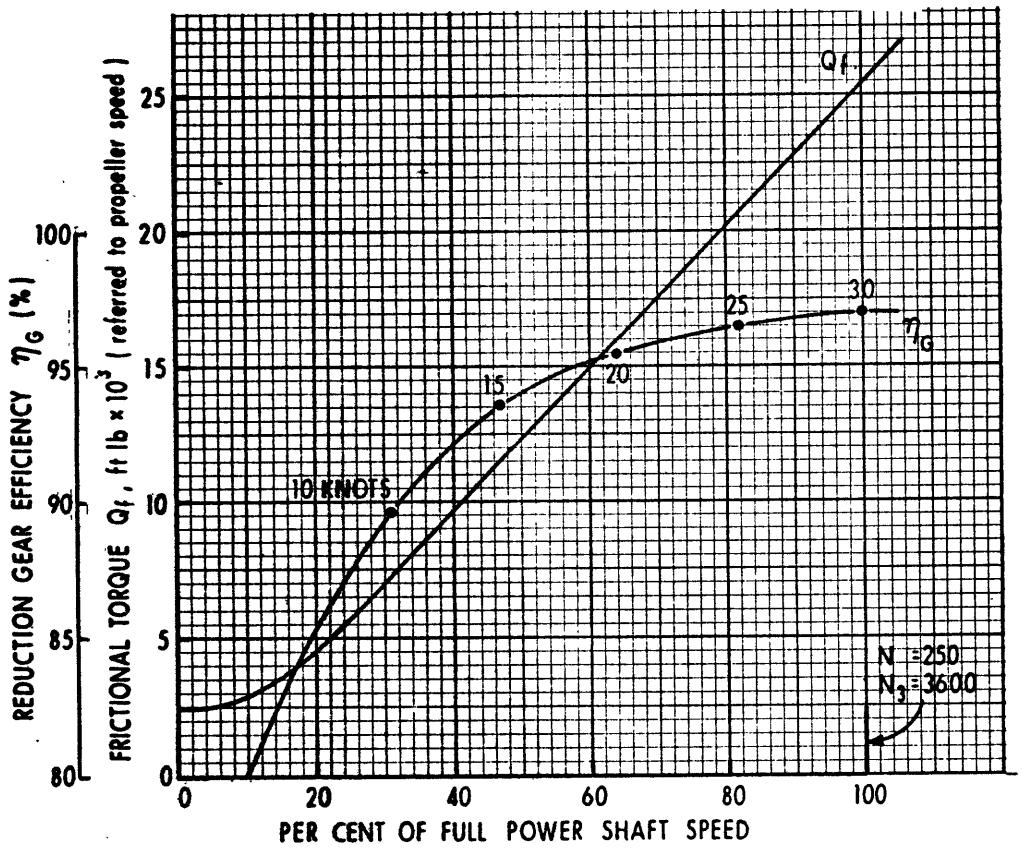

Figure 16 - Assumed Reduction Gear/Bearing Efficiency and Frictional Torque Versus Percent of Full Power Speed

The full power speed was nominally assumed to be 30 knots for which the reduction gear efficiency, η_G, is 97%. Thus, the corresponding plots of ship speed versus SHP, Figure 1, and engine power versus free turbine speed differ by the amount of the speed-dependent gear efficiency curve. The relationship between them is

$$SHP = \eta_G P_{ENG} .$$

REDUCTION GEAR AND BEARING FRICTIONAL TORQUE

A typical efficiency curve for the transmission system including the double reduction gear and shafting was assumed. From Figure 16 it can be seen that the efficiency, η_G, is shaft speed dependent, with the efficiency varying from 97% at full speed to about 90% at 1/3 full speed. For the efficiency and frictional torque calculations, a maximum nominal shaft speed of 250 rpm, corresponding to a ship speed of 30 knots, was used. The frictional torque, Q_f, corresponding to the speed-dependent efficiency curve, is also shown in Figure 16. This curve is a linearized fit based on the equation,

$$Q_f = (1 - \eta_G) Q_d ,$$

where Q_d = torque delivered by the engine(s) to the propeller shaft. A breakaway torque corresponding to 10% of full load frictional torque was assumed.

The frictional torque curve versus percent of shaft speed was used in this study to describe the total frictional torque of the system as required in the torque equation.

It should be noted that this friction representation is not exact since the friction load varies both with speed and propeller torque. For example, at 40% of maximum speed there is about a 2% change in efficiency between 10% and 100% of maximum propeller torque.[30] However, this refinement was not considered significant enough to include in this study.

ENGINE RESPONSE CHARACTERISTICS

The transient response of the engines is required in any dynamic simulation of the ship and its propulsion system. A gas turbine is a highly nonlinear system, and so its response is not predictable by linear methods of analysis. Consequently, there is no "transfer function," as such, for a gas turbine. Small-signal, linearized transfer functions can be used to approximate the gas-turbine behavior for small variations about an operating point, and these linearized transfer functions will vary from one

operating point to another. Therefore, they are of limited value in the investigation of performance where transients over the whole dynamic range of the machine are being investigated.

Gas-turbine simulation is now done almost exclusively with computers. Some of the simulation models used are linear models with constant coefficients. The engine is represented as a collection of multivariable functions which are linearized by writing them in total differential form. An improvement in the linearized model is the method of variable partial derivatives in which the coefficients of the total derivatives vary with the operating point. Both of these methods are limited in accuracy and flexibility because of the limited excursions from a base point of operation. The most successful and accurate method of simulating gas turbines is the functional or component method in which the characteristics of the compressors, turbines, etc are stored in the computer or generated as functions and solved as a multivariable problem by either an analog or a digital computer. Such simulations calculate the rotor speeds from the dynamics of the unbalanced torques on the turbine or turbines after subtracting the torque necessary to drive the compressor or compressors. Usually these simulations include compressor and enthalpy maps for the engine and consider the effects of transport delays and temperature lags at various points within the engine.

Several investigators[9 10 17 22 32] have used the above methods in simulating gas-turbine engines.

The approach taken in this report in modeling the transient response of the gas-turbine engines is a pseudo-steady-state representation with only the principal external engine characteristics such as fuel flow rate, engine torque, and engine speed used in the model. The method of computer solution discussed in greater detail later uses a stored engine torque map and a stored maximum fuel flow rate of change to calculate the engine torque. The solution of the two nonlinear differential equations of the ship-propulsion system results in a shaft speed and a corresponding engine speed, N_3. After the digital computer solution is begun, a previous solution giving N_3 is used to find the incremental change in engine torque. Since a new solution is computed for every 0.1 second or less, the engine torque-speed change in a computation interval based on steady-state characteristics is very small. Thus, the transient behavior is predicted from a continuous solution of extremely small steady-state intervals which depend on the solution of the entire ship-propulsion system of equations.

Ultimately it is hoped to incorporate a more sophisticated engine model of the component type in a computer subroutine. From such a model the behavior of internal engine characteristics, such as stage temperatures, pressures, and gas flow rates, can be readily predicted for any condition of ship maneuvering.

To obtain transient response verification of the FT4A-2 engine, it was tested at NAVSECPHILADIV for various types of fuel commands at a number of power levels with the speed governor both operational and disabled. In addition, the water brake load was varied at several engine power levels. The results obtained were used as a verification of the engine model used in this report. Subsequent reports will discuss engine computer simulations and experimental test results for the FT4A-2 gas-turbine engine.

Experimental test results for one of the gas-turbine transient tests are shown in Figure 17. In this test a step fuel flow command was given with the speed governor disabled and with a water brake load whose power increased approximately as the cube of speed. The inertia of the water brake load at the free turbine shaft for this test was 2000 lb-ft^2. The free turbine inertia is 5009 lb-ft^2. By comparison, the drive train moment of inertia at the free turbine shaft for the study ship in the base load condition is 23,000 lb-ft^2. Thus, the inertia of the test load was less than 1/10 of the study-ship drive-train inertia, although the torque loading characteristics were similar.

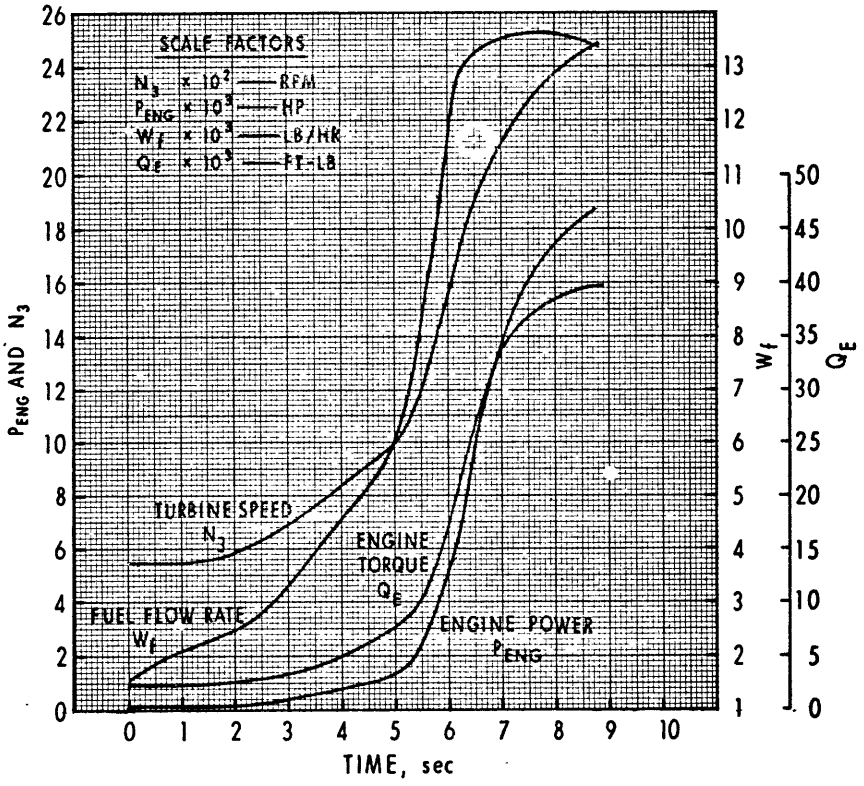

Figure 17 - Gas-Turbine Transient Test for FT4A-2 Engine
Step Throttle Increase - Idle to 20,000 HP
(Speed Governor Disabled)

These and other transient data taken at various power levels indicate that the engine torque lags the fuel flow rate by 1 second or more, depending on the power level. In the engine model used in this report, this lag was not considered; consequently, the engine torque follows the fuel-flow rate with no delay.

The rate of change of fuel-flow rate with time for a step change in commanded fuel-flow rate agrees within about 1 second with the assumed performance used in the analysis and shown in Figure 18.

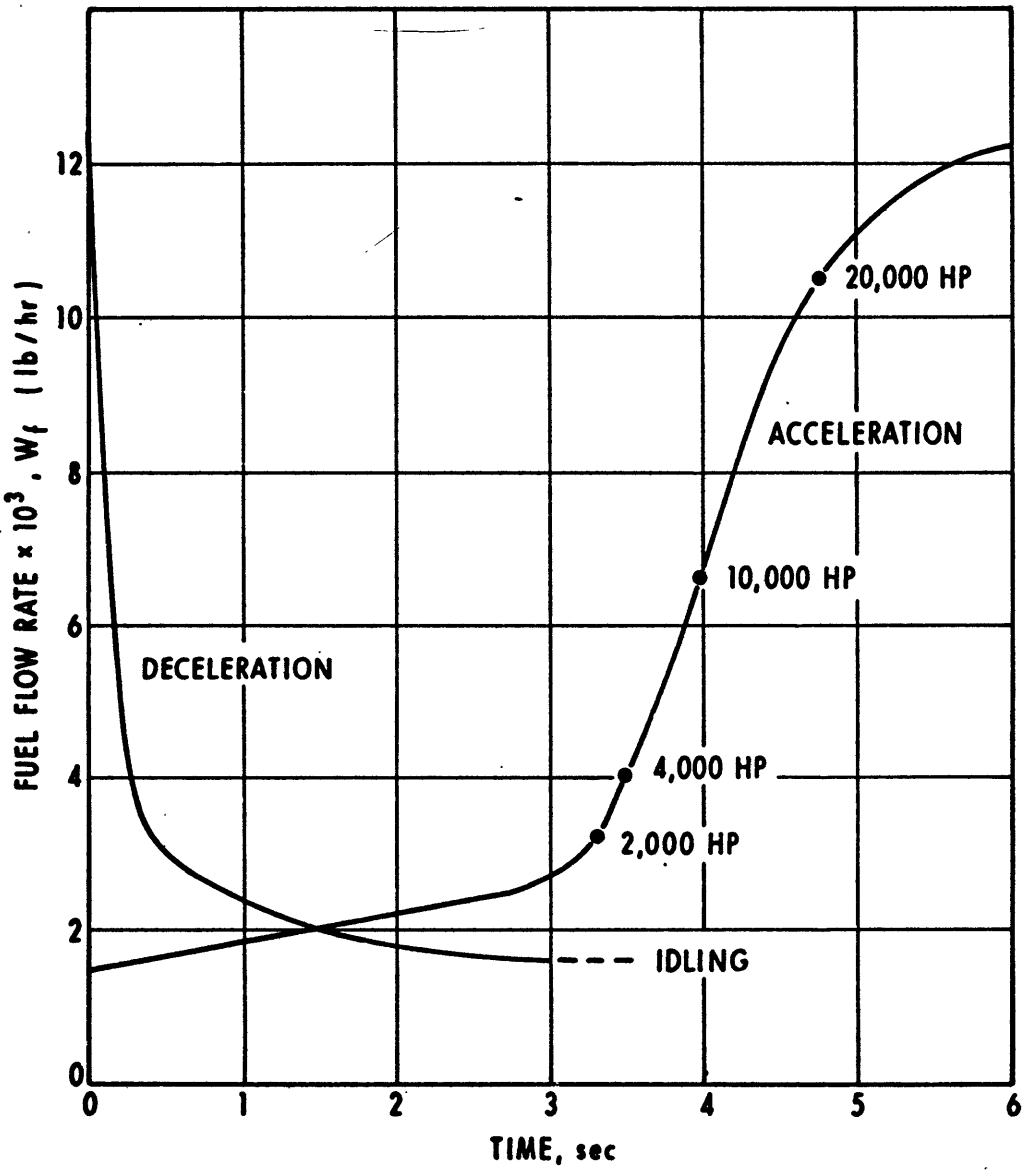

Figure 18
Fuel Flow Acceleration and Deceleration Rates

The engine model used in the present first-phase study is for an open-loop, fuel-scheduled gas generator; that is, no attempt was made to simulate the particular gas-turbine control system used by the manufacturer. In later studies a gas-turbine control system will be synthesized as part of the overall ship combined plant throttle control system. This control system will provide the fuel flow rate commands to the gas turbines and is called the "shaft error signal conditioner and load sharing control." This approach was taken because of the greater generality in the investigation of a gas-turbine control system whose parameters could be varied during the simulation and is an intimate part of the total ship and propulsion-plant simulation. Thus, it allows an investigation of open- and closed-loop operation for both speed and power governing. However, in the later studies it is anticipated that performance of the existing gas-turbine control systems will be evaluated. It should be noted that for the manufacturer's standard control systems for the FT4A-2 engine (either the hydromechanical fuel control system or the electronic fuel control system), it is only by means of fuel flow rate that the engine is controlled.

The following brief descriptions of both types of control systems are taken from the manufacturer's publications[15, 16] where detailed descriptions of the engine and control systems are given.

Hydromechanical Fuel Control System

> "The FT4 fuel control operates in conjunction with a free turbine speed governor and controls free turbine speed by controlling gas generator output. The speed governor senses free turbine speed (N_3)* and, through appropriate linkages, transmits the N_3 speed signal to the fuel control power lever. The fuel control, in turn, meters fuel to the gas generator in accordance with gas generator speed, burner pressure, and fuel control power lever angle. The fuel control provides the correct fuel flow schedule during starting and acceleration/deceleration transients and during steady state operation. A maximum fuel flow stop provides limiting power output in accordance with the specific rating of the engine. Additional free turbine speed sensing is provided, which will initiate a signal for rapid emergency fuel shutoff in the event of a free turbine overspeed condition.

*For consistency with the engine manufacturer's notation, N_3 is the free turbine speed. N_1 and N_2 refer to the low- and high-pressure compressor speeds, respectively, and are not used in this report.

"The JFC25-28 model fuel control for FT4 marine gas turbines is a high capacity hydro-mechanical fuel flow metering device. Two control levers are provided on the control. One lever controls the gas generator during operation and is mechanically linked to the output lever of the free turbine governor. The other control lever is used to effect gas generator starting and shutdown by opening and closing a fuel shutoff valve within the control and sending a signal to the manifold drain valve (pressurizing and dump valve assembly).

"Due to the characteristics of the gas generator, it is necessary that fuel flow be maintained within certain limits which vary depending upon operating conditions. The limits imposed are those of burner pressure and gas generator speed. Subject to these limits the control is capable of accurately maintaining gas generator speed during steady-state operation by the use of a permanent droop system in conjunction with the speed setting governor (in the fuel control). During acceleration and starting, the control senses burner pressure and gas generator speed, and as a result, schedules fuel flow to permit the maximum rate of acceleration allowable within the gas generator operating temperature limits while avoiding compressor surge and rich blowout. During deceleration, the fuel control schedules fuel flow as a function of burner pressure to ensure the maintenance of sufficient fuel flow at the minimum level to support combustion, thus, preventing lean die-out, yet permitting a maximum rate of deceleration. In addition, the fuel control incorporates a fixed mechanical stop on the metering valve to limit maximum fuel flow, thus, limiting maximum engine power and free turbine torque at rated speed."

Electronic Fuel Control System

This system controls the turbine by metering fuel to the gas generator by means of the SPC2 fuel control.

"The electronic control system provides three principle functions in controlling the fuel supplied to the FT4 gas generator, (1) speed governing, (2) acceleration limiting, and (3) shutdown protection. Basically, the system is a gas generator or free turbine speed governor that maintains a preset reference speed. The control continuously measures speed error and regulates fuel flow to maintain

a minimum error condition. Acceleration is regulated by limiting gas generator exhaust gas temperature to a predetermined schedule of temperature versus speed, thus, providing optimum acceleration times, yet protecting the gas generator against excessive exhaust gas temperature. Protection features are incorporated which provide monitoring of certain engine parameters, comparison with preset limits and initiation of gas generator shutdown for excessive conditions.

"The basic electronic controller is a remote-mounted speed governor that controls the gas generator fuel supply to maintain a preset gas generator speed.

"The controller is of the feedback servo-mechanism type, utilizing feedback compensation techniques which continuously measure any speed errors and corrects these errors to maintain the system at minimum error. To accomplish this, the controller speed sense module receives an a. c. signal from the speed transducer and generates a d. c. voltage proportional to speed. This signal is biased by the output of the inlet air temperature sensor in order to limit gas generator power or exhaust gas temperature. The corrected speed signal is compared to the reference speed and the summation, or error signal is fed to a selector circuit. The selector circuit sees speed error and exhaust gas temperature error (acceleration limiting) and sends one control signal to the power amplifier -- that is, the signal calling for the lesser fuel flow. The amplified controlling error signal drives the liquid metering valve actuator in the direction to reduce the error. The basic controller will control gas generator transient response by limiting its exhaust gas temperature to a pre-determined schedule of temperature versus gas generator speed. This limiting will prevent excessive temperature during acceleration, yet permit optimum acceleration response rates. The controller will also automatically initiate an engine shutdown for excessive exhaust gas temperature."

Fuel Flow Rate

Since the fuel flow rate controls the engine speed and power, certain limits on the rate at which the fuel flow rate can be changed are incorporated in the engine fuel control as previously discussed. From manufacturer's data on the FT4A-2 engine relating engine response time to engine speed and torque for both acceleration and deceleration, fuel flow acceleration and deceleration rates were computed as a function of time,

shown in Figure 18. These curves are the assumed maximum allowable rates of fuel change for the FT4A-2 engine. The computer simulation discussed later in this report allows fuel flow rate to vary no faster than these rates regardless of the commanded rate. It should be noted that the time required to effect a fuel rate change varies with the power level, the smallest rate of change occurring between idling and about 2000 horsepower. The fuel response rate from any power level has been corrected in the computer program to bias the time scale about any operating point on the acceleration or deceleration curves to permit simulation of power changes at any desired level.

An engine "torque map" was calculated from the engine data shown in Figures 14 and 15. The free turbine torque (Q_E) versus free turbine speed (N_3) and fuel flow rate (W_f) were plotted from these data and are shown in Figure 19.

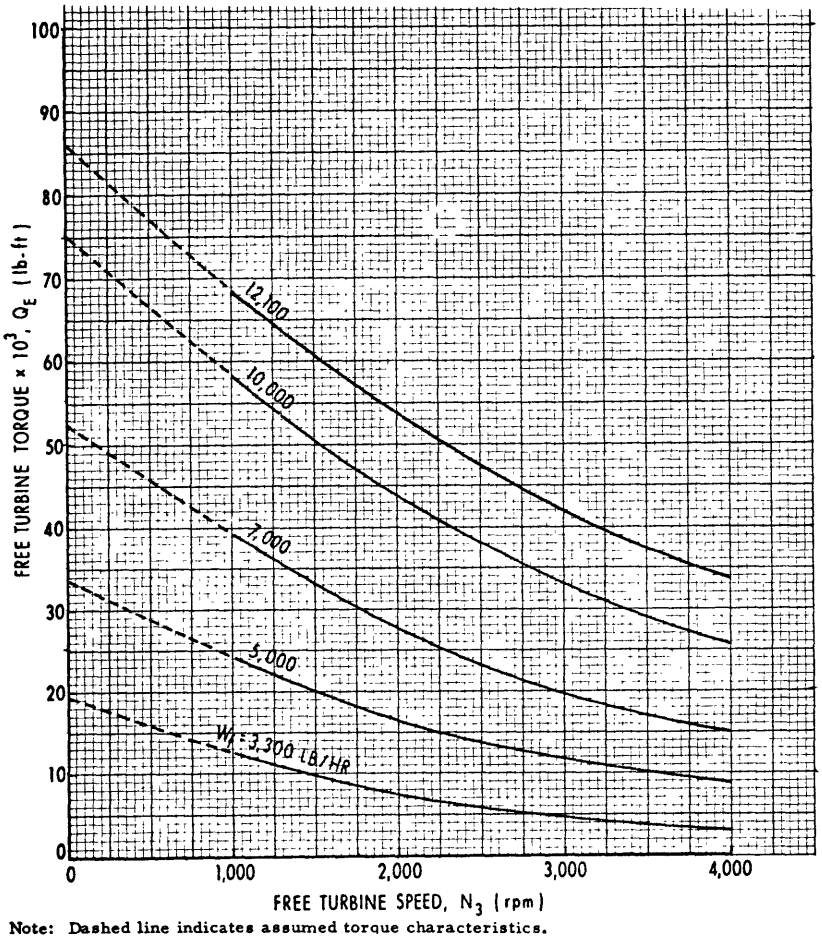

Note: Dashed line indicates assumed torque characteristics.

Figure 19 - Engine Torque Versus Engine Speed and Fuel Flow Rate

This engine torque representation applies to both the base and boost gas turbines. The calculations from the horsepower to torque methods of representation were computed from the two expressions,

$$Q_E = \frac{5252\ P_{ENG}}{N_3} \qquad \text{(engine torque)}$$

and

$$W_f = SFC \times P_{ENG} \qquad \text{(fuel flow rate)} \ .$$

It should be noted that both the engine representations are steady-state engine characteristics. The engine torque versus speed and fuel-flow rate is a very important engine description in this simulation because the driving function in the solution of the differential equations of the propulsion system is torque and the independent variable is engine fuel-flow rate. Any change in commanded speed is accomplished by a change in the fuel-flow rate.

In the steady-state condition, the fuel-flow rate (W_f) required to achieve a certain turbine speed and a corresponding ship speed can be computed from the propeller load characteristic plotted on the engine-power (P_{ENG}) versus engine-speed (N_3) curves shown in Figures 14 and 15. From these curves the fuel-flow rate versus engine speed for both the base and boost turbines was computed and is shown in Figure 20. It should be noted that these curves of fuel flow rate versus speed are along the steady-state propeller characteristic, as shown in Figures 14 and 15, describing the ship power/speed profile. The base turbine fuel-flow rate is normally limited to about 10,500 lb per hr which corresponds to about 20,000 engine horsepower.

These curves can be interpreted as the "fuel-flow schedule" relating required fuel-flow rate to achieve a particular engine and ship speed. Thus, there is a direct correspondence between engine and shaft speed and fuel-flow rate via these curves.

Engine Idling Conditions and Windage Losses

The engine torque map, Figure 19, does not describe conditions for an idling engine. Tests were conducted at NAVSECPHILADIV to establish the engine torque and speed characteristics at low speeds corresponding to an idling fuel-flow rate.

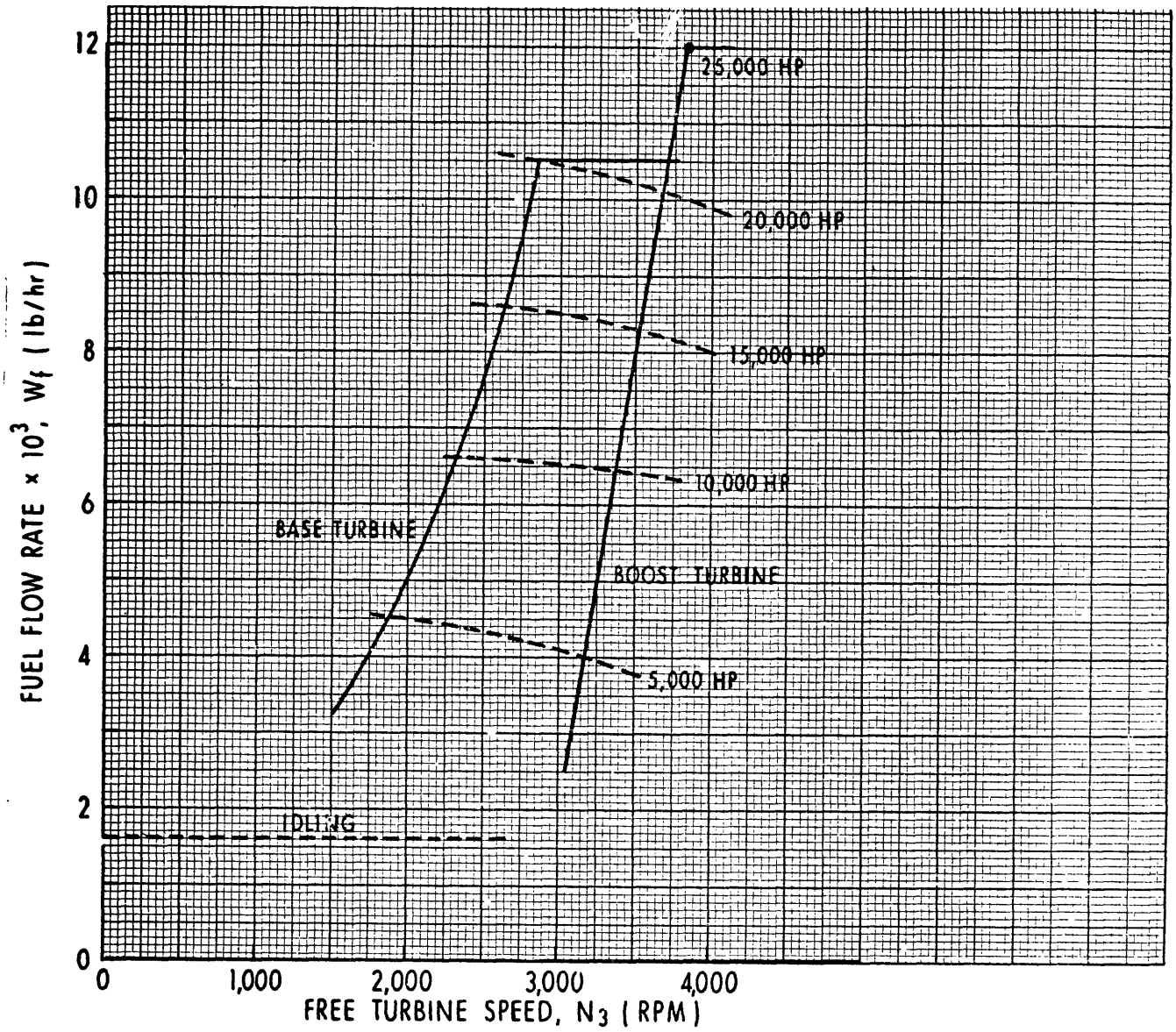

Figure 20
Turbine Fuel Flow Rate Versus Turbine Speed

Figure 21 shows the experimental data for a fuel flow rate, W_f, of about 1600 lb per hr for several conditions of free turbine speed and torque. The torque changes were produced by changing the load on the gas-turbine water brakes and reading the resultant torque and free turbine speed under a steady-state condition. The resultant readings were corrected to correspond to an engine inlet temperature, t_{t2}, of 80° F.

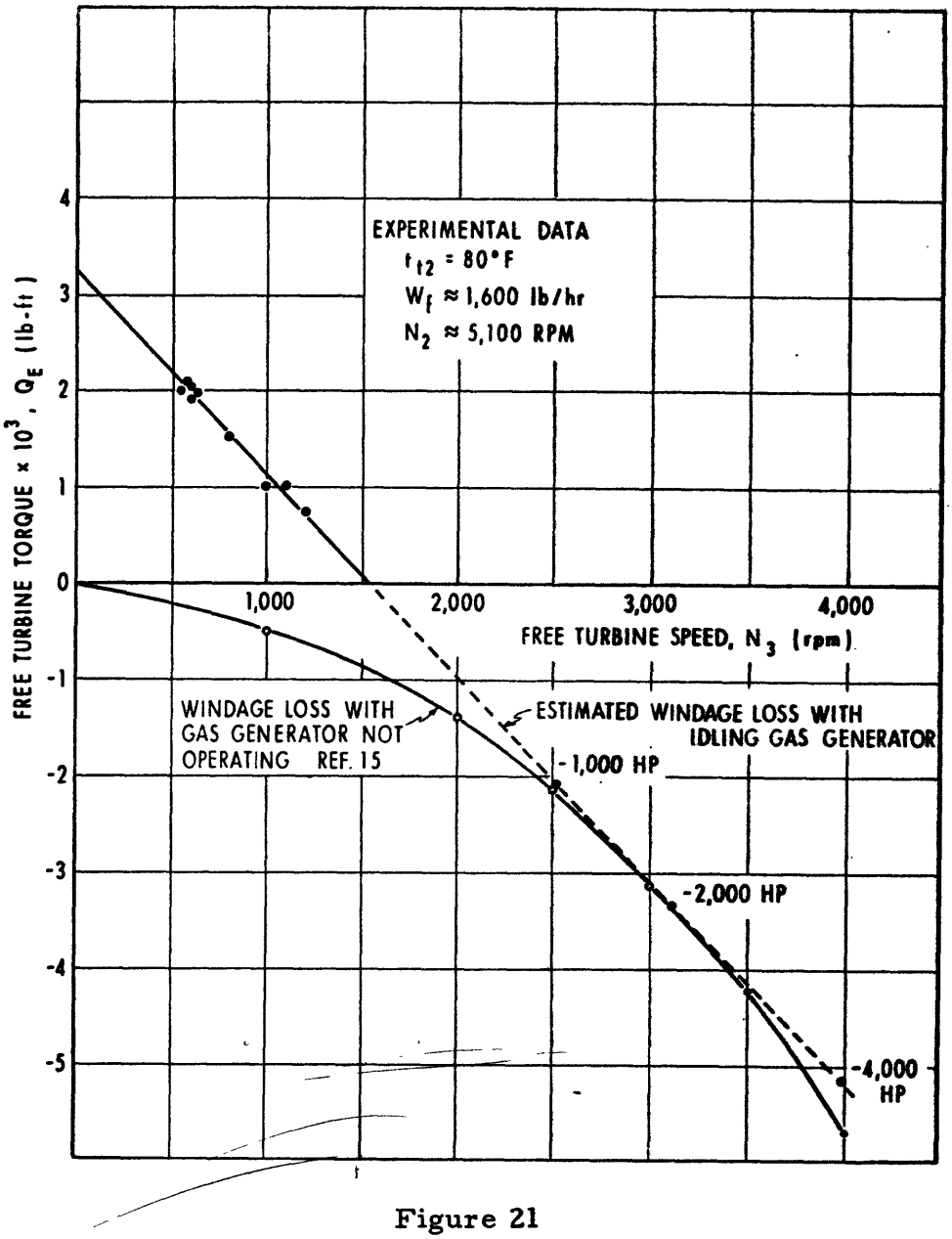

Figure 21
Free Turbine Idle and Windage Torque
for FT4A-2 Gas-Turbine Engine

From these data it can be seen that the torque available from the engine is zero at a speed of about 1500 rpm and the engine idle stall torque (N_3 = 0) is about 3200 lb-ft for a fuel flow rate of about 1600 lb per hr. A linear extrapolation of this curve for speeds between 1500 and 4000 rpm is the estimated windage loss curve with an idling gas generator. Thus, if the free turbine is rotated between 1500 and 4000 rpm, power must be

supplied to overcome the windmilling losses which reach approximately 4000 hp at 4000 rpm. Consequently, the engine torque and horsepower are defined as negative in this region. It should be noted that the windage loss predicted by this method in this range matches fairly closely the estimated windage loss by the manufacturer for the gas turbine with the gas generator not operating (FT4 Gas Turbine Engine Installation Handbook,[15] Curve No. INST. 30184).

The significance of the windmilling torque is that when the gas generator power is cut to idle during a stopping or reversing maneuver, the windmilling torque extracts power from the water milling shaft and tends to slow the shaft speed. This sort of dynamic braking adds to the braking exerted by the water brake and the friction clutches.

The computer simulation discussed later includes the idling and windmilling torque in the solution of the ship-propulsion equations. The engine torque map, Figure 19, is used when the fuel flow rate is in excess of 1600 lb per hr. When the fuel flow rate goes to idling at 1600 lb per hr, the computer switches to the idling torque representation, Figure 21, which includes the windage losses.

It should be noted that with the torque representation shown in Figure 21, the engine torque changes sign in the computer program as the gas-turbine speed passes through 1500 rpm. For example, during a deceleration the torque map is changed when the idling fuel flow rate goes to 1600 lb per hr. The engine torque becomes negative, and as speed decreases, it goes in the positive direction and eventually becomes positive again.

SHIP-PROPULSION EQUATIONS

The ship-propulsion equations for calm water and with no turning maneuvers are the two first-order, nonlinear, time-varying differential equations given below:

$$m \frac{dv}{dt} = T_p - R_T \qquad \text{(thrust equation)}$$

$$2\pi I \frac{dn}{dt} = \Sigma Q \qquad \text{(torque equation)} ,$$

where T_p, R_T, and Q are nonlinear functions of V and n and

m = ship mass including entrained water, lb-sec^2/ft

V = ship speed, fps

T_p = propeller net thrust, lb

R_T = total ship resistance, lb

I = drive train moment of inertia, lb-ft-sec^2

n = propeller angular speed, rps

ΣQ = torque summation acting on propeller shaft, lb-ft.

The propeller thrust is a function of two variables for a fixed pitch propeller. These are: n, the angular speed of the propeller, and V_p, the propeller speed of advance.

The propeller speed of advance, V_p, is calculated from a stored computer table of wake fraction, w, versus ship velocity, V, from the equation

$$V_p = V (1 - w) .$$

The propeller net thrust, T_p, is calculated in the simulation by correcting the propeller open water thrust, T, by the thrust-deduction factor (1 - t). The thrust-deduction factor versus ship velocity is a stored computer table.* Thus,

$$T_p = T (1 - t) .$$

Open water propeller thrust, T, is found from the equation

$$T = C_T \rho D^2 (V_p^2 + n^2 D^2) .$$

This equation is computed from a stored map of the propeller thrust coefficient, C_T, versus σ (Figure 8). The second modified advance coefficient, σ, is computed from the propeller speed of advance and the propeller speed:

$$\sigma = \frac{nD}{\sqrt{V_p^2 + n^2 D^2}} .$$

*Appendix B describes the logic flow diagram for the computer solution of the propulsion equations.

Total ship resistance, R_T, is another computer look-up table giving R_T versus ship speed, V.

The thrust and torque equations are both solved on the digital computer by an iteration procedure with an integration every 0.1 second. For each integration interval the table look-up functions are changed from the previous value by a linear interpolation, the equations are updated, the new torques and thrusts are computed, and the solution progresses until a steady-state condition is reached.

The thrust and torque equations are coupled through the propeller thrust and torque coefficients which are functions of both V_p and n.

The shaft torque and acceleration are related by the torque equation,

$$2\pi I \frac{dn}{dt} = \Sigma Q \ .$$

During various ship maneuvers, both the total drive train inertia, I (referred to the propeller shaft), and the torques acting on the shaft change; consequently, the appropriate moment of inertia and torque must be used in the torque equation, depending on the situation. The direction of free turbine and propeller rotation is clockwise when viewed from the shaft end, and the propeller angular speed, n, is defined as positive for forward ship motion. All the torques are considered positive when acting in the direction of positive n (Figure 22).

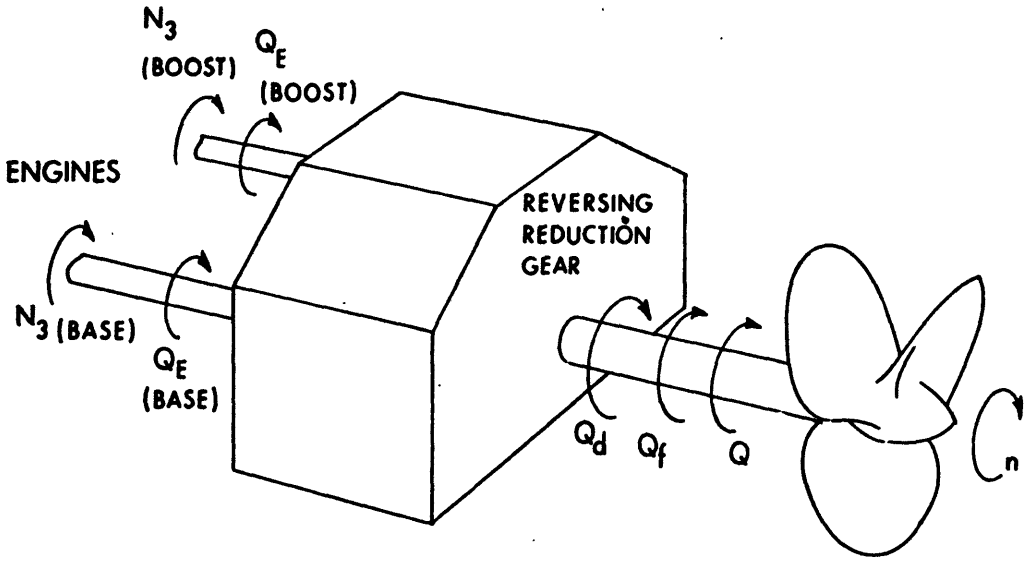

Speed and Torque Notation (all quantities positive in direction shown)

Figure 22
Reversing Reduction Gear Transmission

The torque, Q_d, developed by the engine on the propeller shaft is given by

$$Q_d = k_g \, (Q_{E_{base}}) \qquad \text{(when in the base engine only mode)}$$

and

$$Q_d = k_g \, (Q_{E_{base}} + Q_{E_{boost}}) \qquad \text{(when in the base + boost engine mode)} ,$$

where k_g is the reduction gear ratio.

The propeller torque required to drive the shaft at a speed, n, is from a previous discussion:

$$Q = C_Q \rho D^3 \, (V_p^2 + n^2 D^2) \quad .$$

The torque coefficient, C_Q, versus σ is a stored computer map from which C_Q is found for every value of σ (Figure 9), and then a new value of torque is computed.

The propeller speed, n (rps), is related to the engine speed, N_3 (rpm), through the reduction gear ratio:

$$N_3 = 60 \, k_g \, n \qquad \text{(rpm)} \quad .$$

The frictional torque of the reduction gear and line shaft bearings is Q_f (referred to the propeller side). This torque is a speed-dependent quantity and is obtained from a computer look-up table for any value of shaft speed from Figure 16.

An engine windmilling torque is present with an idling or shut-down gas generator for free turbine speeds in excess of about 1500 rpm. This torque is present when the engine speed is decreased from any value in excess of about 1500 rpm; so it must be considered in coast down, dynamic braking, and reversing ship maneuvers. The windmilling torque is included in the engine torque map, Q_E, which was discussed in a previous section.

- Acceleration (Base Engine Only). The single engine torque equation is

$$2\pi I_1 \frac{dn}{dt} = Q_d - Q_f - Q$$

$$Q_d > (Q_f + Q) \qquad \frac{dn}{dt} \text{ positive},$$

where

I_1 = drive train moment of inertia in the ahead direction with base turbine only (Table 1, see page 53)

$Q_d = k_g \, Q_{E_{base}}$.

- Acceleration (Base + Boost Engines). In this condition the total engine torque, Q_d, is for both engines; the moment of inertia, I_2, is for both engines; and the torque equation is

$$2\pi I_2 \frac{dn}{dt} = Q_d - Q_f - Q$$

$$Q_d > (Q_f + Q) \qquad \frac{dn}{dt} \text{ positive},$$

where

I_2 = drive train moment of inertia in the ahead direction with both the base and boost engines engaged (Table 1)

$Q_d = k_g \, (Q_{E_{base}} + Q_{E_{boost}})$.

Note that the sign of the propeller torque, Q, is always positive during acceleration due to the fact that the torque coefficient, C_Q, is always positive in acceleration.

- Coast Down Deceleration. In this condition the engine torque delivered to the shaft, Q_d, is decreased corresponding to a decrease in the engine fuel flow rate. The forward clutch(s) remain engaged.

Either I_1 or I_2 is used as the moment of inertia in the torque equation, depending on whether the base or base plus boost engines are engaged. The torque equation is still

$$2\pi I \frac{dn}{dt} = Q_d - Q_f - Q \ ;$$

however,

$$Q_d < (Q_f + Q) \qquad \frac{dn}{dt} \text{ negative .}$$

During this phase the shaft continues to rotate in the positive direction, but the speed is decreasing. Since the shaft speed, n, is greater than zero, there is an effective torque provided by the large drive train inertia, even though Q_d goes to zero. This comes from the initial condition on the above differential equation at the start of the coast down phase.

If a water brake is used for dynamic braking of the propeller shaft prior to clutch reversing, the water brake torque, Q_b, absorbs the inertial and water milling energy of the shaft in slowing the shaft speed and then the clutches are reversed. The water brake torque characteristic is essentially a "cube law" with speed, and the magnitude of the torque for any speed is obtained from a computer look-up table derived from Figure 13 giving Q_b versus N_s (where Q_b is at the propeller speed). Water brake losses with an empty water brake were neglected in the study.

The torque equation with a water brake is:

$$2\pi I \frac{dn}{dt} = Q_d - Q_b - Q_f - Q \ ,$$

where I = drive train moment of inertia with turbine or turbines and water brake ($I = I_{1\,b}$ for one turbine and the water brake, $I = I_{2\,b}$ for two turbines and the water brake) (Table 1). The sign of the propeller torque, Q, changes to a negative value when the combination of n and V_p results in a σ of 0.64 or less. The sign of Q is negative over almost the entire dynamic braking phase.

- Reverse Clutching Deceleration. After an interval involving coast down with or without dynamic braking, the forward clutches are disengaged and the reverse clutches are engaged. Clutch slipping (with rapid shaft deceleration) occurs until clutch "lockup," and finally a full reversal of the propeller, takes place.

Reverse clutching deceleration involves a derivation of the clutch equations for the reversing reduction gear of the "Falk" type.

The torque equations with clutching are treated in the next section.

CLUTCHING EQUATIONS

The amount of torque that the clutch can pass without slipping is a function of the number of paralleled clutches, the type of clutch, and the net air pressure used to engage the clutch. The maximum clutch torque capability, Q_C, for 35-inch-diameter clutches is given by:*

$$Q_C = 4550\ p_{net} \text{ (both turbines, 16 clutches)} \quad \text{(lb-ft)}$$

$$Q_C = 2275\ p_{net} \text{ (single turbine, 8 clutches)} \quad \text{(lb-ft)} ,$$

where p_{net} = net air pressure activating the clutch (psi).

The clutch glands which expand the clutch shoes to make contact with the clutch face expand inwardly against the centrifugal force of the rotating clutch assembly. Consequently, the air pressure, p_c, required to counteract this force subtracts from the supply pressure. Thus, the net air pressure to the clutch glands is

$$p_{net} = p_s - p_c \quad \text{(psi)} .$$

The supply pressure, p_s, typically increases for inflation at the rate of 5 psi per sec and decreases on deflation at 30 psi per sec. Thus, for a typical supply pressure of 150 psi and with t in seconds,

$$p_s = 150 - 30\ t \quad \text{(deflation supply pressure, psi)}$$

$$p_s = 5\ t \quad \text{(inflation supply pressure, psi)} .$$

The pressure, p_c, required to counteract centrifugal force is given by

$$p_c = 5 + (5.9 \times 10^{-5})\ N_g^2 ,*$$

where N_g = speed (rpm) of the gland pinion.

*Data on the clutches and reduction gear were supplied by the Falk Corporation via an unpublished memorandum.

But

$$N_g = 60\ nk_3\ ,$$

where

n = propeller speed (rps)

k_3 = forward low-speed pinion gear ratio (4.3197) .

Thus, p_c in terms of n is

$$p_c = 5 + 4\ n^2\ .$$

Combining the equations gives (for the combined plant):

$$Q_C = 4550\ (5\ t - 5 - 4\ n^2) \qquad \text{(clutch engaging equation)}$$

$$Q_C = 4550\ (145 - 30\ t - 4\ n^2) \qquad \text{(clutch disengaging equation)}\ .$$

During a reversing maneuver, the turbine is brought to an idle condition and the "ahead" clutch disengagement and the "reverse" clutch engagement begin. Figure 23 shows the shaft speeds on the reduction gear during reversing. The clutch control system with the typical rates given above prevents simultaneous engagement of both clutches.

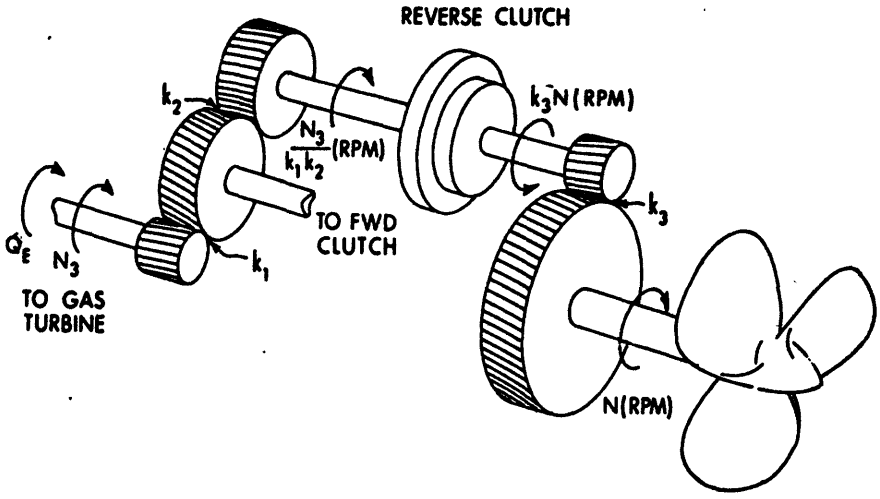

Figure 23 - Reverse Clutch Engaging
(Showing one turbine and one drive section only)

REVERSING EQUATIONS

In reversing (assumed from 31 knots with both gas turbines) both turbine fuel commands are decreased to idle and the engine and propeller torque fall off rapidly. Since the forward clutch is being disengaged and the reverse clutch is being engaged during the reversing maneuver, the clutch torque is:

$$Q_{CR} = 4550\ (5\ t - 5 - 4\ n^2) \qquad \text{(reverse clutch torque)}$$

$$Q_{CF} = 4550\ (145 - 30\ t - 4\ n^2) \qquad \text{(forward clutch torque)}\ .$$

The clutch signals are supplied by the FWD/REV clutch control from commands issued by the start-stop-reverse sequencer, Figures 11 and 12.

During the coast down phase with both turbines engaged, the torque equation as discussed previously is

$$2\pi I_2 \frac{dn}{dt} = Q_d - Q_f - Q\ ,$$

where I_2 = total drive train inertia (referred to the propeller shaft) with both turbines and all forward clutches engaged (Appendix A and Table 1).

Starting at t = 0 (the beginning of the coast down phase), the program solves the equation for Q_{CF} involving n by a solution of the ship-propulsion equations.

When

$$|k_3\ Q_{CF}| < |Q|\ , \qquad t = t_D \quad \text{(forward clutch disengages)}$$

where t_D = declutching time.

Note that this definition of clutch disengagement is adequate but not exact; it assumes the clutch disengages when it starts to slip and that disengagement once begun is immediate.

During the open clutch-reclutching phase, two torque equations are required because of the uncoupled gas-turbine and propeller systems whose speeds and inertias are now both different. The propeller and gas-turbine torque equations in the interval between opening the forward clutch and lockup of the reverse clutch are now:

$$2\pi I_{2p} \frac{dn}{dt} = 4550 (5t - 5 - 4n^2) k_3 - \frac{Q_f}{2} - Q \quad \text{(propeller torque equation)},$$

where I_{2p} = open drive train moment of inertia (referred to the propeller shaft) (Appendix A and Table 1).

$$2\pi I_{2T} \frac{dn_T}{dt} = Q_E - \frac{Q_f}{2k_g} - \frac{4550}{k_1 k_2} (5t - 5 - 4n^2) \quad \text{(gas-turbine torque equation)},$$

where

$n_T = N_3/60$ (turbine speed, rps)

I_{2T} = open drive train moment of inertia on gas-turbine shaft (referred to turbine shaft) (Appendix A and Table 1).

Table 1
Drive Train Moments of Inertia

Condition	I (symbol)	I, lb-ft-sec^2
One engine only	I_1	1.79×10^5
Two engines	I_2	2.88×10^5
One engine and water brake*	I_{1b}	1.79×10^5
Two engines and water brake*	I_{2b}	2.88×10^5
Two engines with open drive (propeller side)	I_{2p}	0.71×10^5
Two engines with open drive (turbine side)	I_{2T}	1.05×10^3
One engine with open drive (propeller side)	I_{1p}	0.71×10^5
One engine with open drive (turbine side)	I_{1T}	0.53×10^5

*The water brake inertia is negligible relative to the drive train.

It is important to note that the above two equations are correct only in the interval,

$$t_L > t > t_D \ ,$$

where

t_L = clutch lockup time at reverse clutch lockup

t_D = declutch time at declutch of forward clutch.

For $t < t_D$, the term $(5\,t - 5 - 4\,n^2)$ has no meaning because it is negative which simply means the air pressure is not high enough to engage the reverse clutch. Thus, for all values $(5\,t - 5 - 4\,n^2) \leq 0$, the computer program interprets this term as zero. During this phase then, the gas turbines and propellers are freewheeling into an open drive train and their rates of deceleration are independent of each other.

The frictional torque, Q_f, is simplified by splitting it in half between both drive trains.

The reverse clutch engages when

$$Q_{CR} > 0 \qquad t = t_E \ .$$

Clutch energy dissipation begins from time, t_E, until lockup at t_L.

During this phase there is a slip speed across the clutch; when the slip speed becomes zero, this is defined as clutch "lockup." The slip speed across the clutch is

$$N_{SLIP} = k_3 N - \left(\frac{-N_3}{k_1 k_2}\right) \ ,$$

where N = propeller speed (rpm), and $k_3 N$ is defined in the positive direction as shown.

Note that when $N_{SLIP} = 0$, the clutch pinion speed is the same on both sides of the clutch, and the propeller speed is

$$N = \frac{-N_3}{k_1 k_2 k_3} = \frac{-N_3}{k_g k_2} \approx \frac{-N_3}{10} \ .$$

Thus, lockup time, t_L, is defined as follows (assuming t = 0 at the start of the reversing maneuver):

$$t = t_L \quad \text{when} \quad N_{SLIP} = 0 \quad \text{or} \quad N \approx \frac{-N_3}{10} .$$

During this braking phase (depending on initial speed), the gas turbines may be slowed to a complete stop and then be driven backward by the water milling propeller. The propeller is correspondingly stopped or driven in reverse. Most of the braking torque on the gas-turbine side comes from the large kinetic energy of the turbine, since the near-idling or idling fuel-rate provides little opposing torque.

The clutch torques are shown as a function of time in Figure 24 for a typical reversing maneuver.

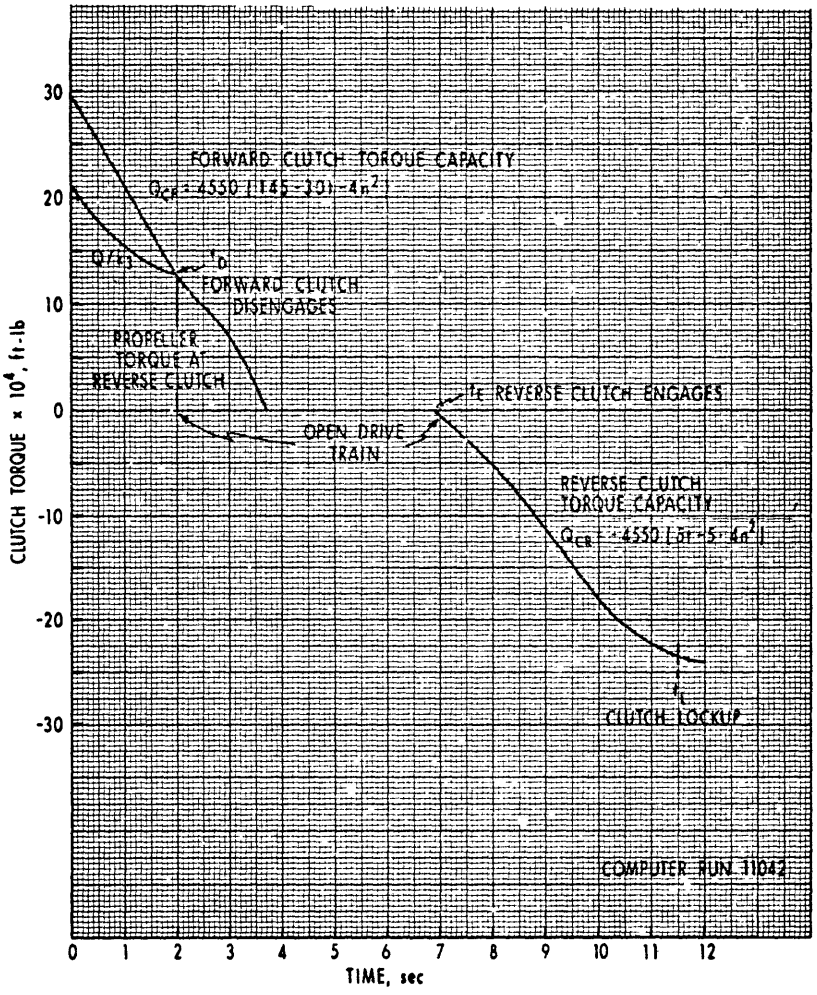

Figure 24 - Clutch Torques Versus Time (for Reverse Clutching Deceleration from 31.3 Knots)

It can be shown very readily that the kinetic energy of the rotating gas turbine and the reduction gear on the gas-turbine side is in excess of the kinetic energy of the rotating elements on the propeller side of the clutches.

The turbine kinetic energy, E_T, at a speed, ω_T, is

$$E_T = 1/2\ I_T\omega_T^2 = 1/2\ I_T \left(\frac{2\pi N_3}{60}\right)^2 \qquad \text{(ft-lb)} \ ,$$

where

$$\omega_T = \frac{2\pi N_3}{60} \qquad \text{(turbine angular speed, radians/sec)} \ .$$

The propeller side of the drive train kinetic energy, E_P, at a speed, ω_P, is

$$E_P = 1/2\ I_P\omega_P^2 = 1/2\ I_P \left(\frac{2\pi N}{60}\right)^2 \qquad \text{(ft-lb)} \ ,$$

where

$$\omega_P = \frac{2\pi N}{60} \qquad \text{(propeller angular speed, radians/sec)} \ .$$

Thus, the ratio of turbine to propeller kinetic energy is

$$\frac{E_T}{E_P} = \frac{I_T}{I_P} \left(\frac{N_3}{N}\right)^2 \ .$$

At the start of a reversing maneuver this ratio is independent of speed since $N_3 = k_g N$, and this ratio becomes

$$\frac{E_T}{E_P} = \frac{I_T}{I_P}\ k_g^2 = \frac{1050}{70,500} \times 206.2 = 3.07 \quad \text{(for the two-turbine case)} \ .$$

After the forward clutch disengages, N_3 is independent of N and at reverse clutch engagement (for the 31.3-knot case, Computer Run 11042), the ratio is

$$\frac{E_T}{E_P} = \frac{I_{3T}}{I_{3P}} \left(\frac{N_3}{N}\right)^2 = \frac{1050}{70,500} \left(\frac{2670}{160}\right)^2 = 4.16 \ .$$

The kinetic energy of the turbine is used to overcome the kinetic and water milling energy of the propeller in stopping the propeller rotation. This total energy is dissipated in the reversing clutch during the r eversing maneuver. The power absorbed by the clutches during the braking maneuver is

$$P_C = \frac{N_{SLIP}\, Q_{CR}}{5252} \Bigg|_{t = t_E}^{t = t_L} \qquad \text{(hp)}$$

$$P_C = \frac{\left(k_3 N + \frac{N_3}{k_1 k_2} \right) 4550\ (5\ t - 5 - 4\ n^2)}{5252} \Bigg|_{t = t_E}^{t = t_L} .$$

The total energy absorbed in the interval between clutch engagement and lockup is given by the time integral of the absorbed clutch power

$$E_C = 550 \int_{t = t_E}^{t = t_L} P_C\, dt \qquad \text{(ft-lb)} .$$

Note that for the calculations in reversing from a one-turbine condition (base plant only), the previous equations are changed only in the replacement of 2275 for 4550 everywhere this constant occurs and change to the appropriate moments of inertia.

DYNAMIC BRAKING EQUATIONS

The propeller speed can be brought down quickly from some large value during the coast down phase by dynamic braking. Depending on the prime mover and transmission system, dynamic braking is accomplished by electric power dissipation (with electric drive), clutches (reversing gear), air compression (diesel engine), or with a water brake. A water brake was investigated in this study with the characteristics shown in Figure 13.

During dynamic braking, the power delivered by the drive train must be equal to the power absorbed by the braking system and the losses. Since the drive train with its large inertia is being decelerated rapidly, there is a large "transient inertial horsepower" due to the shaft and propeller speed deceleration as well as a rotational power. Thus,

$$P_{(\text{rotational})} + P_{(\text{inertial})} = P_{(\text{brake})} + P_{(\text{windage})} + P_{(\text{friction})} \quad \text{(horsepower)}.$$

Referred to shaft speed, N, the corresponding terms in this equation are:

$$\frac{NQ}{5252} + 2 \times 10^{-6}\ IN\ \frac{dN}{dt} = \frac{1}{5252}\left[Q_b N + Q_w N + Q_f N\right] .$$

The windage torque, Q_w, was not explicitly defined in the torque summation previously discussed, since it is lumped with the engine torque, Q_d. That is, when Q_d goes negative, $Q_d = Q_w$. The sign of all the terms on both sides of the braking equation is considered positive.

The inertial power term can be derived from the kinetic energy of the drive train, E.

$$E = 1/2\ I\omega^2 ,$$

where

I = drive train inertia referred to propeller speed (lb-ft-sec^2)

ω = angular speed of propeller (radians/sec).

$$\text{Power} = P = \frac{1}{550}\ \frac{dE}{dt} = \frac{I\omega}{550}\ \frac{d\omega}{dt} \quad \text{(horsepower)} .$$

In terms of shaft speed, N (rpm), since $\omega = 2\pi N/60$,

$$P = \frac{4\pi^2}{(550)(60)(60)}\ IN\frac{dN}{dt} = 2 \times 10^{-6}\ IN\ \frac{dN}{dt} \quad \text{(horsepower)} .$$

An example of the magnitudes involved in the braking equation is available from a typical computer run (10151) discussed in greater detail later. This is a ship coast down from 24.8 knots with dynamic braking. The water brake is filled along a 6-second time ramp, and the results are shown in Figures 39 and 41. Thus, at t = 4 seconds after the fuel flow rate idling command is given, the following conditions prevail:

$t = 4$ sec	$Q = 110.1 \times 10^3$ lb-ft	$N = 107.8$ rpm
$N_3 = 1550$ rpm	$I = 1.79 \times 10^5$ lb-ft-sec^2	$Q_w = 1.59 \times 10^3$ lb-ft
$Q_f = 10.63 \times 10^3$ lb-ft	$\frac{dN}{dt} = -25.9$ rpm/sec	$Q_b = 18,000$ lb-ft .

At 4 seconds, the water brake torque is 2/3 of the fully effective torque at 6 seconds when the water brake is completely filled.

Substituting these values into the braking equation and rounding off to the nearest 10 hp gives

$$P_{(rotational)} + P_{(inertial)} = P_{(brake)} + P_{(windage)} + P_{(friction)}$$

$$2260 + 9980 = 11,990 + 30 + 220$$

The windage horsepower is small for this condition because of the low turbine speed, N_3 (1550 rpm) where the windage torque is almost zero. When braking from 31 knots, the windage horsepower term is somewhat in excess of 2000 horsepower.

A large part of the power required in slowing the propeller is to overcome the kinetic energy lost by the propeller and drive train, especially at the beginning of the braking period. At the end of the braking period where shaft deceleration becomes small, the $P_{(inertial)}$ term approaches zero.

The water brake torque, Q_b, at the propeller shaft is computed from the stored map of water brake power versus free turbine speed, N_3. For reverse clutching deceleration with dynamic braking, the water brake torque is set equal to zero at Time t_D when the forward clutch disengages.

ACCELERATION PERFORMANCE

A number of open-loop acceleration runs with fuel flow rate, W_f, as the ordered variable were made. The results are summarized in Table 2 and the major variables are plotted in Figures 25 through 30.

Table 2 - Acceleration Performance

Computer Run	Fuel Ramp sec	Maximum Ship Speed knots	t_{AV} sec	S_{AV} ft	Condition
10233	0	14.8	128.0	1800	Base turbine only
10211	0	20.0	97.1	1830	Base turbine only
10071	0	24.8	78.0	1792	Base turbine only
11142	10	24.8	80.0	1792	Base turbine only
10141	0	24.8-31.3	20.1	890	Boost turbine added from maximum base plant speed
10261	0	32.0	53.0	1470	Both turbines simultaneously (maximum power)
10291	10	32.0	55.0	1474	Both turbines simultaneously (maximum power)
10301	20	32.0	59.6	1490	Both turbines simultaneously (maximum power)
10302	30	32.0	65.0	1548	Both turbines simultaneously (maximum power)

t_{AV} - time to reach 90% of final ship speed
S_{AV} - head reach at t_{AV}

Several fuel flow ramps were used, and a 0-second ramp is the maximum fuel flow acceleration rate shown in Figure 33 (see page 72). For example, a 10-second ramp means the normal maximum fuel flow rate acceleration multiplied by a ramp which rises at the rate of 10% per second. For speeds up to 24.8 knots, only the base turbine was used in the simulation. To reach 31.3 knots from a top base plant speed of 24.8 knots (limiting the base turbine to W_f = 10,500 lb per hr and P_{ENG} to 20,000 hp), the boost engine was added with a fuel flow rate of 12,100 lb per hr, corresponding to 25,000 hp for the boost turbine. This run (10141) is particularly interesting because it shows the boost capability situation, i.e., the response to an order to reach top speed from a cruising condition after the idling boost turbine is put on the line.

Crash acceleration runs (1 to 32 knots) were made under the condition of maximum power delivered by both turbines (W_f = 12,100 lb per hr fuel

flow rate for each turbine) and for several fuel ramp rates. All the acceleration runs indicate that the propeller torque, speed, and thrust are extremely fast in buildup and closely follow the rate of change of the fuel flow rate even for the relatively large drive train inertia for this ship. These three variables reach most of their final excursions within 10 seconds after the fuel flow rate order is given for a 0-second ramp. The gas turbine has sufficient torque to rapidly accelerate the shaft and results in large overtorques relative to the steady-state values. To control the overtorques and overthrusts on the propeller shaft, several runs with a ramped fuel flow rate were made. These are discussed later.

The transient engine torque during all the acceleration runs was computed. A plot of the engine torque, Q_E, during an acceleration transient plotted as a function of engine speed, N_3, and time is shown in Figure 31. The plot in this figure which reaches the higher peak torque is for an acceleration run from 1 to 24.8 knots on the base plant with an ordered fuel flow rate of 10,500 lb per hr at the maximum acceleration rate. The second plot showing a lower peak engine torque is for the same condition except that the total drive train inertia was decreased by half. The situation with the higher moment of inertia is the case for this ship where the reversing reduction gear approximately doubles the drive train inertia over the typical nonreversing gear. Halving the inertia of the drive train decreases the peak engine torque by about 12%. In both cases the peak engine torque occurs at about 5 seconds after the fuel flow rate command is given, and this corresponds to the time peak fuel flow rate is reached.

The transient engine torque characteristic (Figure 31) increases rapidly from an idling fuel-flow rate of 1600 lb per hr, reaches a peak, and then decreases along a line of constant ordered fuel flow of 10,500 lb per hr as the engine speed increases and finally reaches the steady-state torque line in about 200 seconds. The excess torque between the transient and steady-state values in the torque speed plane is used to accelerate the shaft and ship to the new steady-state speed.

The corresponding engine power, P_{ENG}, during the acceleration transient from 1 to 24.8 knots is shown in Figure 32. In this figure the transient engine power is shown as a function of both engine speed, N_3, and time. The lower curve corresponds to an acceleration from 1 to 24.8 knots, and the upper curve is for the boost turbine where a fuel flow rate of 12,100 lb per hr was ordered for the boost turbine to bring the ship speed from 24.8 to 31.3 knots. The excess engine power between the transient and steady-state conditions at 200 seconds is used in accelerating the shaft and the ship to the new steady-state value(s).

System performance was investigated using a fuel-flow ramp to control the rate of change of the fuel-flow rate for fuel ramps from 0 to 40 seconds in length. The minimum time to achieve a maximum fuel-flow rate is approximately 5 seconds, as shown in Figure 18. This was defined

as the 0-second ramp (which would be a step function). Additional ramps from 10 to 40 seconds were obtained by multiplying the zero-ramp, fuel-flow rate times a linear ramp with a time base from 10 to 40 seconds. The fuel ramps are shown in Figure 33.

A fuel ramp of 10 seconds produces only a 2-second increase in the time to reach 90% of ordered speed for the crash acceleration case (1 to 32 knots) and essentially no difference in head reach. A fuel ramp of 20 seconds increases the acceleration time and head reach by about 7 seconds and 20 feet, respectively. For acceleration from 1 to 24.8 knots, the 10-second ramp increases the acceleration and head reach by 2 seconds and 0 feet, respectively. These results are summarized in Table 2.

While the effect of fuel ramps of as long as 20 seconds has a relatively insignificant effect on ship acceleration time, there is a pronounced effect on engine and shaft peak torque. Table 3 and Figure 33 summarize the effects of thrust and torque during acceleration for varying fuel ramp lengths.

Table 3
Peak Torques and Thrust on the Shaft
during Acceleration Transients

Computer Run	Fuel Ramp sec	Ship Speed knots	Q_d (peak) lb-ft x 10^3	t at Q_d (peak) sec	Q_{ds} lb-ft x 10^3	$\frac{Q_d \text{ (peak)}}{Q_{ds}}$	$\frac{Q_d \text{ (peak)}}{Q_{ds}(max)}$	T (peak) lb x 10^3	t at T (peak) sec	T_S lb x 10^3	$\frac{T \text{ (peak)}}{T_S}$	$\frac{T \text{ (peak)}}{T_S(max)}$
10233	0	14.8	287	3.6	179	1.60	0.29	90	27.0	62	1.44	0.25
10211	0	20.0	576	4.0	329	1.75	0.58	169	23.0	117	1.44	0.47
10072*	0	24.8	786	4.7	523	1.50	0.80	273	19.0	189	1.45	0.76
10071	0	24.8	890	4.7	523	1.70	0.90	269	20.0	189	1.43	0.75
11132	10	24.8	703	10.0	523	1.34	0.72	269	21.4	189	1.42	0.75
11151	20	24.8	660	20.0	523	1.26	0.67	269	26.2	189	1.42	0.75
10141	0	24.8-31.3	1085	5.0	918	1.18	1.10	355	13.0	334	1.06	0.99
11041	0	32.0	1850	5.0	985		1.88	508	16.3	359		1.42
11072	10	32.0	1361	10	985		1.38	507	18.3	359		1.41
11081	20	32.0	1258	20	985		1.28	500	22.9	359		1.39
11084	30	32.0	1204	30	985		1.22	449	33.2	359		1.25
11086	40	32.0	1166	40	985		1.18	435	43.4	359		1.21

*The drive train inertia is half that of Computer Run 10071.

Q_d (peak), T (peak) - peak values of shaft torque and thrust during acceleration
Q_{ds}, T_S - steady-state values of torque and thrust after 200 seconds of acceleration
Q_{ds} (max), T_S)max) - steady-state values of torque and thrust at 32 knots
(Q_{ds} (max) = 985 lb-ft, T_S (max) = 359 lb)

The ratio of peak torque, $Q_{d(peak)}$, to the steady value, Q_{ds}, varies from 1.60 to 1.75 for three comparable zero fuel ramp computer runs (10233, 10211, and 10071). This torque ratio indicates by how much the peak torque exceeds the final steady-state value at a particular speed. A second ratio, $Q_{d(peak)}/Q_{ds(max)}$, indicates the torque ratio relative to the torque at 32 knots.

A zero fuel ramp with ship acceleration from 1 to 32 knots produces the largest $Q_{d(peak)}/Q_{ds(max)}$ ratio of 1.88. This ratio decreases rapidly with fuel ramp length to 1.28 at a ramp length of 20 seconds. Increasing the fuel ramp further provides only a small decrease in the torque ratio while increasing the ship acceleration time.

Performance comparing torque ratio for acceleration to 24.8 knots is also shown in Figure 33 and Table 3. This graph and table also compare the effect of shaft thrusts for various conditions of acceleration and fuel ramp lengths. It is interesting to note that for a 0-second ramp, the ratio of peak thrust to steady-state thrust, $T_{(peak)}/T_S$, is essentially the same at about 1.44 for all comparable conditions of acceleration.

A fuel-flow ramp has a minor effect on the thrust ratio. For a 20-second fuel ramp there is a very slight difference in the thrust ratio from the 0-second ramp case for acceleration from 1 to 32 knots. For acceleration from 1 to 24.8 knots, the thrust ratio is constant at 0.75 and is independent of ramp length.

The propeller second modified advance coefficient for the acceleration from 1 to 24.8 knots with a zero fuel ramp time goes from 0.905 at 1 second to about 0.990 in 10 seconds and comes back down to 0.779 in 200 seconds where steady state is reached. This behavior is indicated in Figure 34, showing the propeller thrust coefficient, C_T, versus the second modified advance coefficient, σ.

The steady-state values for all the computer runs were established at 200 seconds where further changes in the variables were no longer significant. These steady-state values were used for all comparisons and constitute the specifications for the "standard ship" used in this study. Table 4 gives the steady-state parameters, and the major ones are plotted in Figure 35.

Table 4
Steady-State Conditions
(at end of 200-second acceleration runs)

Computer Run	Q_d lb-ft $\times 10^3$	σ	V knots	W_f lb/hr $\times 10^3$	T lb $\times 10^3$	P_{ENG} hp $\times 10^3$	Q lb-ft $\times 10^3$	N rpm	N_3 rpm	Q_E lb-ft $\times 10^3$	R_T lb $\times 10^3$	S ft $\times 10^3$	Q_f lb-ft $\times 10^3$
11043	115	0.774	11.3	2.50	39	2.0	105	93.5	1340	8.0	32	2.58	8.9
10233	179	0.772	14.8	4.00	62	4.0	167	118.6	1700	12.5	55	3.54	11.5
11044	239	0.773	17.2	5.00	84	6.2	225	137.2	1970	16.6	75	4.30	13.5
10211	329	0.777	20.0	6.56	117	10.0	312	159.6	2290	22.9	105	5.21	16.1
11051	429	0.776	23.1	8.50	154	15.0	410	183.9	2640	29.8	141	6.13	18.7
10071	523	0.779	24.8	10.50	189	20.0	503	201.1	2890	36.4	174	6.81	20.3
11052	677	0.778	28.0	16.55	245	29.7	653	230.5	3370	47.0	230	9.31	23.3
10141	918	0.782	31.3	22.60	334	46.5	891	265.9	3820	63.9	333	10.35	27.0
10261	985	0.784	32.0	24.20	359	51.4	956	274.1	3940	68.6	362	9.36	27.8

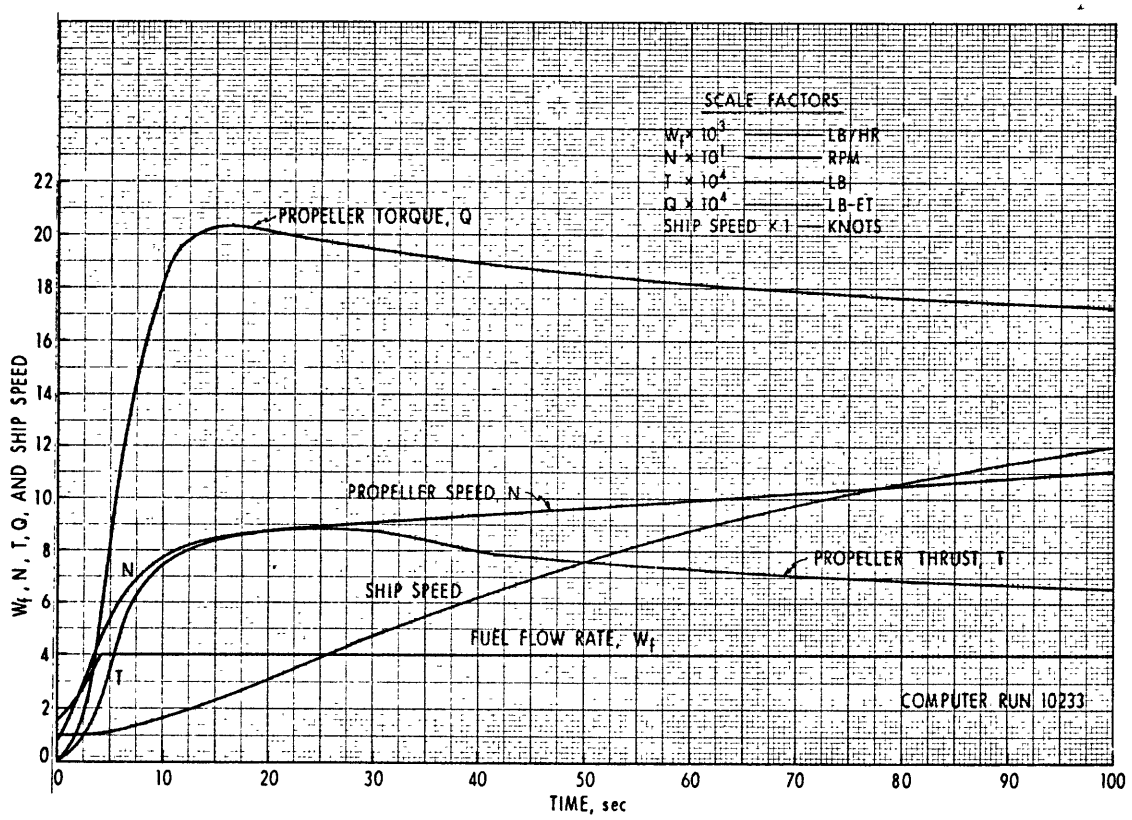

Figure 25 - Acceleration (1 to 14.8 Knots)
(Maximum Acceleration on Base Turbine
with Ordered Fuel Flow Rate of 4000 Lb per Hr)

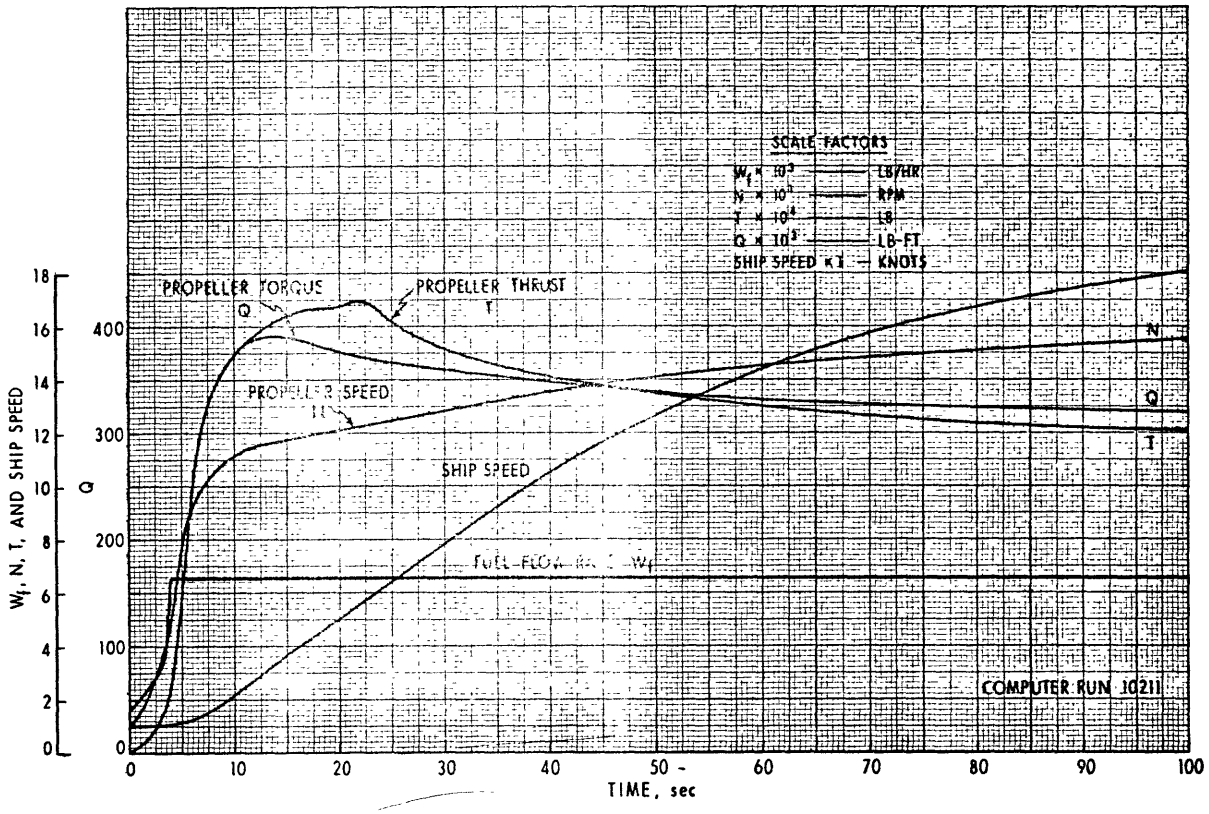

Figure 26

Acceleration (1 to 20 Knots)
(Maximum Acceleration on Base Turbine
with Ordered Fuel Flow Rate of 6560 Lb per Hr)

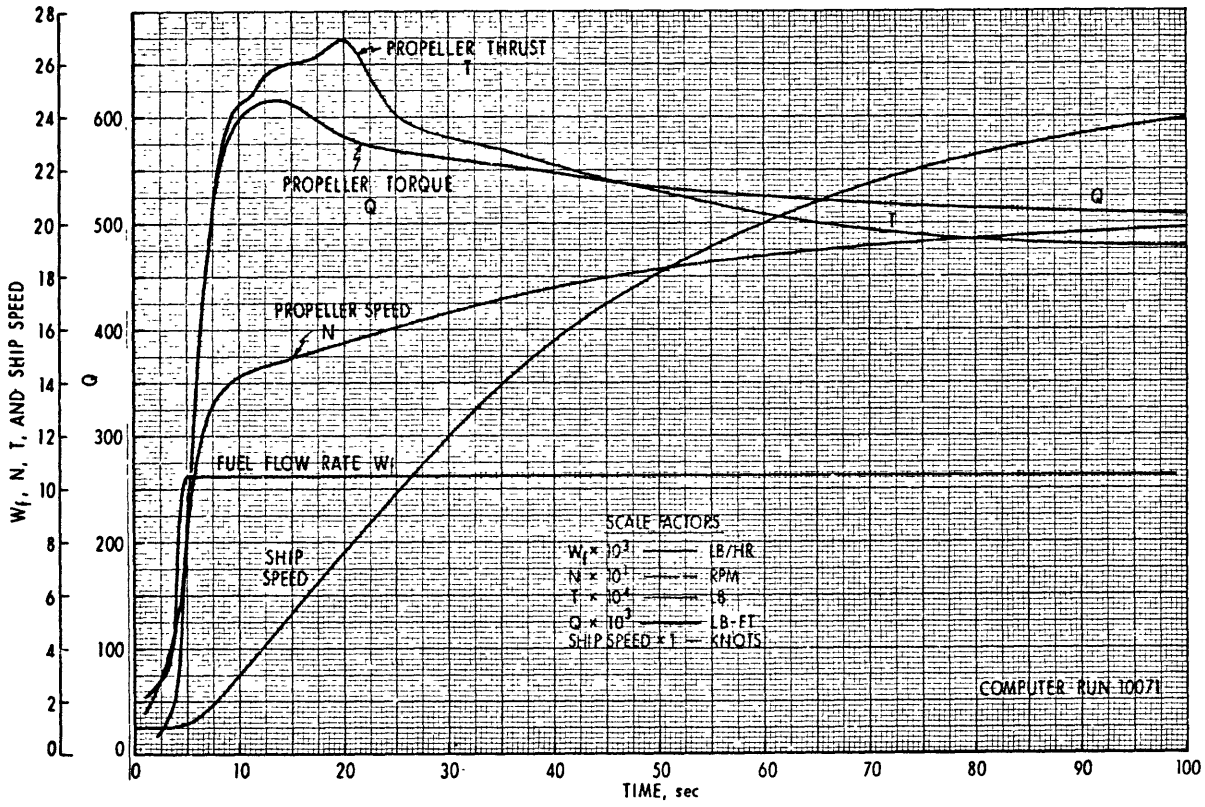

Figure 27

Acceleration (1 to 24.8 Knots)
Base Engine Only
(Maximum Acceleration on Base Turbine
with Ordered Fuel Flow Rate of 10,500 Lb per Hr)

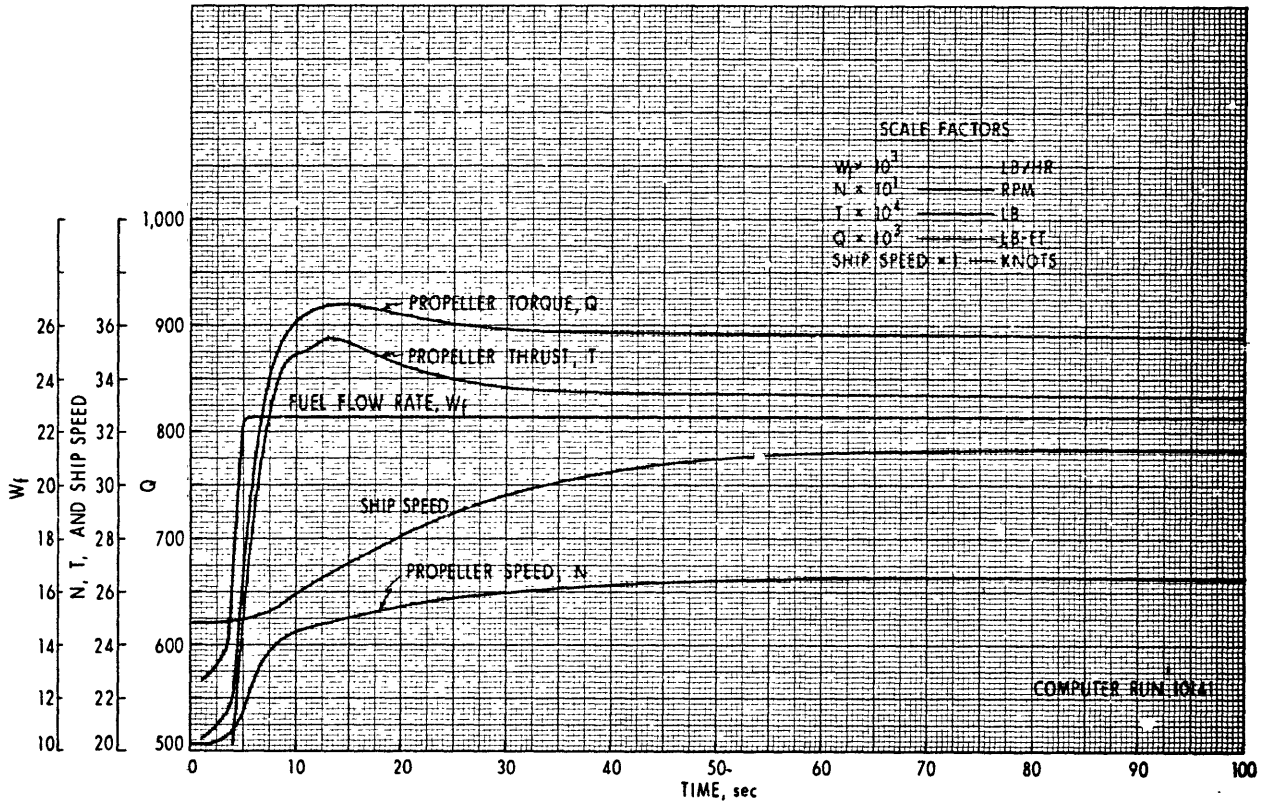

Figure 28

Acceleration (24.8 to 31.3 Knots)
Base and Boost Engines
(Maximum Acceleration on Boost Turbine
with Ordered Fuel Flow Rate of 12,100 Lb per Hr;
Base Turbine at 10,500 Lb per Hr)

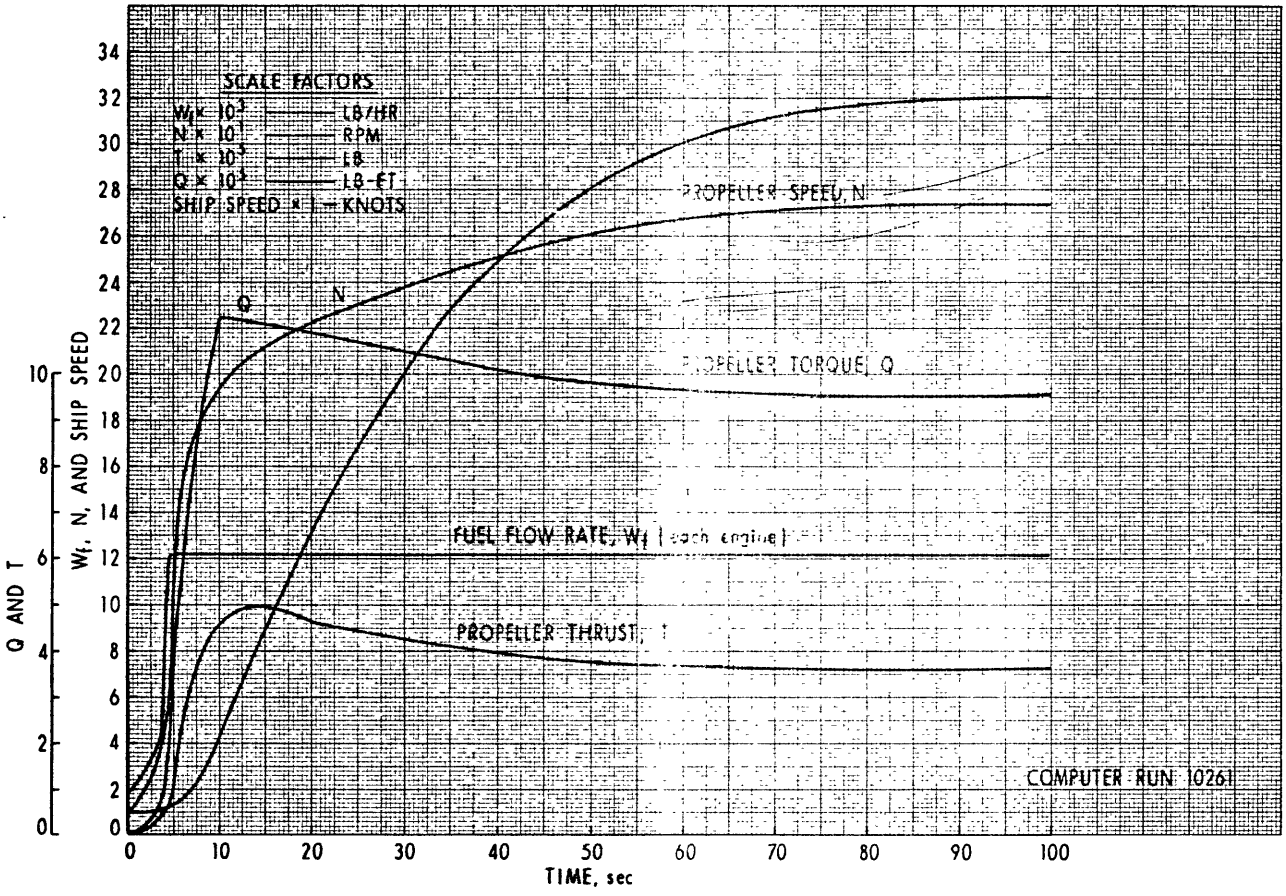

Figure 29

Acceleration (1 to 32 Knots)
(Maximum Acceleration on Both Turbines
with Ordered Fuel Flow Rate of 12,100 Lb per Hr Each Ship Speed)

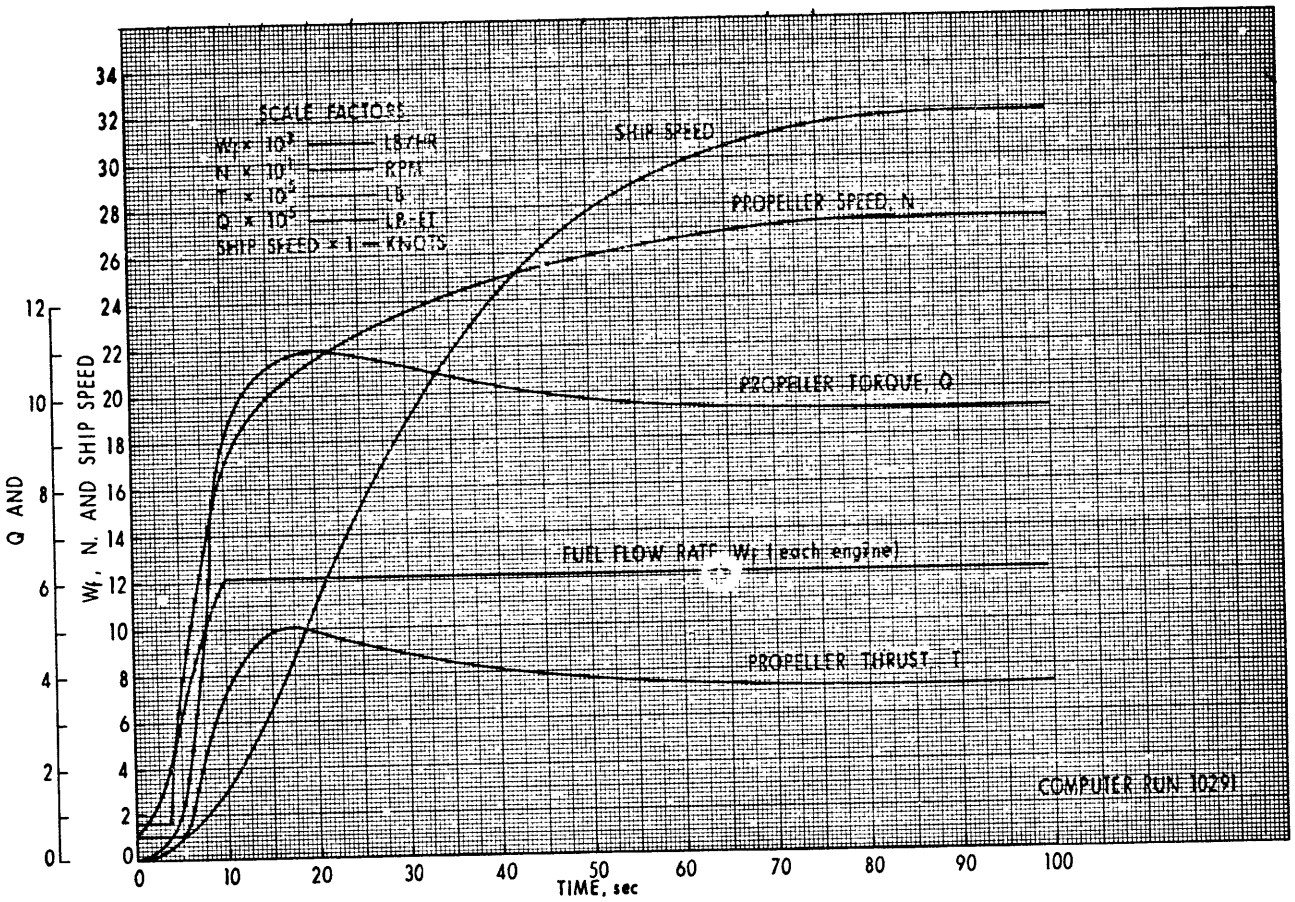

Figure 30

Acceleration (1 to 32 Knots)
(10-Second Fuel Ramp on Both Turbines
with Ordered Fuel Flow Rate of 12,100 Lb per Hr Each)

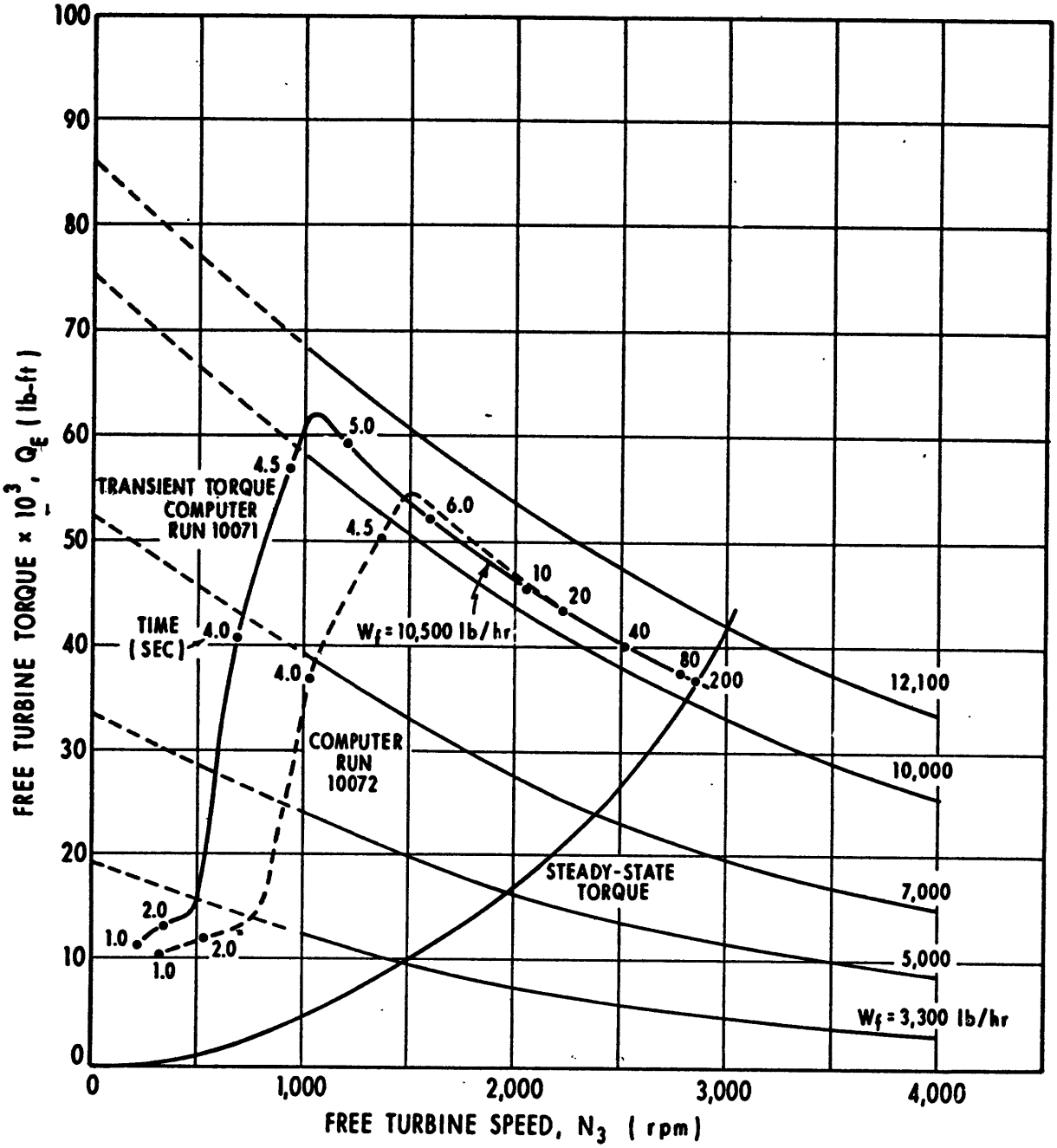

Note: Dashed curve is for drive train inertia, I, of half of solid line inertia.

Figure 31
Transient and Steady-State Engine Torque Versus Engine Speed
(for Single Engine Maximum Acceleration Maneuver, W_f = 10,500 Lb)

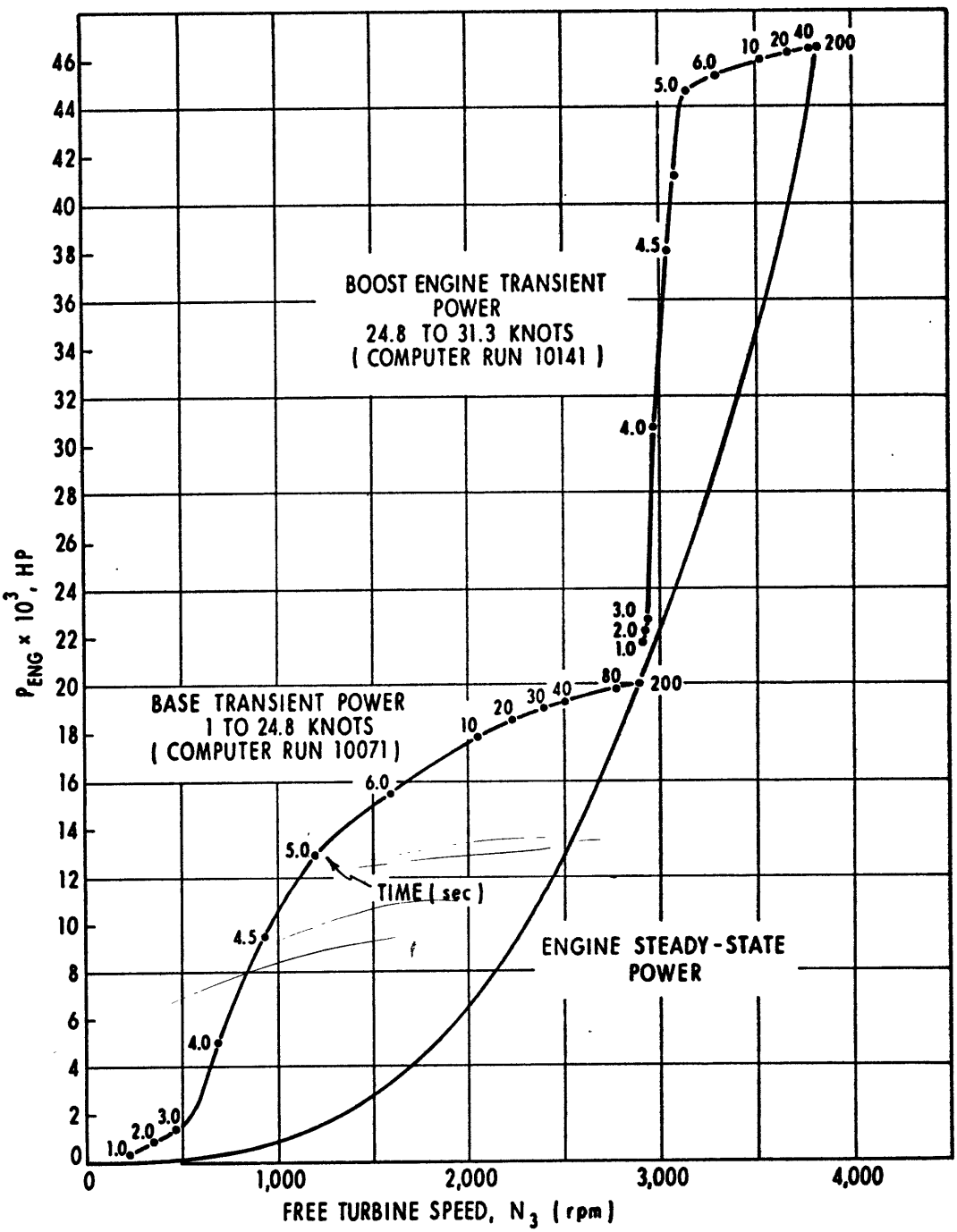

Figure 32 - Transient and Steady-State Engine Power Versus Engine Speed

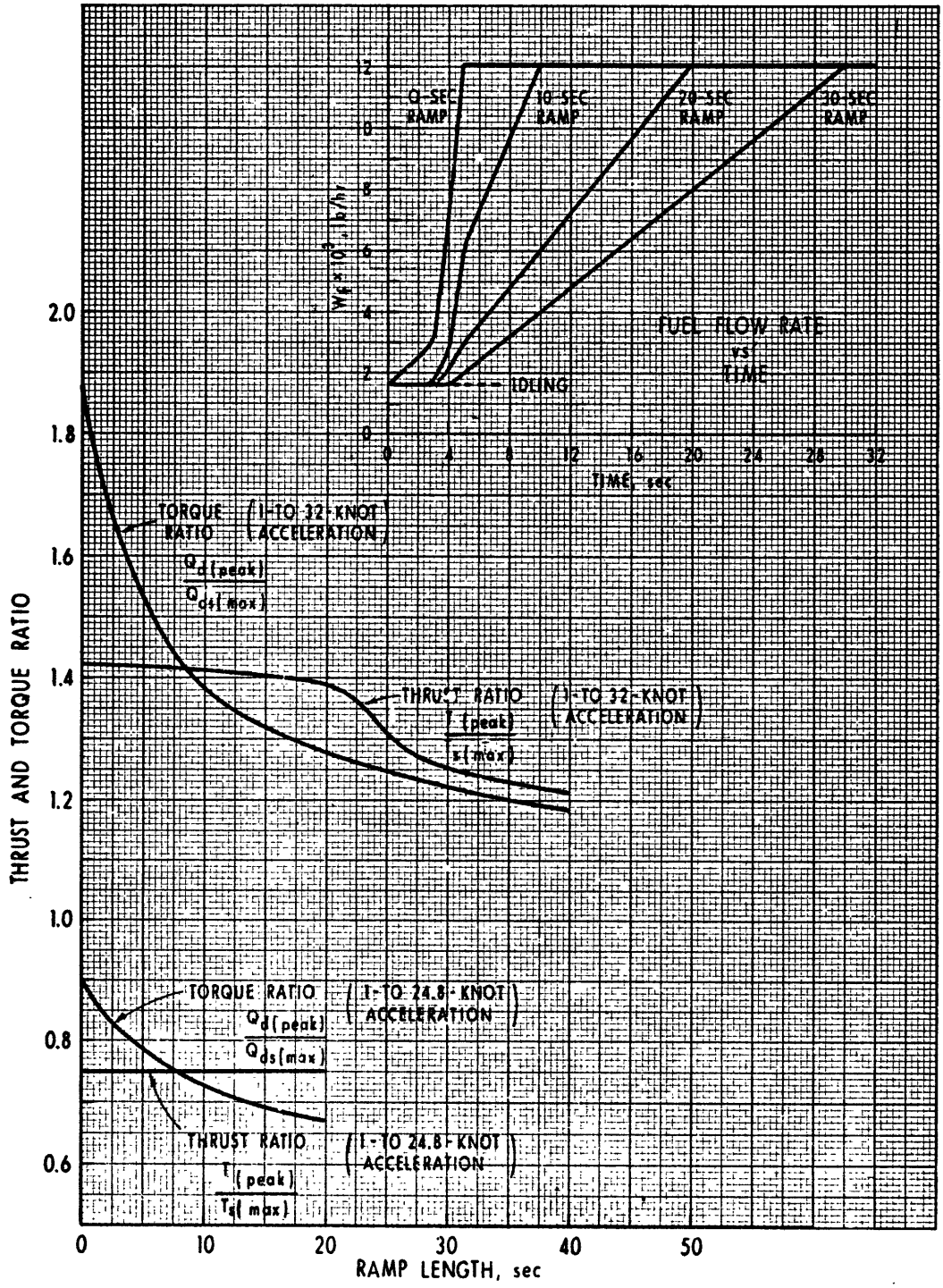

Figure 33 - Thrust and Torque Ratio
Versus Fuel Flow Ramp Length

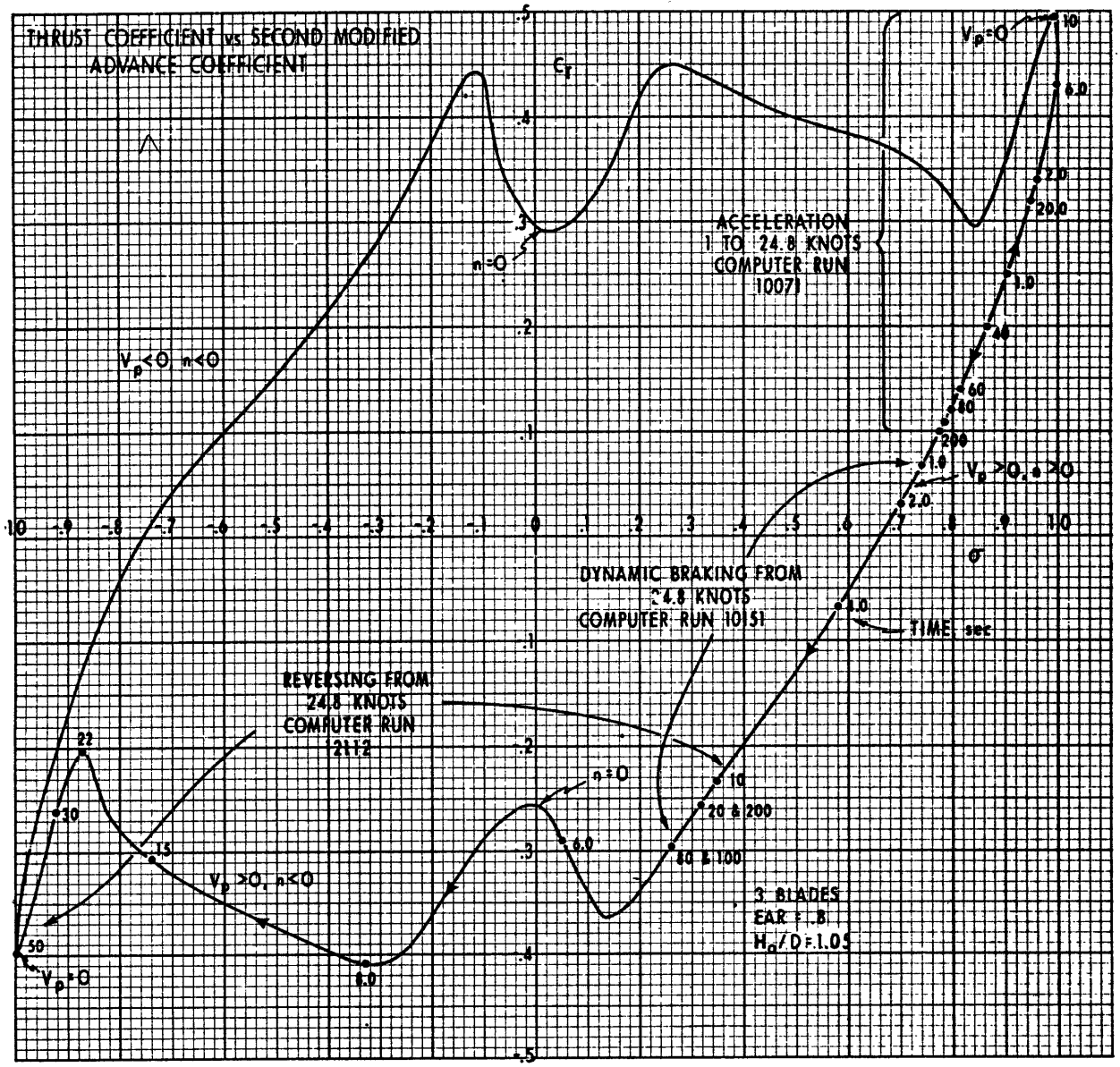

Figure 34 - Locus of C_T and σ with Time for Acceleration and Dynamic Braking

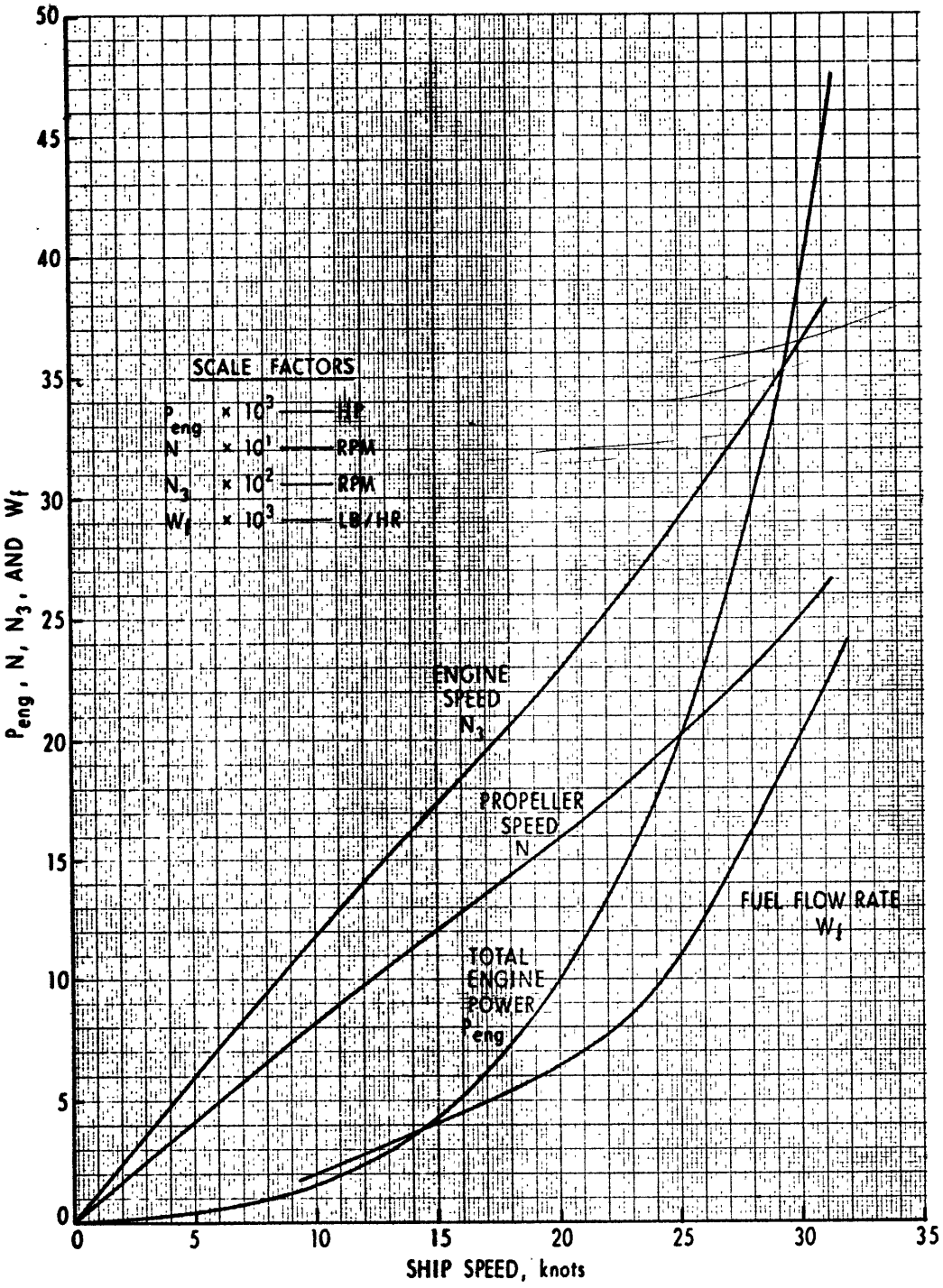

Figure 35 - Total Engine Power, Propeller Speed, Engine Speed, and Fuel Flow Rate Versus Ship Speed (Steady-State Conditions)

DECELERATION AND REVERSING PERFORMANCE

COAST DOWN

Coast down from initial ship speeds of 24.8 and 31.3 knots was investigated with no braking and compared with corresponding conditions with dynamic braking.

Coast down from an initial speed of 24.8 knots and a shaft speed of 201 rpm is shown in Figure 36. For this maneuver, the fuel flow rate, W_f, was ordered to an idling value at the maximum fuel deceleration rate (Figure 18) which brings the fuel rate almost to idling in about 1 second. Propeller speed drops off rapidly for about the first 10 seconds and then decreases much more slowly.

The propeller torque, Q, drops off very rapidly, reaching almost zero in about 10 seconds; whereas the propeller thrust goes negative at about 6 seconds, reaching a small negative peak at 15 seconds.

During all the deceleration and reversing runs, the engine torque map is switched to the idling condition when the fuel flow rate reaches 1600 lb per hr. This torque map includes the windage loss which creates a negative engine torque until the engine speed, N_3, falls below 1500 rpm. Below 1500 rpm the engine torque goes positive slightly. It should be noted that in all the subsequent plots, the propeller hydrodynamic torque, Q, and not the engine torque, Q_d, developed on the shaft are plotted.

The coast down from 31.3 knots with both turbines on the line is shown in Figure 37. In this maneuver the fuel-flow rate for each turbine is brought to the idling condition of 1600 lb per hr.

The propeller deceleration versus propeller speed (phase plane plot) is indicated in Figure 38 for coast down and for several other conditions including braking and clutching deceleration. This figure contains coast downs from 24.8 and 31.3 knots. The deceleration peaks in both cases at about 0.4 second after the throttle idling order is given and decays to almost zero in 40 seconds. The sharp discontinuity at 3 seconds is the increase in deceleration due to free turbine windage torque as the engine torque map changes to the idling fuel flow rate torque when the fuel flow rate reaches 1600 lb per hr.

Table 5 (see page 79) summarizes deceleration performance for coast down and other deceleration maneuvers. For example, the time required for the ship speed to decrease to half the initial speed is 59 and 76 seconds for the 31.3- and 24.8-knot speeds, respectively.

COAST DOWN WITH DYNAMIC BRAKING

Coast down with dynamic braking from 24.8 and 31.3 knots is shown in Figures 39 and 40. The water brake torque is computed from the stored water brake characteristic (Figure 13) and is then multiplied by a ramp function with a 6-second time base to simulate increasing water brake effectiveness as the water brake cavity is filled. At 6 seconds the water brake is 100% effective. The resulting braking torque is then summed with the other torques acting on the propeller shaft to solve the torque equation. The water brake is both time (due to the 6-second ramp) and speed dependent. The torque extracted from the system falls rapidly as the water brake/turbine speed decreases. Figure 41 shows the power absorbed by the water brake for dynamic braking from 24.8 and 31.3 knots.

During dynamic braking the braking equation discussed earlier is satisfied, i.e., there is a power balance between the power delivered by the shaft and the power absorbed by the system. A breakdown of the individual power terms for dynamic braking from 24.8 knots was given earlier where this computer run was used as an example of braking performance.

Figures 39 and 40 indicate that with dynamic braking, a large negative propeller thrust and torque is developed, with peaks occurring at between 6 and 10 seconds after deceleration is begun. The propeller speed falls rapidly from 201 to about 51 rpm in 10 seconds for deceleration from 24.8 knots and from 266 to about 75 rpm for deceleration from 31.3 knots.

The maximum power extracted from the shaft by the water brake is 12,000 and 21,600 hp for deceleration from 24.8 and 31.3 knots, respectively.

Propeller deceleration versus propeller speed with dynamic braking from 24.8 knots is shown in Figure 38. From this figure it can be seen that the deceleration follows the curve for the coast down case with no braking (10142) until about 0.3 second; then the deceleration by the water brake is maintained well in excess of the no-braking deceleration until about 10 seconds.

The relatively large negative propeller thrusts developed during dynamic braking decrease the ship speed in each case by about 5 knots below the normal coast down case at 50 seconds after deceleration is begun.

REVERSE CLUTCHING DECELERATION

Propeller reversing maneuvers accomplished with the reversing reduction gear with no dynamic braking are referred to in this study as reverse clutching deceleration. These maneuvers were simulated for

initial ship speeds of 31.3 knots (Figures 42 and 43) and 24.8 knots (Figures 44 and 45). They represent the "crash reverse" capability of the ship.

Idling torque and windage torque characteristics discussed previously are incorporated in the reverse clutching deceleration computer runs.

The reverse and forward clutches are located at the intermediate reduction gear pinions operating at a speed (k_3 N) of approximately 4.32 times the propeller speed.

For these maneuvers, fuel idling commands to the turbine(s), forward clutch deflation, and reverse clutch inflation begin simultaneously at time t = 0. The decrease in forward clutch torque capacity is determined by the air deflation rate and the clutch speed according to the equation for Q_{CF} (this discussion is concerned with the 31.3-knot case). The forward clutch torque capacity goes to zero at 3.7 seconds, but clutch slipping occurs at 2 seconds where the clutch torque capacity goes below the torque required to hold the propeller torque at the clutch (Q/k_3). Clutch disengagement occurs at Time t_D, the drive train is open, and the computation now involves the solving of two independent torque equations with the appropriate inertias. In the open drive train condition between t_D and t_E (reverse clutch engagement), turbine speed, N_3, and propeller speed, N, both decrease independently.

The reverse clutch begins to engage at t_E = 6.9 seconds according to the equation for Q_{CR} developing a negative torque opposing the porpeller torque, Q/k_3, on the other side of the reverse clutch. While Q_{CR} is always positive, the negative sign for Q_{CR} is included in the propeller torque equation. A large slip speed across the reversing clutch (initially about 1850 rpm) and an increasing torque, Q_{CR}, rapidly develop a large absorbed power, P_C, in the reversing clutch. The absorbed clutch power rises to a peak of 32,400 hp at 9.4 seconds and falls to zero at 11.7 seconds where clutch lockup occurs at t_L. In the 4.8 seconds during which the reverse clutch is absorbing power, the turbine, propeller, and slip speeds decrease very rapidly.

The total absorbed energy by the clutch, E_C, is the time integral of the absorbed power curve; the total energy reaches about 50×10^6 ft-lb at clutch lockup.

The propeller and turbine speeds (N and N_3) are about -10 and 100 rpm, respectively, at clutch lockup.

Ship and propeller performance during reverse clutching deceleration from 31.3 knots is indicated in Figure 43.

Propeller torque falls rapidly to about 5% of the maximum value in 4 seconds. Reverse clutching causes propeller torque to go negative, and it becomes very large by the time clutch lockup is achieved. Propeller thrust goes negative at 3.5 seconds and stays very slightly negative during the open drive train interval. At reverse clutch engagement the thrust begins to increase negatively, reaching a very large value at clutch lockup (11.7 seconds). The corresponding ship speed and head reach at clutch lockup are 25 knots and 570 feet, respectively.

With the reverse clutch locked up, the reversing system is fully effective and the turbine power can be increased as desired to achieve the required propeller speed in reverse.

A comparison between reverse clutching deceleration from 31.3 and 24.8 knots (Figures 44 and 45) indicates that absorbed clutch power decreases from 50×10^6 to 18×10^6 ft-lb. It should be noted, however, that for this case, only half the clutches were used because the boost turbine is declutched. As indicated earlier, the constants used in the clutching equations are 2275 for the 24.8-knot case and 4550 for 31.3 knots. Correspondingly, the drive train inertia is for a single engine.

The interval between forward clutch disengagement and reverse clutch engagement decreases from 4.9 seconds at 31.3 knots to 1.7 seconds at 24.8 knots. This is due to the fact that at lower speeds, the forward clutch takes longer to release and the reverse clutch begins engagement earlier. Both these effects are a result of the speed-dependent centrifugal force term ($- 4n^2$) in the clutching equations.

Large decelerations of the propeller are experienced during reverse clutching deceleration. The deceleration versus speed for the propeller is indicated for both 31.3 and 24.8 knots in Figure 38.

Table 5
Coast Down, Braking, and Reversing Performance

Computer Run	Initial Ship Speed knots	t_{DV} sec	S_{DV} ft	t_{DN} sec	t_L sec	S_L ft	t_T sec	S_T ft	E_C ft-lb	Condition
10212	31.3	59.0	2170	19.0						Coast down, both engines
11251	31.3	32.0	1220	5.7						Coast down, both engines with braking
11042	31.3			8.5	11.7	570			50×10^6	Reverse clutching deceleration
12051	31.3			4.6	18.4	800			7×10^6	Reverse clutching deceleration with braking
12131	31.3	26.3	1070	8.5	11.7	570	38.0	1380	50×10^6	Reversing until ship speed = 0
12132	31.3	29.1	1130	4.6	18.4	800	52.9	1450	7×10^6	Reversing until ship speed = 0, with braking
10142	24.8	76.0	2210	29.0						Coast down, base engine
10151	24.8	37.5	1130	4.3						Coast down, base engine with braking
11071	24.8			8.0	10.7	430			18×10^6	Reverse clutching deceleration
12062	24.8			4.3	19.3	690			5×10^6	Reverse clutching deceleration with braking
12112	24.8	31.3	1019	8.0	10.7	430	62.7	1350	18×10^6	Reversing until ship speed = 0
12161	24.8	33.9	1062	4.3	19.3	690	66.0	1400	5×10^6	Reversing until ship speed = 0, with braking

t_{DV} = time to reach 50% of initial ship speed
S_{DV} = head reach at t_{DV}
t_{DN} = time to reach 50% of initial propeller speed
t_L = time to achieve clutch lockup
S_L = head reach at clutch lockup
t_T = time to achieve zero ship speed
S_T = head reach at t_T
E_C = absorbed clutch energy at t_L

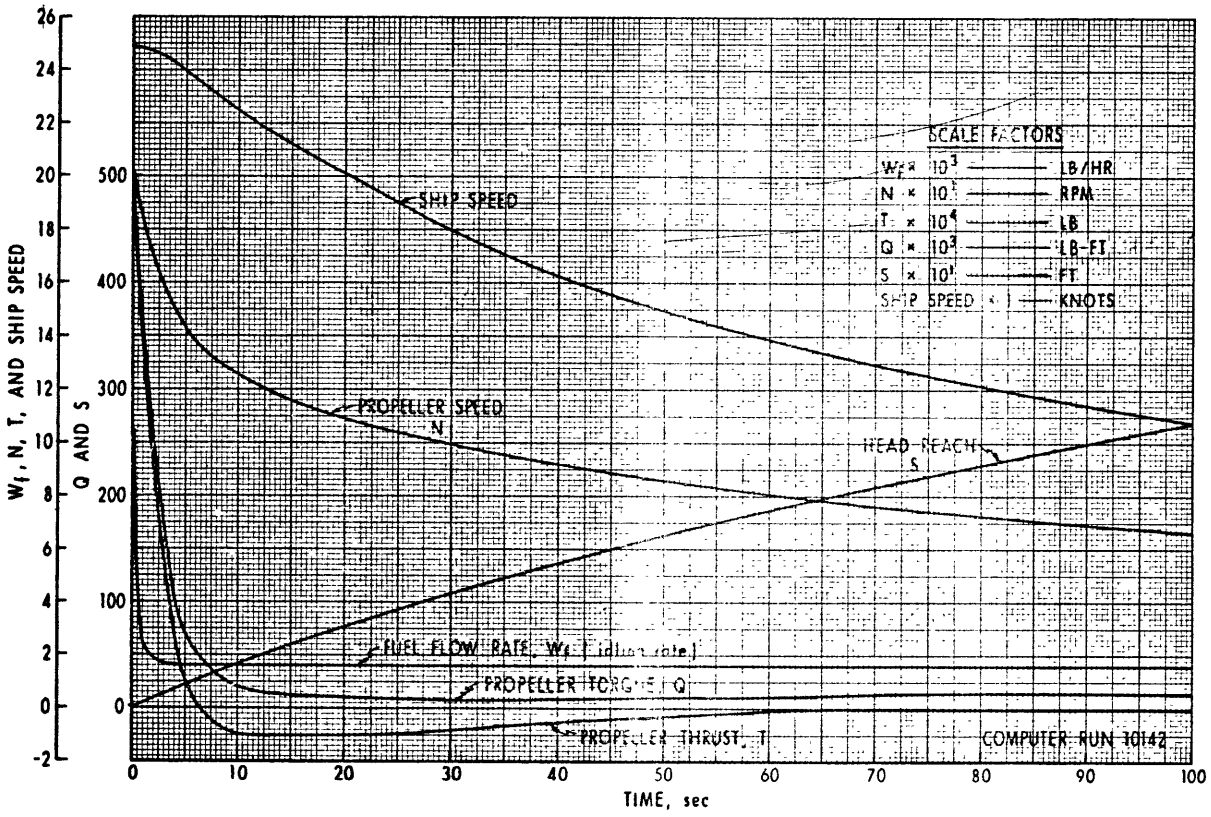

Figure 36
Coast Down from 24.8 Knots, Base Engine Only
(Maximum Deceleration on Base Turbine, No Braking)

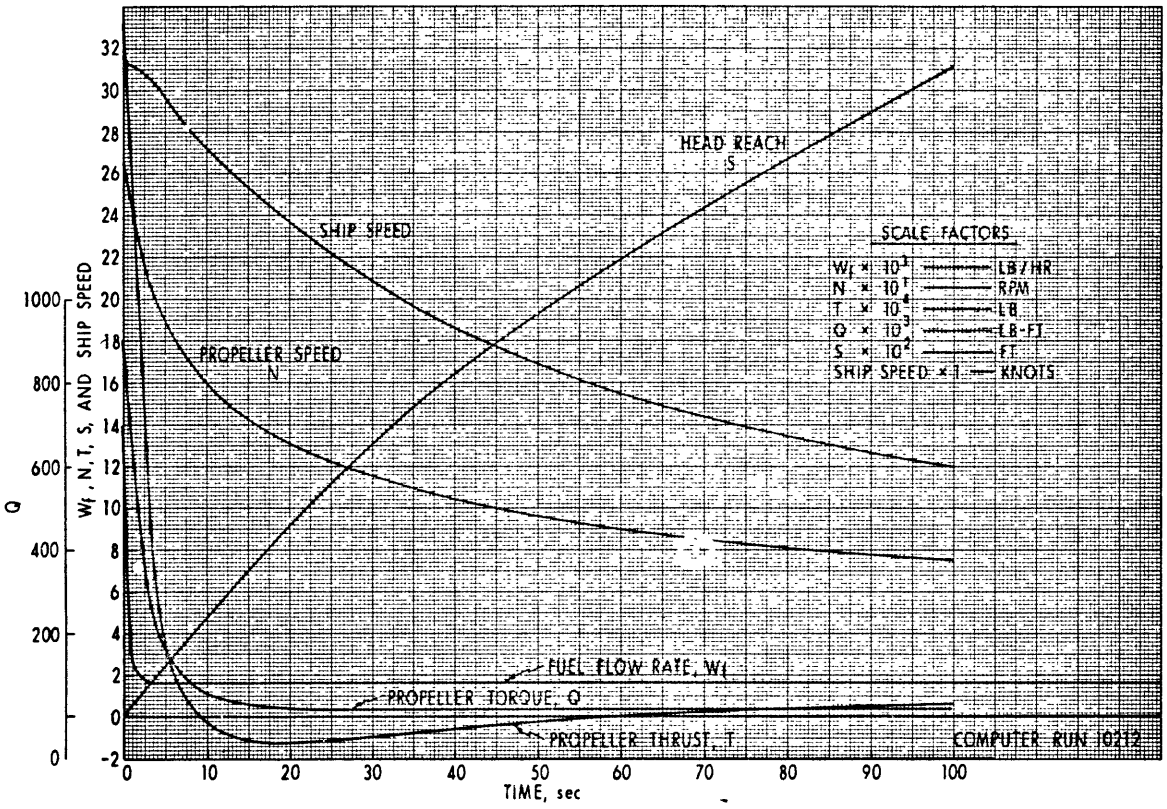

Figure 37
Coast Down from 31.3 Knots, Both Engines
(Maximum Deceleration on Both Engines, No Braking)

Computer Run	Condition
10212	Coast Down from 31.3 Knots, No Braking
11042	Reverse Clutching Deceleration from 31.3 Knots, No Braking
10142	Coast Down from 24.8 Knots, No Braking
10151	Coast Down from 24.8 Knots, with Braking
11071	Reverse Clutching Deceleration from 24.8 Knots, No Braking

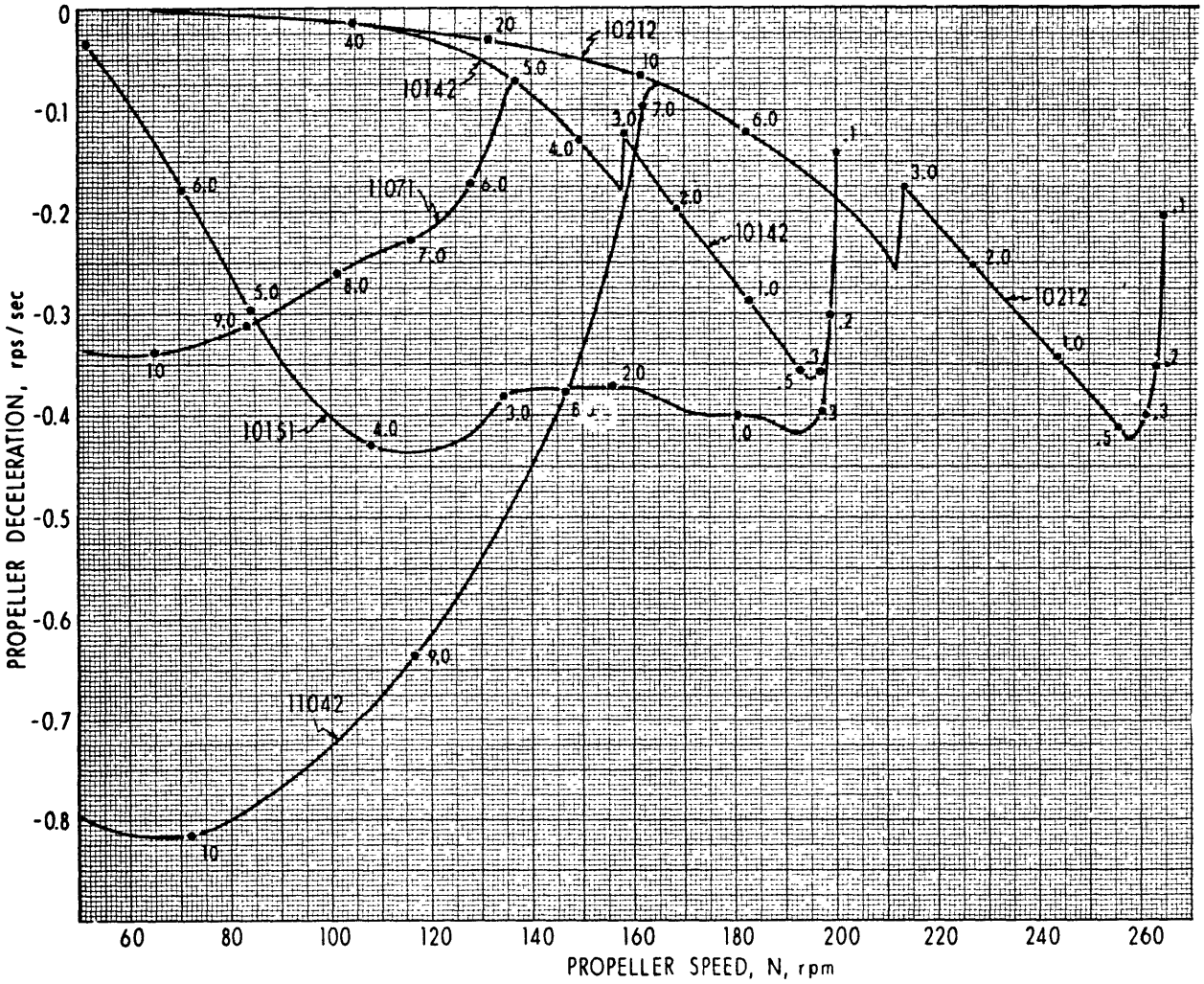

Figure 38
Propeller Deceleration Versus Propeller Speed
for Various Conditions of Deceleration

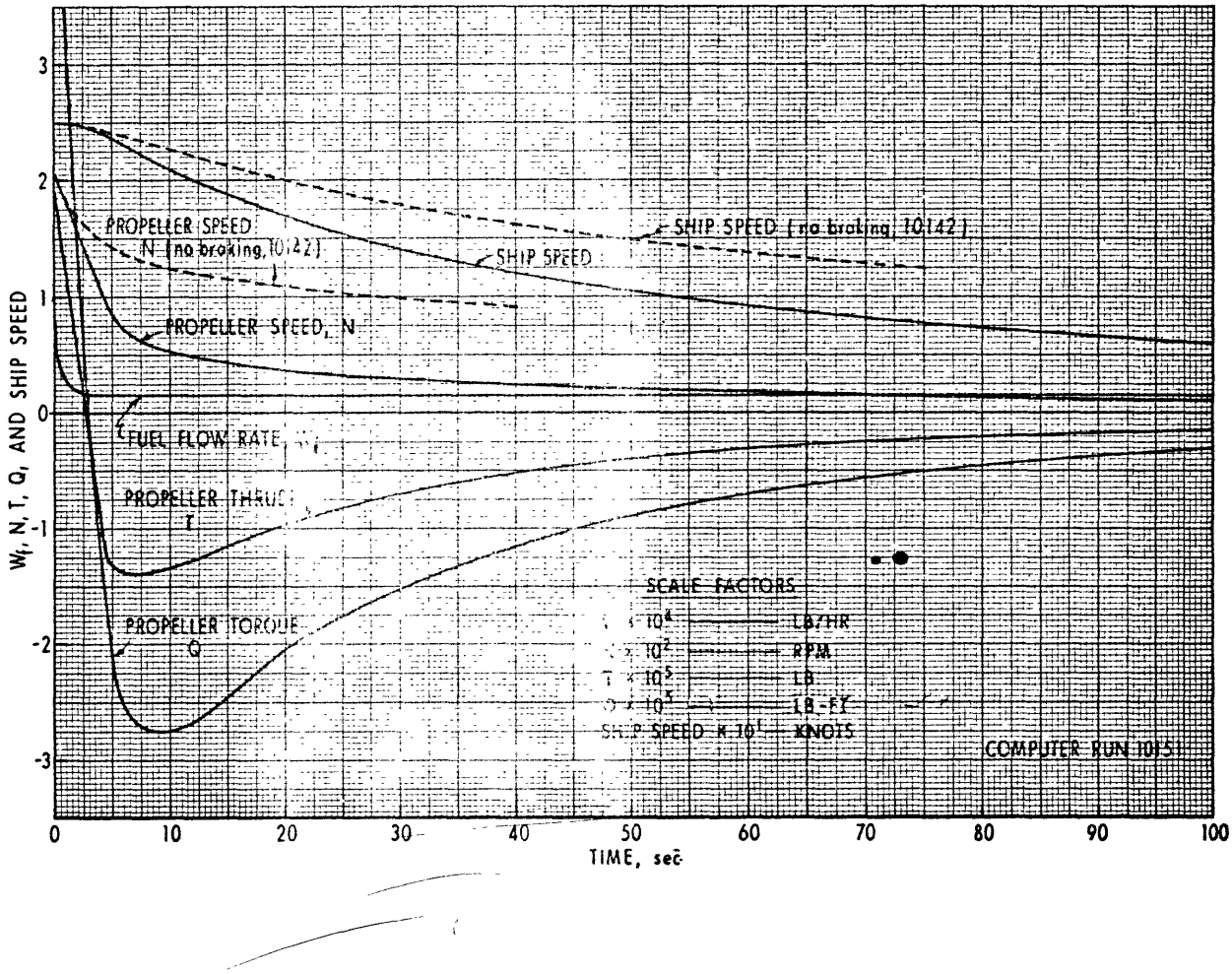

Figure 39
Coast Down from 24.8 Knots, Base Engine Only
(Maximum Deceleration on Base Turbine with Dynamic Braking)

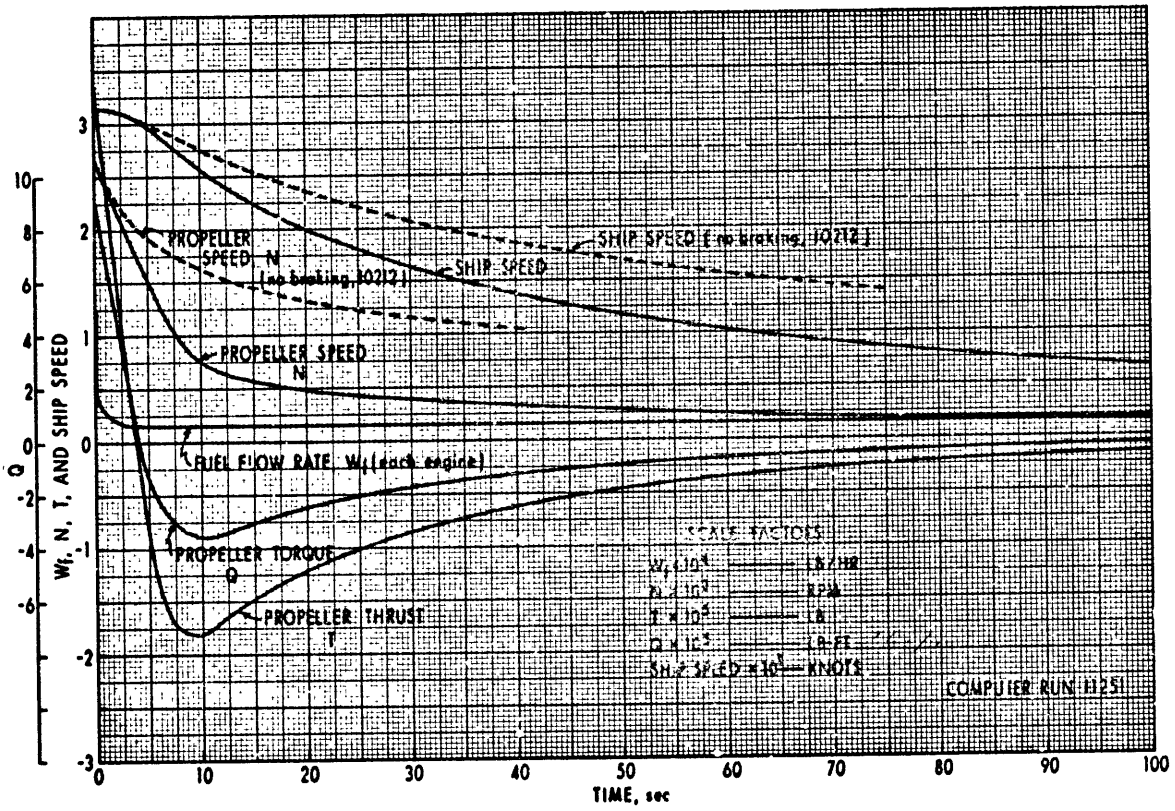

Figure 40
Coast Down from 31.3 Knots, Both Engines
(Maximum Deceleration on Both Engines with Dynamic Braking)

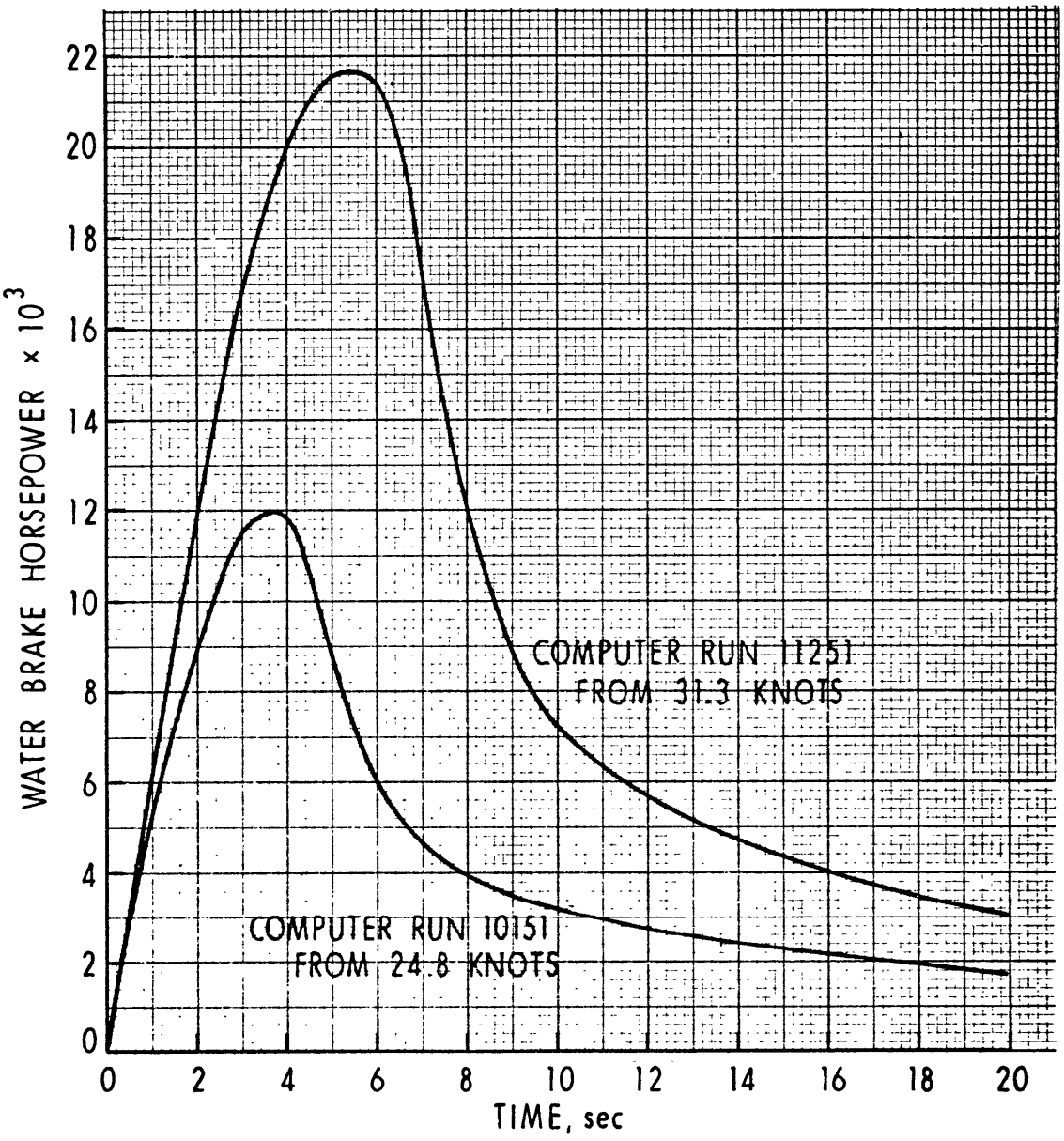

Figure 41
Water Brake Power Versus Time
(for Dynamic Braking from 24.8 and 31.3 Knots
with 6.0-Second Ramp)

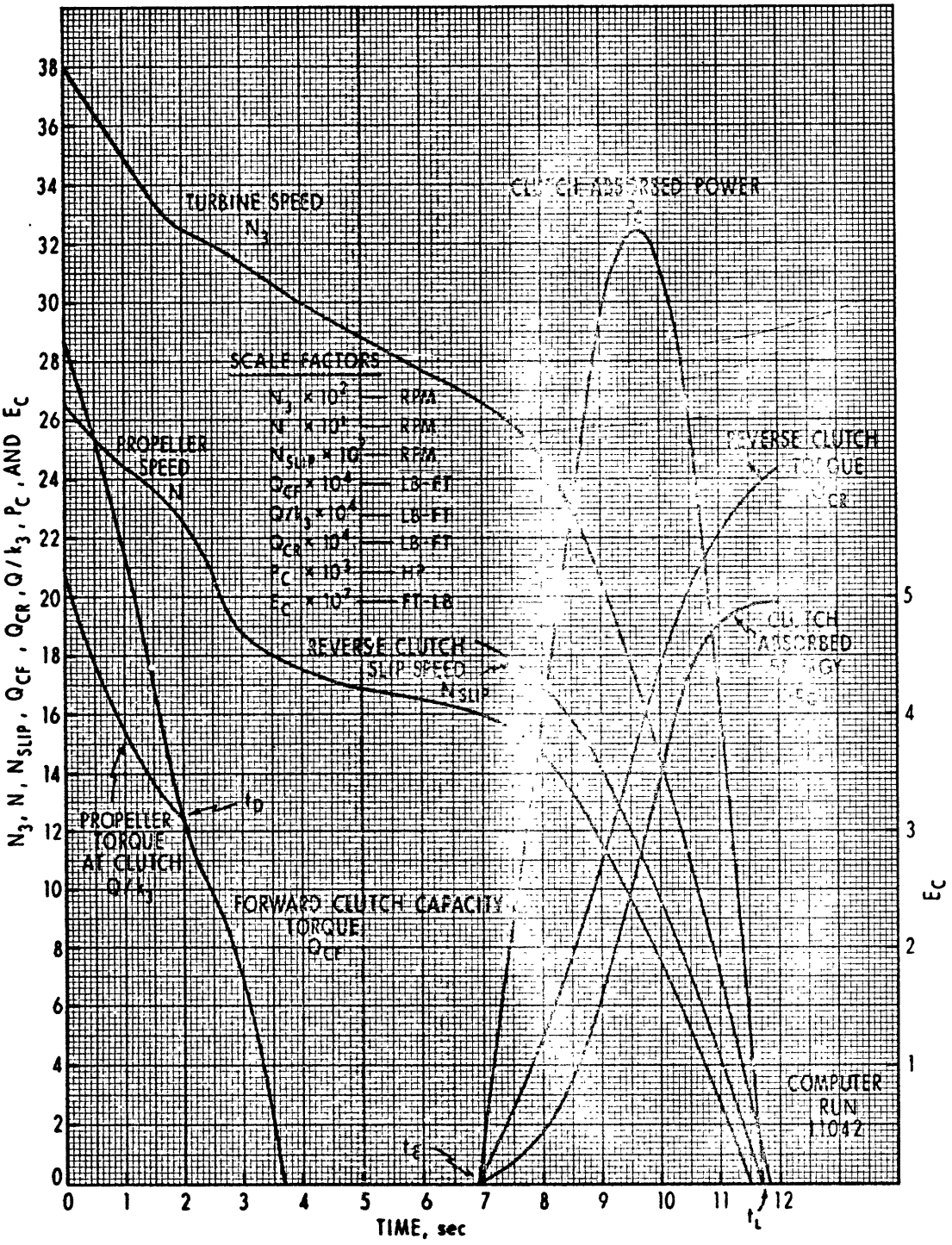

Figure 42
Reverse Clutching Deceleration from 31.3 Knots

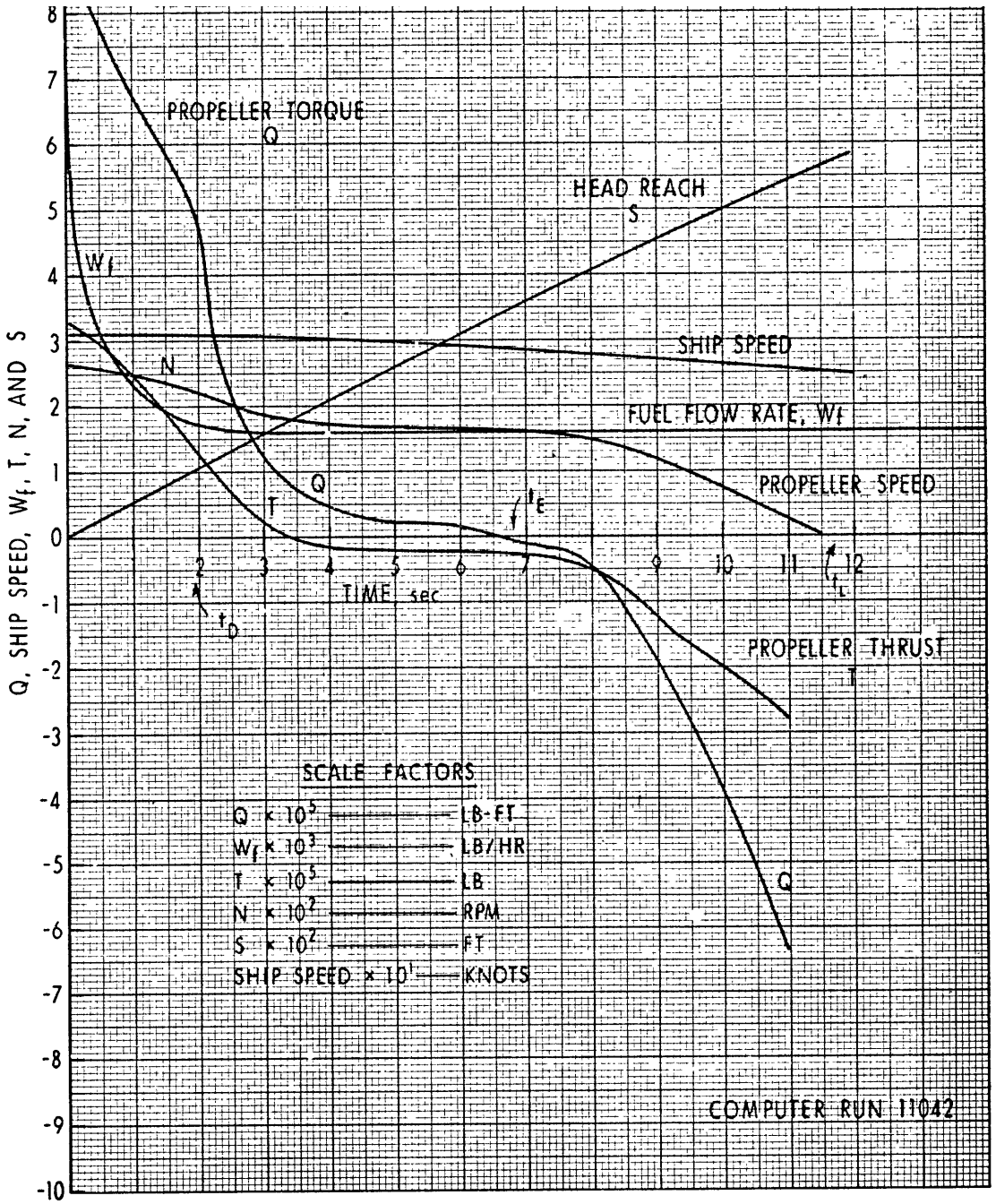
Q, SHIP SPEED, W_f, T, N, AND S
TIME, sec
PROPELLER TORQUE
Q
HEAD REACH
S
W_f
SHIP SPEED
N
FUEL FLOW RATE, W_f
Q
PROPELLER SPEED
T
t_E
t_D
t_L
PROPELLER THRUST
T
Q
SCALE FACTORS
$Q \times 10^5$ —— LB-FT
$W_f \times 10^3$ —— LB/HR
$T \times 10^5$ —— LB
$N \times 10^2$ —— RPM
$S \times 10^2$ —— FT
SHIP SPEED $\times 10^1$ —— KNOTS
COMPUTER RUN 11042

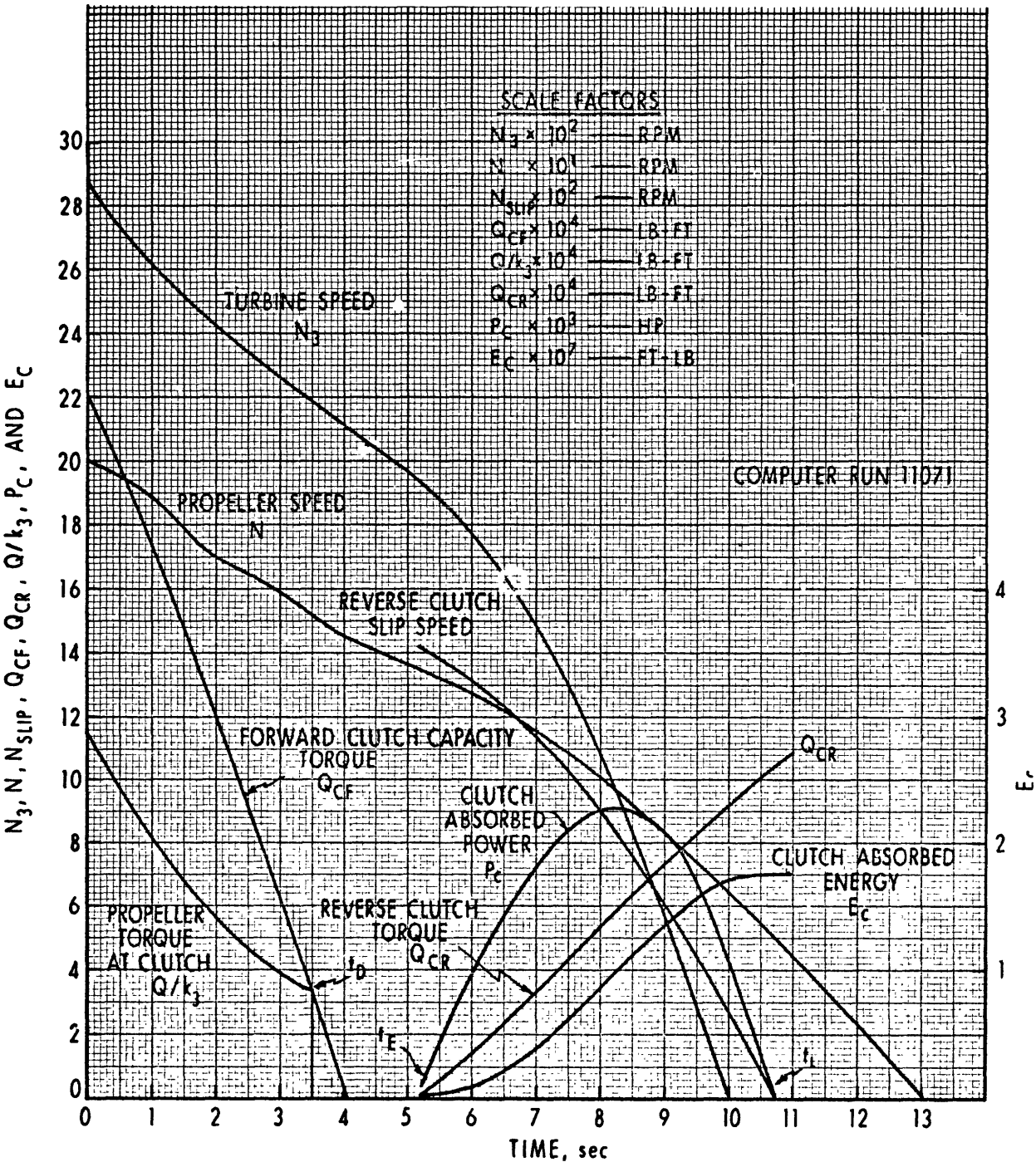

Figure 44
Reverse Clutching Deceleration from 24.8 Knots

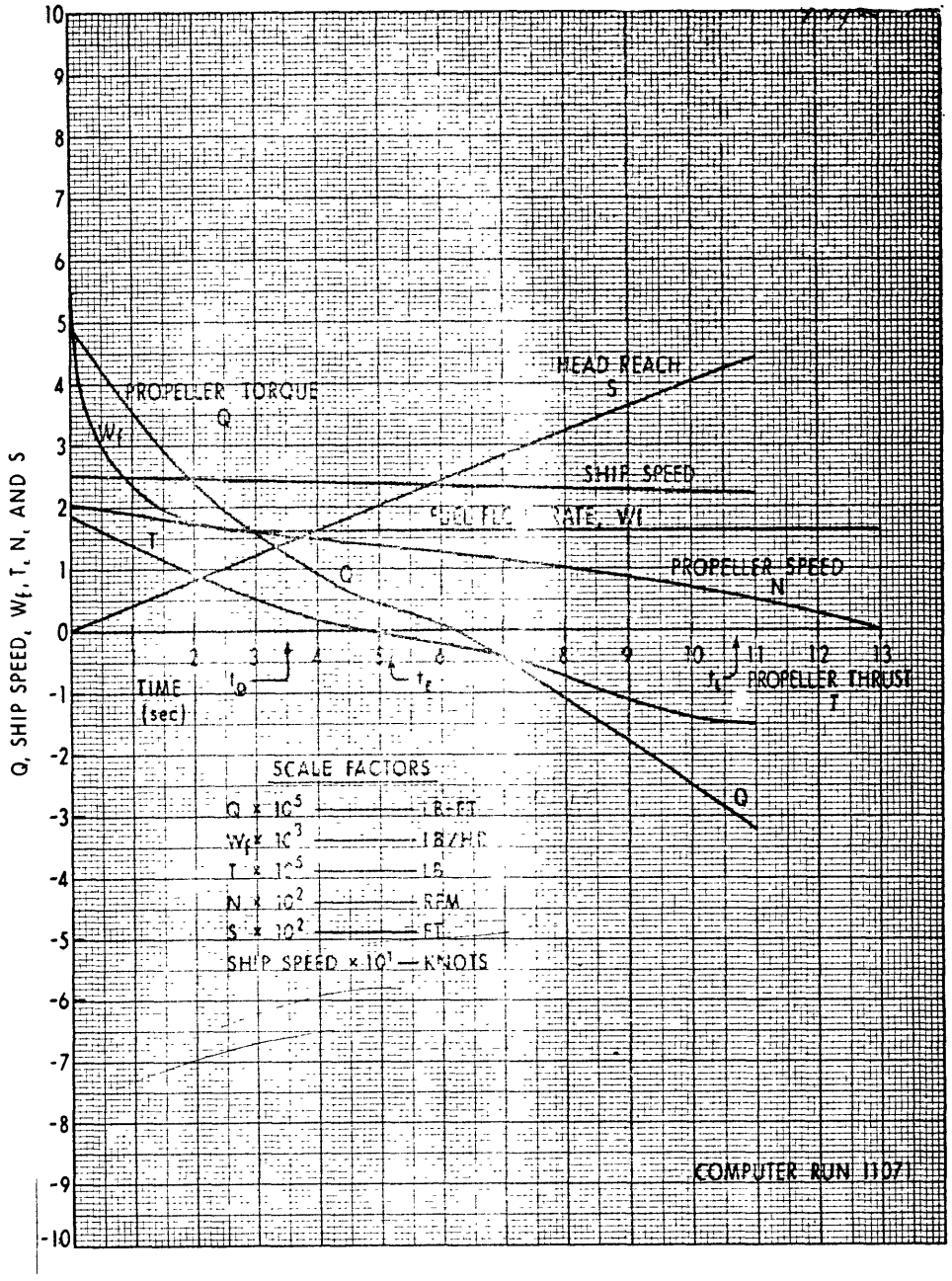

Figure 45
Reverse Clutching Deceleration from 24.8 Knots

REVERSE CLUTCHING DECELERATION WITH DYNAMIC BRAKING

In order to decrease the absorbed clutch power and energy in reversing maneuvers, the reverse clutching decelerations from 31.3 and 24.8 knots were repeated with dynamic braking prior to clutching (Figures 46, 47, 48, and 49). The water brake effectiveness was again simulated with a 6-second ramp, and the clutching equations were delayed by 10 seconds or more while large braking power was still effective. The braking torque, Q_b, was summed in the single torque equation and then set to zero at Time t_D when the forward clutch disengaged.

Clutch overlap occurs with braking because the rapid decrease in turbine and propeller speed delays forward clutch disengagement while shortening the time to engage the reverse clutch. To minimize overlap the forward declutching is begun at 10 seconds and the reverse clutching is begun at 12 seconds after the fuel flow rate is cut to idling.

While the reverse clutch torque is increasing in the interval between t_E and t_L, the water brake torque is set to zero at t_D, and there is an increase in propeller speed and then a decrease when sufficient reversing torque is provided to overcome the propeller torque. The tendency of the propeller to increase in speed while the reverse clutch is engaging is due to the low propeller speed created by braking for that ship speed.

Clutch lockup is achieved for a propeller speed well above zero (50 rpm) with the turbine driven in reverse (-500 rpm) for the 31.3-knot case. However, the important consideration is to achieve clutch lockup quickly and with as little dissipated clutch energy as possible since the propeller can be very quickly reversed with the application of turbine power, once lockup is achieved.

Dynamic braking has a very pronounced and desirable effect in decreasing the total dissipated energy from 50×10^6 to 7×10^6 ft-lb for the 31.3-knot braking/reversing maneuver while increasing the head reach from the comparable run with no braking by only 230 feet. The corresponding results for braking/reversing from 24.8 knots are a decrease in clutch energy from 18×10^6 to 5×10^6 ft-lb and a head reach increase of 260 feet.

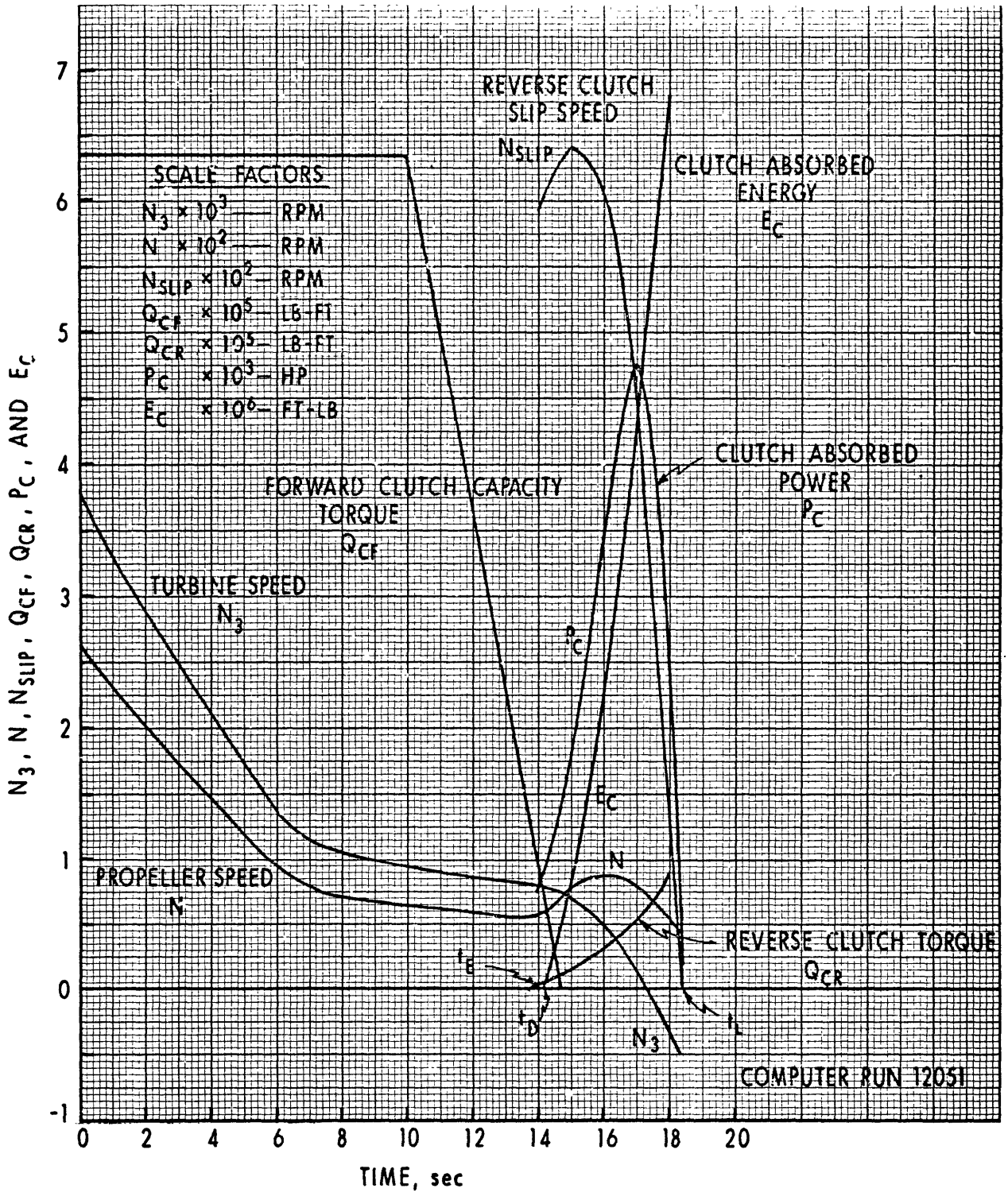

Figure 46 - Reverse Clutching Deceleration with Dynamic Braking from 31.3 Knots

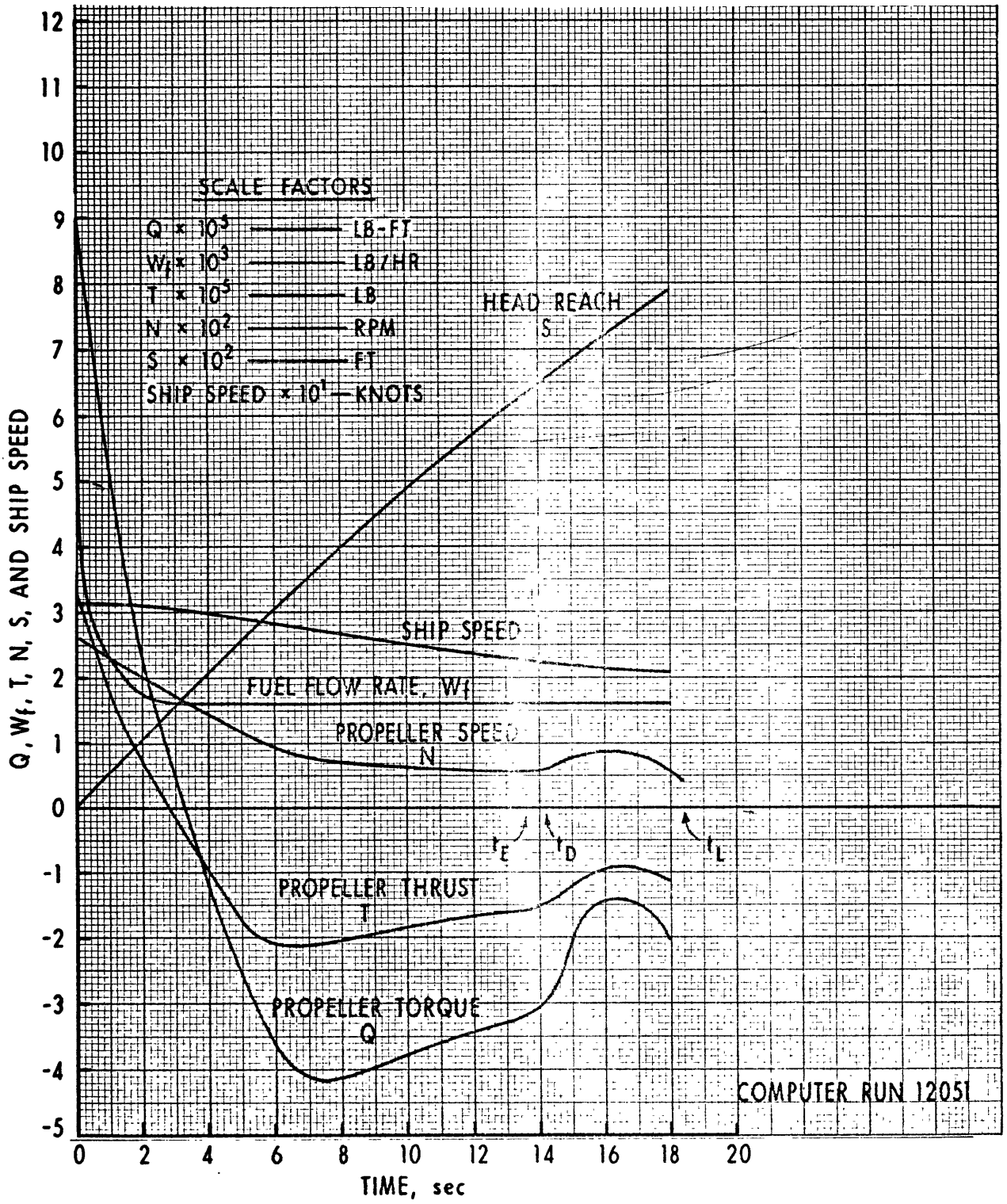

Figure 47 - Reverse Clutching Deceleration with Dynamic Braking from 31.3 Knots

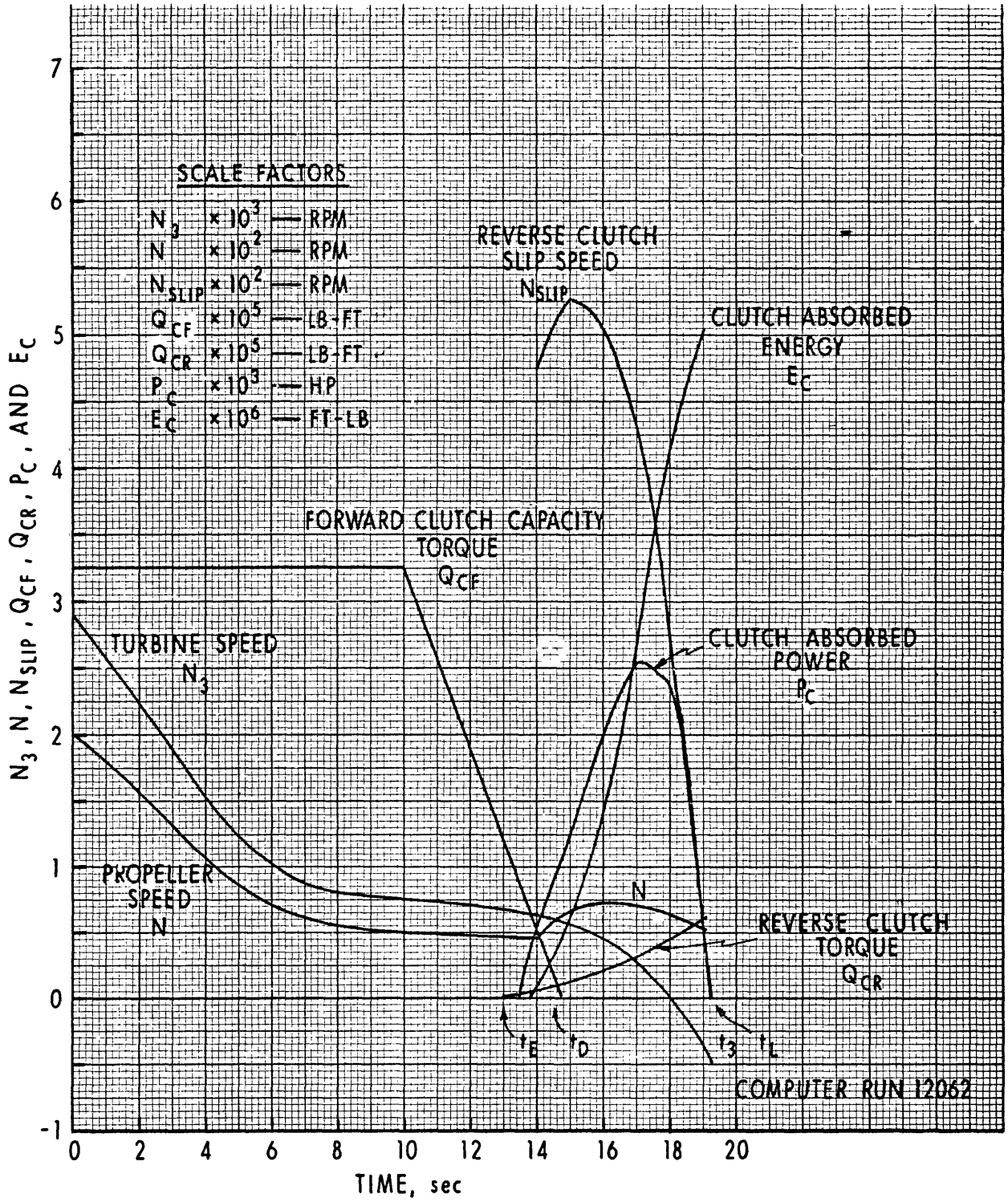

Figure 48 - Reverse Clutching Deceleration with Dynamic Braking from 24.8 Knots

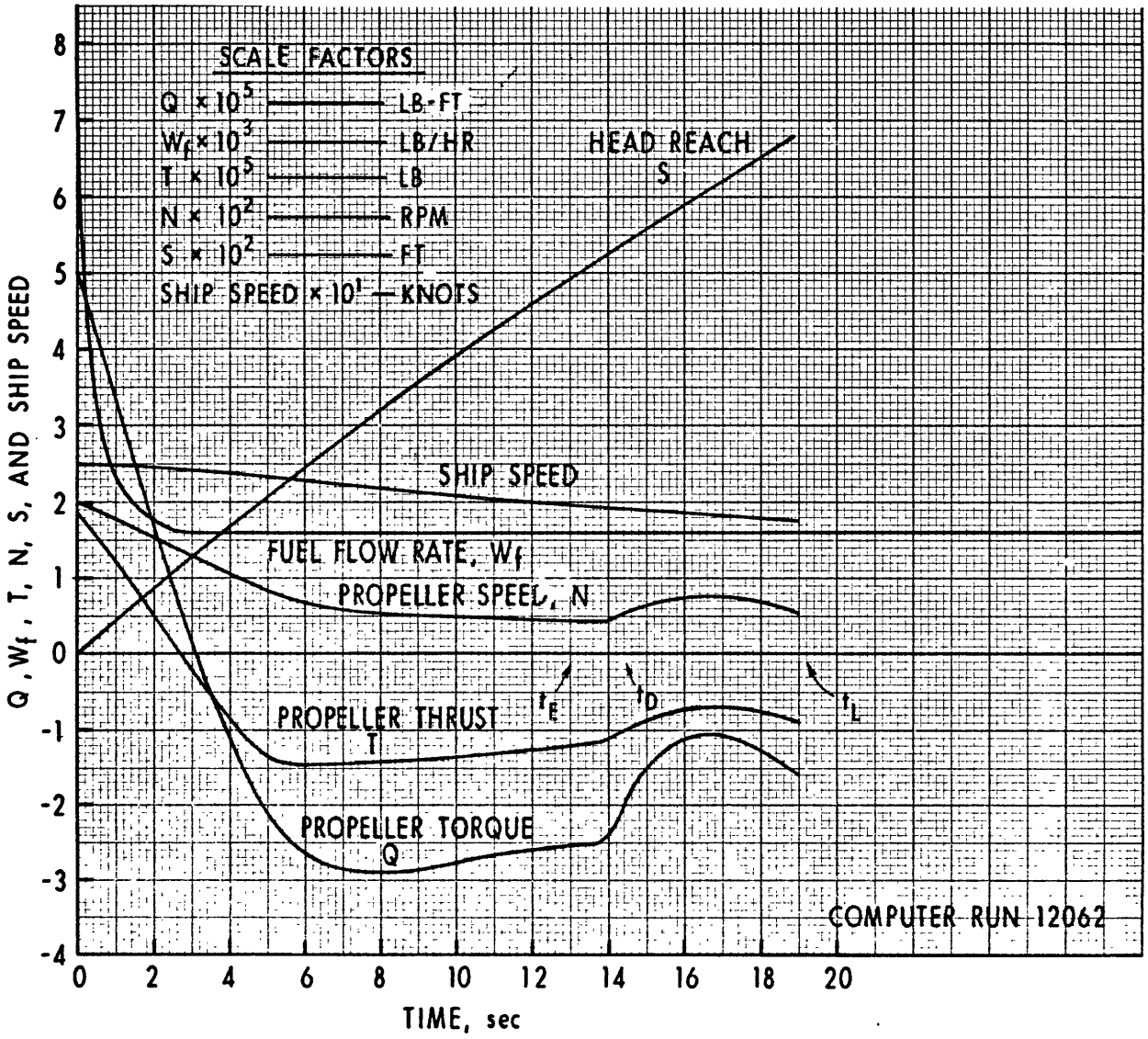

Figure 49 - Reverse Clutching Deceleration
with Dynamic Braking from 24.8 Knots

REVERSING

Performance in reversing was investigated for initial ship speeds of 31.3 and 24.8 knots after the clutch was locked up in reverse following reverse clutching deceleration both with and without dynamic braking. Each computer run for reversing was started beginning at clutch lockup (at Time $t = t_L$). The initial conditions existing at t_L were used in starting the computer runs which terminated when the ship speed was reduced to zero.

During reversing, the propeller characteristics for the thrust and torque computations fall in the quadrant where $V_p > 0$ $n < 0$. Wake and thrust fractions and ship resistance were unchanged (only forward ship motion was analyzed). The gear ratio in reverse is $k_1 k_2 k_3 = k_2 k_g = 0.6990 \times 14.3589 \approx 10$. With the reverse clutch(s) fully engaged there is only one torque equation for the system.

Initially, the turbine is operating in reverse due to reverse clutching and the water milling propeller (Computer Run 12112). Starting at t_L, the fuel flow rate is advanced to $W_f = 10,500$ lb per hr for the single engine or $W_f = 10,500$ lb per hr for each engine.

The gas flow first decelerates the power turbine from its reverse direction then accelerates it driving the propeller in reverse. During the engine torque buildup where $|Q_d| < |Q|$ the propeller speed increases slightly due to propeller water milling (for about 3 seconds in the 24.8-knot case, Run 12112). The large engine torque then rapidly brings the propeller speed back to zero in about 3 additional seconds and continues to accelerate the propeller in reverse.

The engine torque map for the engine initially operating in reverse is an extension of the torque speed characteristics of Figure 19 into the region of negative N_3. Operation in the region of negative N_3 and the transient engine torque versus engine speed and time is shown in Figure 52 for reversing from 24.8 knots (Computer Run 12112).

Figures 50 and 51 show reversing from initial ship speeds of 31.3 and 24.8 knots following reverse clutching deceleration with no braking. It should be noted that in all the reversing runs the computation was begun at clutch lockup, t_L; consequently, the values in Table 5 for total head reach total time t_T, t_{DV}, and S_{DV} are the sum of the values in the appropriate computer runs.

Due to the low or negative turbine speeds at the beginning of the propeller reversing phase when the fuel flow rate is increased, the engine torques developed on the propeller shaft are very large. To limit the torque, the fuel flow rate in reverse was limited to 10,500 lb per hr for each engine. For reversing from 31.3 knots (Computer Run 12131) the initial ship and

propeller speeds following clutch lockup are 25.2 knots and -0.8 rpm, respectively. The engine torque developed on the propeller shaft (with both engines) reaches a peak of 1.53×10^6 lb-ft. This represents an overtorque ratio of $(1530 \times 10^3)/(985 \times 10^3) = 1.5$ relative to the maximum forward torque at 32 knots.

All the reversing runs indicate that the propeller is absorbing a large torque and produces large negative thrusts of about 200×10^3 to 300×10^3 pounds within almost 10 seconds after reversing is begun. The peak power developed by the engine(s) is 15×10^3 and 35×10^3 hp for reversing from 24.8 and 31.3 knots.

It should be noted that in all cases the propeller reaches a maximum negative speed and then decreases slowly in speed. This is due principally to the propeller characteristics in the quadrant where $V_p > 0$ $n < 0$ and also the fact that the total ship resistance is decreasing rapidly with time as the ship slows down. The variations in thrust and torque during the maneuvers are due to the propeller characteristics which are referenced in Figures 50 and 51 by showing σ at various points on the thrust curves.

Computer runs with reversing begun at clutch lockup following reverse clutching deceleration with dynamic braking are shown in Figures 53 and 54.

The total time to stop the ship, t_T, and the total head reach, S_T, for all the runs are shown in Table 5. For example, the total head reach, S_T, with no braking from 31.3 knots (Run 12131) is 1380 feet and the time is 38 seconds. With dynamic braking the time is increased to 52.9 seconds with a head reach of 1450 feet. The apparent discrepancy between time and head reach in the two cases is due to the fact that with dynamic braking, the ship speed is about 4 knots less than for no braking when the reversing maneuver is begun.

Finally, it is recognized that these results as well as those for acceleration are optimistic because the effects of propeller cavitation and transient wake and thrust fractions were not simulated.

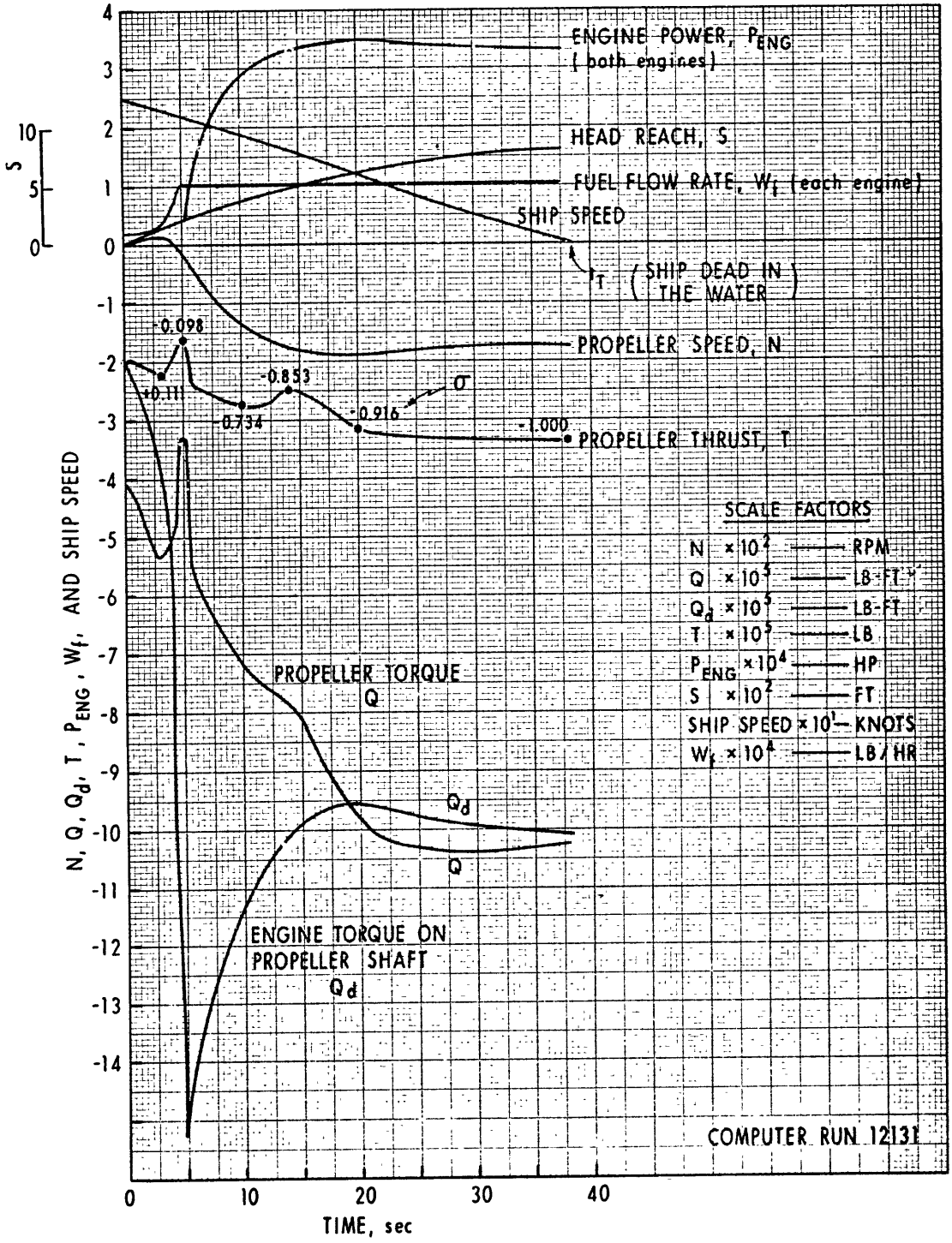

Figure 50 - Reversing from 31.3 Knots until Ship Speed = 0 (both engines)

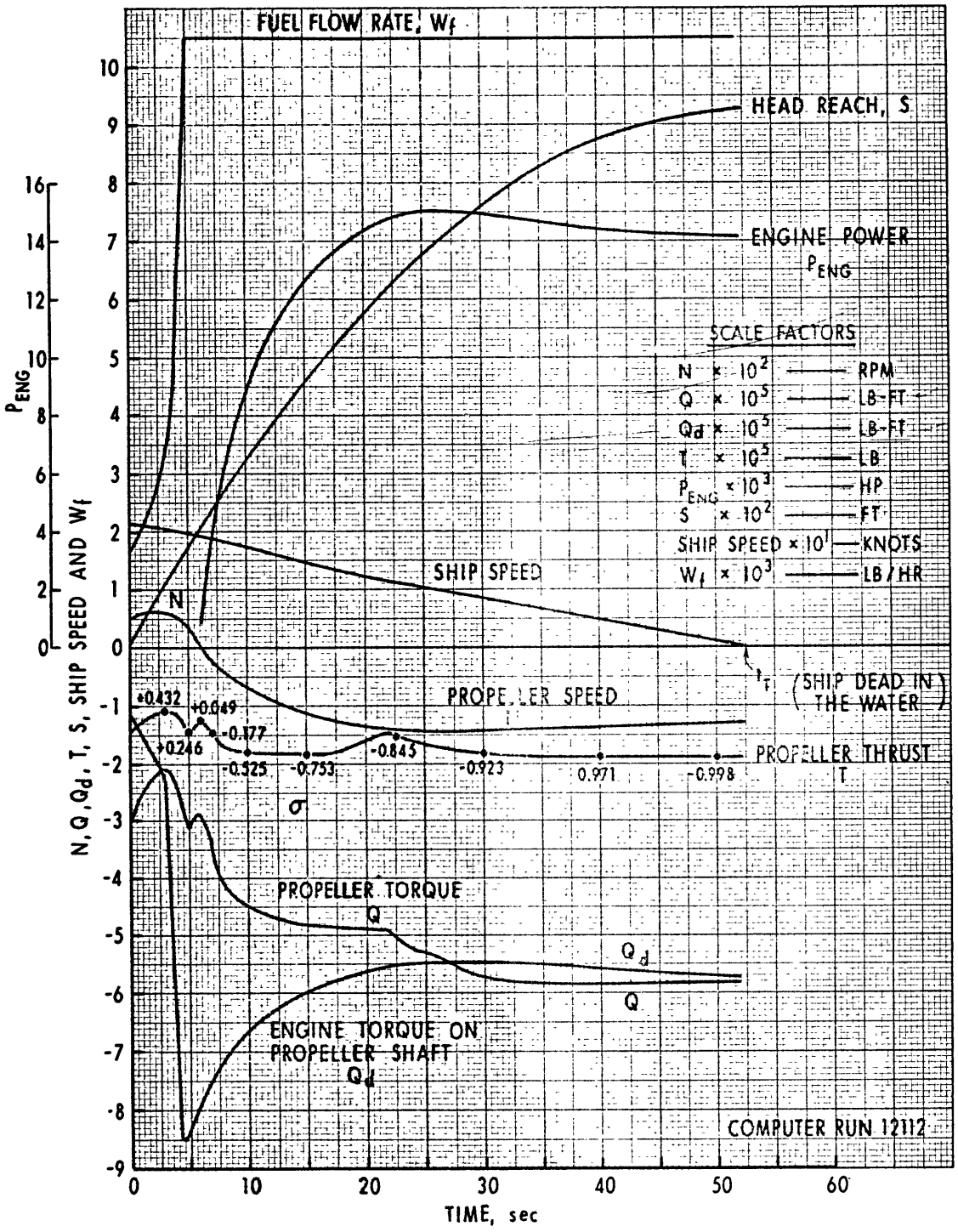

Figure 51 - Reversing from 24.8 Knots until Ship Speed = 0 (base engine only)

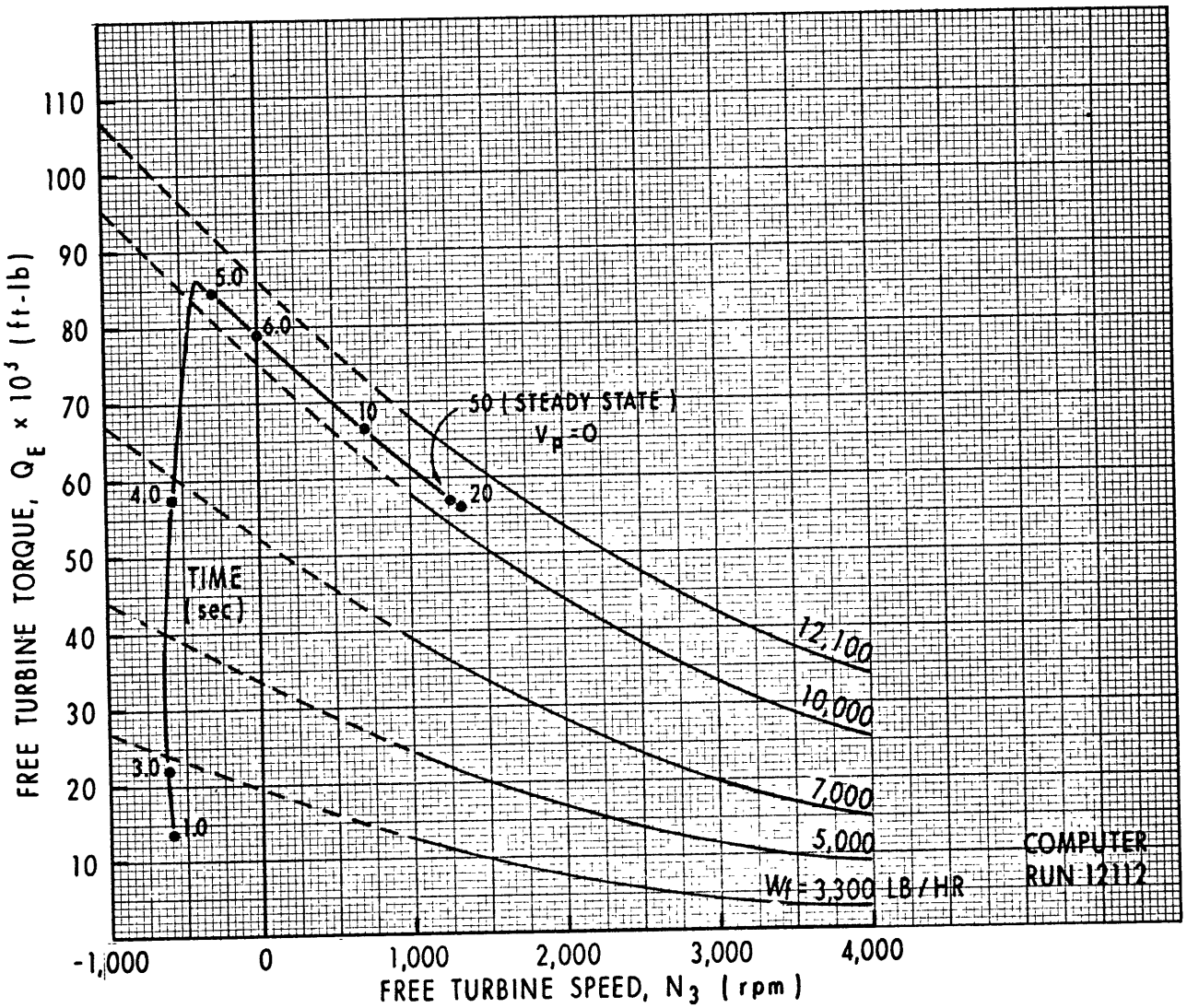

Figure 52
Transient Engine Torque Versus
Engine Speed for Reversing

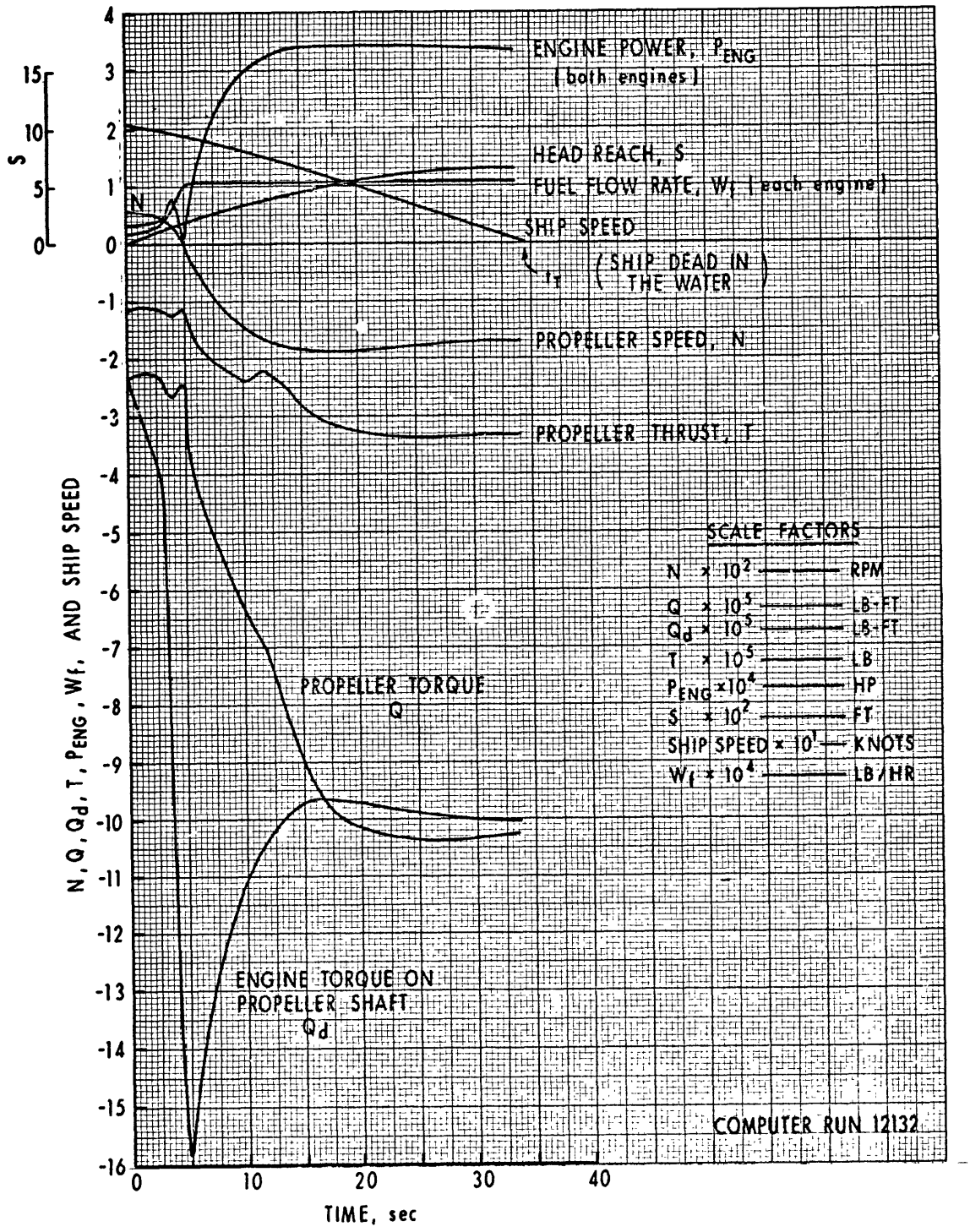

Figure 53 - Reversing from 31.3 Knots until Ship Speed = 0 (both engines and with braking)

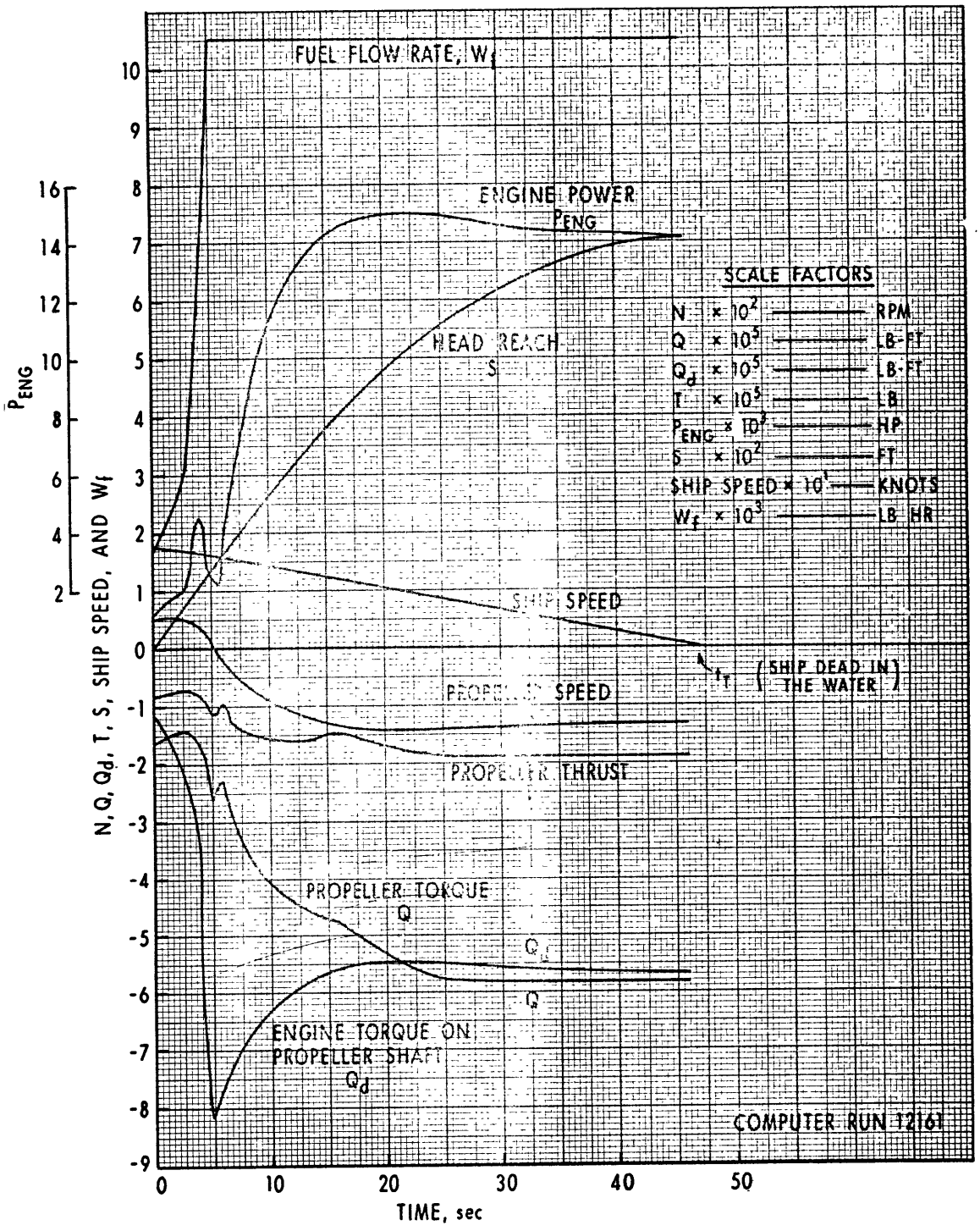

Figure 54 - Reversing from 24.8 Knots
until Ship Speed = 0 (both engines and with braking)

CONCLUSIONS

The objective of the ship-propulsion dynamics studies is to predict ship- and propulsion-plant performance for a variety of conditions and to derive the design theory for the development of automated, high-performance ship-propulsion control systems.

Modeling and analytical prediction of the behavior of complex propulsion systems provide immediate, though still theoretical, answers to many difficult problems frequently encountered in matching components of the ship-propulsion system and the design of ship-propulsion plants to ship's characteristics. Naturally, the transient phenomenon of propulsion dynamics is the most complex and also the least explored. Consequently, the major emphasis of the propulsion dynamics studies will be devoted to transient phenomena associated with acceleration, deceleration, reversing, load sharing, maneuvering, and sea-state effects. The last half of this report represents conclusions from the results of many computer runs which are given in graphs and tables to describe the conditions for a number of situations involving acceleration, dynamic braking, and reversing. Computer programs are now available for further studies in propulsion dynamics. These programs can be varied and expanded to suit other requirements. For example, a diesel engine was tried as a base plant during this study with little difficulty in implementation.

Additionally, the program can be expanded to include a controllable-reversible pitch propeller and automatic control systems including power or speed governing or both. The succeeding phases of propulsion dynamics work will concentrate in these areas.

It is important to recognize that most of the work reported here is applicable to gas-turbine propulsion plants in general despite the use of a reversing reduction gear in this study.

The salient conclusions of this study are summarized below:

- Ship and propulsion system dynamics can be simulated to provide design data for plant and component selection and optimization.

- The method of a second modified advance coefficient for representing propeller characteristics for simulations is a great improvement over previous methods particularly in the analysis and interpretation of results.

- Acceleration to 90% of the base plant speed of 24.8 knots from an idling condition can be achieved in 78 seconds with a head reach of 1790 feet.

- Acceleration to 30 knots from 24.8 knots with the boost engine is accomplished in 35 seconds.

- Crash acceleration with both turbines at maximum power from an idling condition can bring the ship to 28.8 knots in 53 seconds with a head reach of 1470 feet.

- A decrease in acceleration time by a factor of up to 3.8 is possible for speeds between 15 and 25 knots using base power only (20,000 hp), if a fuel flow rate in excess of the required steady-state value is ordered during acceleration.

- Fuel flow rate ramps are very effective in reducing engine torque. For the worst overtorque condition during acceleration, a 20-second fuel ramp decreases the peak engine overtorque from 1.88 to 1.28. Ramps longer than 20 seconds do not provide any significant reduction in torque.

- Fuel flow ramps of up to 20 seconds have a negligible effect on ship acceleration time and head reach.

- Propeller forward thrust ratio is essentially independent of fuel flow ramp length.

- Reverse clutching deceleration from 31.3 knots, using a reversing reduction gear, can be accomplished in 11.7 seconds to clutch lockup (fully reversed clutch) with a head reach of 570 feet. The peak clutch absorbed power reaches 32,400 hp with a total clutch absorbed energy of 50×10^6 ft-lb.

- Dynamic braking prior to reverse clutching has a very pronounced and desirable effect in reducing total clutch absorbed power and energy while increasing the head reach slightly. For reversing from 31.3 knots, the values are: peak clutch absorbed power = 4750 hp, clutch absorbed energy = 7×10^6 ft-lb, and head reach = 800 feet.

- Dynamic braking prior to reverse clutching from 24.8 knots decreases the clutch absorbed energy by a factor of more than three with a head reach to clutch lockup of 690 feet.

- Head reach for a dead in the water condition from 31.3 knots is 1380 feet and 38 seconds when using a total of 35,000 hp in reverse (a fuel flow rate of 10,500 lb per hr for each turbine).

- Head reach for a dead in the water condition from 31.3 knots with dynamic braking prior to reverse clutching deceleration under the same engine power conditions as above is 1450 feet. Dynamic braking for this

condition increases the total head reach by 70 feet while decreasing the dissipated clutch energy by a factor of more than seven.

- Engine torques delivered to the propeller shaft during reversing from 31.3 knots are on the order of 1.5 or more times the maximum steady-state ahead value at 32 knots. This engine torque can be expected to be greater than 1.5 for fuel flow rates to each engine in excess of 10,500 lb per hr. In this study the gear ratio in reverse is approximately 10 and about 14.36 in the forward direction; consequently, the maximum torques in reverse are less than if the same gear ratio in forward and reverse were used.

- Engine torque limiting in reverse can be controlled with fuel flow ramps as in the ahead condition.

Appendix A

Reversing Reduction Gear Polar Moment of Inertia Calculations

$k_1 = \frac{\text{AHD HS Gear}}{\text{HS Pinion}} = 3.324$

$k_2 = \frac{\text{REV HS Gear}}{\text{AHD HS Gear}} = 0.6990$

$k_3 = \frac{\text{Bull Gear}}{\text{LG Pinions}} = 4.3197$

$k_g = \frac{\text{Bull Gear}}{\text{HS Pinion}} = 14.3589$

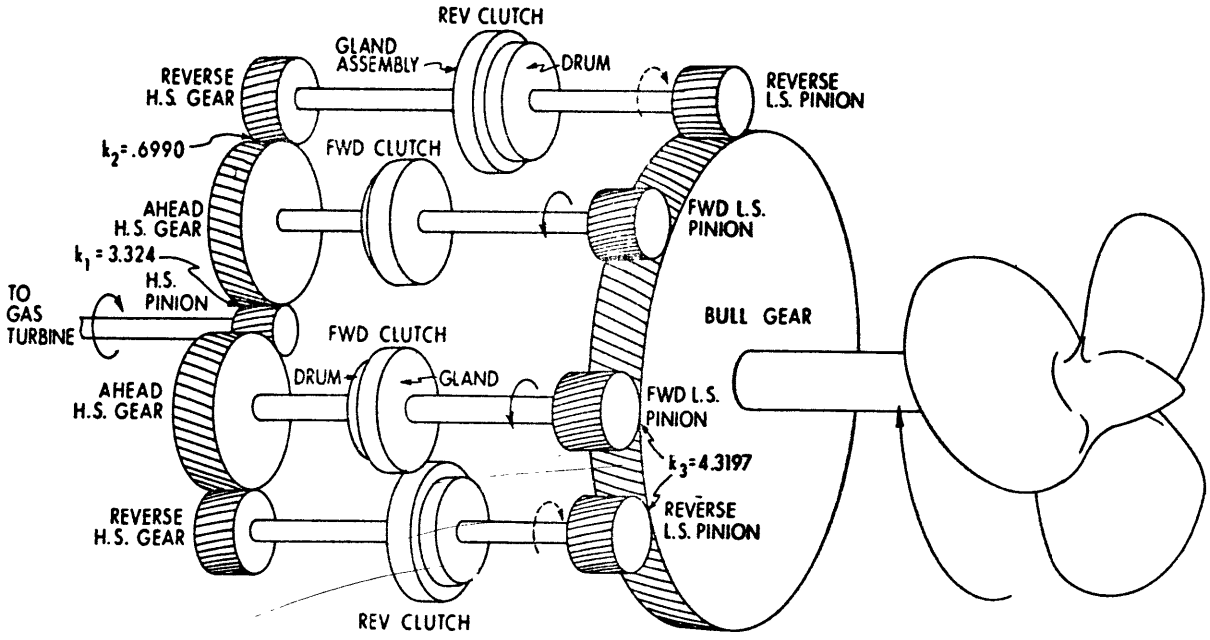

Reversing Reduction Gear
(showing one turbine drive section only)

Moments of Inertia
(referred to themselves) All in lb-ft^2

Gas turbine (GT)	5,009 each
High-speed (H-S) pinion	502 each
Ahead H-S gear	18,675 each
Reverse (rev) H-S gear	12,500 each
Rev clutch drums	5,750 per clutch
Rev clutch gland assembly	6,500 per clutch
Forward (fwd) clutch drums	5,750 per clutch
Fwd clutch gland assembly	6,500 per clutch
Rev and fwd low-speed (L-S) pinions	2,250 each
Bull gear and shaft	590,000
Propeller and entrained water	434,000

Propeller weight estimate $W = 35,000$ lb

Propeller radius of gyration $= 0.21\ D$

Propeller moment of inertia with 25% for entrained water

$$I = (1.25)\ W\ (0.21\ D)^2 = 1.25 \times 347,000$$

$$I \approx 434,000 \text{ lb-ft}^2$$

$$k_1^2 = 11.049$$

$$k_2^2 = 0.4886$$

$$k_3^2 = 18.6598$$

Fwd Direction
(one gas turbine, fwd clutches on boost turbine disengaged)

Gas turbine	5,009
+ H-S Pinion	502
	5,511

Base GT and H-S pinion	$(5,511)\ (k_1^2)\ (k_3^2)$	= 1,136,215
Ahead H-S gears, clutches drums, glands, and L-S pinions (two separate trains/turbine)	$2[18,675 + 6,500 + 5,750 + 2,250]\ k_3^2$	= 1,238,078
Rev H-S gears and rev clutch glands (disengaged rev clutches)	$2[12,500 + 6,500]\ \frac{k_3^2}{k_2^2}$	= 1,451,233
Rev L-S pinions, clutch drums (disengaged rev clutches)	$2[2,250 + 5,750]\ k_3^2$	= 298,557
Bull gear		= 590,000
Propeller and entrained water		= 434,000
Boost turbine fwd L-S pinions and clutch glands	$2[2,250 + 6,500]\ k_3^2$	= 326,547
Boost turbine rev L-S pinions disengaged drums	$2[2,250 + 5,750]\ k_3^2$	= 298,557
	Fwd total$_{(base)}$	5,773,187 (lb-ft^2)

(referred to propeller shaft)

Fwd Direction
(two gas turbines, all fwd, clutches engaged)

Base total		5,773,187
Boost GT and H-S pinion	$(5,511)\ (k_1^2)(k_3^2)$	= 1,136,215
Boost ahead H-S gears and clutch drums	$2[18,675 + 5,750]\ k_3^2$	= 911,531

Boost rev H-S gears and glands	$2[12,500 + 6,500]\frac{k_3^2}{k_2^2}$	= 1,451,233
	Fwd total(base + boost)	9,272,166 (lb-ft²)
	(referred to propeller shaft)	

Rev Direction
(base turbine only, boost turbine clutch disengaged)

Base GT and H-S pinion	$(5,511)(k_1^2)(k_2^2)(k_3^2)$	= 555,155
Ahead H-S gears and clutch drums	$2[18,675 + 5,750](k_2^2)(k_3^2)$	= 445,374
Rev H-S gears, clutches drums, and rev L-S pinions	$2[12,500 + 6,500 + 5,750 + 2,250]k_3^2$	= 1,007,629
Bull gear		= 590,000
Propeller and entrained water		= 434,000
Base turbine fwd L-S pinions and clutch glands	$2[2,250 + 6,500]k_3^2$	= 326,547
Boost turbine fwd L-S pinions and clutch glands	$2[2,250 + 6,500]k_3^2$	= 326,547
Boost turbine rev L-S pinions and drums	$2[2,250 + 5,750]k_3^2$	= 298,557
	Rev total(base)	3,983,809 (lb-ft²)
	(referred to propeller shaft)	

Moment of Inertia Referred to Propeller
(open drive train, all clutches disengaged)
(base and boost fwd and rev L-S pinions always rotating)

Base and boost GT rev & fwd L-S pinions, drums, and glands (two turbines and two trains/turbine)	$2 \times 2[2,250 + 2,250 + 5,750 + 6,500]k_3^2$	= 1,250,206
Bull gear and shaft		= 590,000
Propeller and entrained water		= 434,000
	Total	2,274,206 (lb-ft²)

Moment of Inertia Referred to Gas Turbine
(open drive train, all clutches disengaged)
(base and boost turbines)

Gas turbines and H-S pinions	2 (5, 511)		=	11, 022
Ahead H-S gears and drums	$\frac{2 \times 2}{k_1^2}$	[18, 675 + 5, 750]	=	8, 842
Rev H-S gears and glands	$\frac{2 \times 2}{k_1^2 k_3^2}$	[12, 500 + 6, 500]	=	14, 078
		Total		33, 942 ($lb\text{-}ft^2$)

NOTE: The moment of inertia for the open drive train with a single turbine is as follows: The propeller side remains the same; the turbine side is half the two-turbine value.

Appendix B

Digital Computer Simulation Program

The gas-turbine ship-propulsion dynamics simulation was developed for a digital computer. The computer language used was Fortran IV and was mechanized on an IBM System 360 computer. Logic flow through the program is shown in Figure 1-B for reference in following the computer solution of the equations written for the ship and propeller speeds.

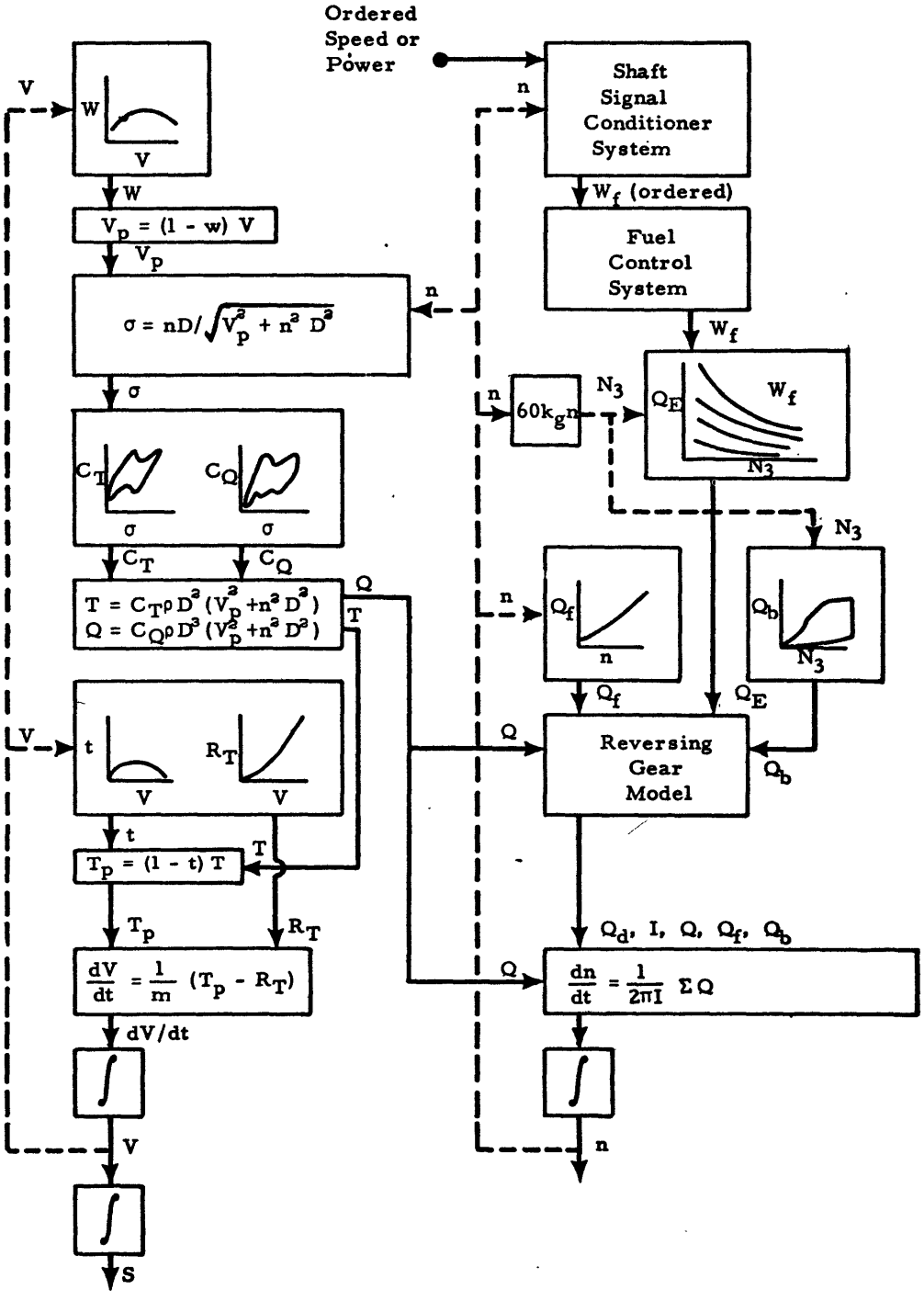

Figure 1-B - Logic Flow Diagram

For the solution of the ship speed (thrust) equation, the program first enters a map of wake fraction versus ship speed and uses a first-order interpolation to obtain the required wake fraction for a particular speed. This first-order interpolation is used on all stored maps in the program. The propeller speed of advance (V_p) is then calculated and along with the propeller speed (n) and diameter of the propeller (D) is used in determining the second modified advance coefficient (σ). This advance coefficient (σ) is now used to extract values of thrust coefficient (C_T) and torque coefficient (C_Q) from stored maps for use in the thrust and torque calculations of the propeller. Propeller thrust is reduced by the thrust deduction fraction taken from a stored map as a function of ship speed. Total ship resistance (R_T), also a function of ship's speed, is taken from a stored map and along with the thrust of the propeller and the mass of the ship (m) is used to calculate ship acceleration. Subsequent integrations of the acceleration with respect to time yield the ship speed and the distance traveled (reach). The new value of ship speed after each integration is now used to repeat the calculation for the next discrete time interval. Each integration interval is 0.1 second.

Simultaneously with the thrust equation, the rotational (torque) equation for the propeller is being solved. A shaft signal conditioner is first used to determine a shaft order dependent upon which type of control is used. Present control (for the first-phase study) is open-loop fuel programming. In later studies this will be expanded to include closed-loop shaft speed and power control utilizing feed forward, proportional, and integral control. This ordered shaft command is then used in the fuel control system representation to determine the fuel flow fed to the engine or engines. The fuel control model contains fuel flow rate limits as discussed earlier. The computational cycle continues by entering a stored engine torque map and extracting engine torque as a function of engine shaft speed (N_3) and fuel flow rate (W_f). Frictional gear and bearing torque losses are now determined from a stored map as a function of propeller speed. Water brake torque (Q_b), if required for the particular run, is now taken from a stored map as a function of engine speed (N_3). A double-reduction reversing gear was simulated for this ship study. This representation includes a model of the forward and reverse clutches for both base and boost engines located on intermediate shafts between the two reduction stages. In the ship acceleration mode, only the forward clutches are engaged. In a reversing maneuver from an ahead condition, however, the forward clutches must first disengage and then the reverse clutches begin engagement and finally "lock up" to complete reversal of the propeller. This splitting and reengagement of the drive train requires first one rotational equation to be solved, then two separate rotational equations, and finally, again a single rotational equation. During this maneuver the appropriate values for inertias, clutch torque, water brake torque, and reduction gear/bearing frictional torques along with the engine and propeller torques are then used to calculate the

accelerations of the propeller and engine shafts. The ensuing integration over time results in the shaft speed which is used to start another pass through the program.

The program will automatically continue through the calculations until a predetermined stopping condition is met. Time, ship speed, propeller speed, propeller reversal, or ship direction reversal are typical examples of such stopping conditions. When such a condition is met, the program automatically stops and goes to the next problem.

Appendix C

Bibliography

1 - "Automation Study for a DE Class Steam Powerplant," George G. Sharp, Inc., New York, N. Y., Contract NObs-90498, 30 June 1965
2 - Baker, D. W., and C. L. Patterson, "Representation of Propeller Thrust and Torque Characteristics for Simulations," Tech Note MEL 202/67, AD 830 085L, Apr 1968
3 - Baker, G. S., "Ship Design, Resistance and Screw Propulsion," The Journal of Commerce and Shipping Telegraph, 2 vols., Liverpool, Charles Birchall & Sons, Ltd., 1951
4 - Boatwright, G. M., and J. J. Turner, "Effect of Ship Maneuvers on Machinery Component Design," BUSHIPS Journal, Sep 1965, pp. 18-26
5 - Broersma, Prof. IR. G., Marine Gears, De Technische Uitgeverij H. Stam N. V., Haarlem (The Netherlands), 1961
6 - Dickmann, Hans E., "Schiffskörper Sog, Wellenwiderstand eines Propellers und Wechselwirkung mit Schiffswellen," Ingenieur Archiv, 1938
7 - Dickmann, Hans E., "Wechselwirkung Zwischen Propeller und Schiff unter besonderer Berücksichtigung des Welleneinfluses," Jahrbuch der Schiffboutechnischen Gesellschaft, 40 Band, 1939, pp. 234-297
8 - Dickmann, Hans E., "Wellenwiderstand eines Propellers und Wechselwirkung mit Schiffswellen," Fifth International Congress of Applied Mechanics, Cambridge, Mass., 1938
9 - Duran, Harlan P., "Simulation of Jet Engine Transient Performance," The American Society of Mechanical Engineers, 65-WA/MD-16, 7-11 Nov 1965
10 - "Dynamic Analysis of Closed Loop Limiting Concept for Gas Turbine Engines," Inter-Controls, Inc., Bunawep, BUWEPS Contract NOw 65-0223F, Mar 1966
11 - "Economy and Endurance Trials Code 1952," The Society of Naval Architects and Marine Engineers, 1952
12 - "Engineering Report, Ships Motion Analysis PN51042 Final Report for FY1963," Sperry Piedmont Co., U. S. MARAD Contract MA2720 (Ships BridgeControl Console System), July 1963
13 - "Final Report, Project Suric, Phase V, Vol. I.," Sperry Gyroscope Co. Rept EB-5280-0308, Contract NOnr 2855 (00), July 1963
14 - Frezenius, R., "Das grundsätzliche Wesen der Wechselwirkung zwischen Schiffskörper und Propeller," Schiffban, 1921
15 - FT4 Gas Turbine Engine Installation Handbook, Pratt & Whitney Aircraft Co., 15 Aug 1963
16 - "Fuel Control Systems for FT4 Marine Gas Turbine Engines," Pratt & Whitney Aircraft Co., 3 Feb 1966
17 - "GG3-GG4 Gas Generator Steady State Stability Analysis," Pratt & Whitney Aircraft Co. Rept PWA Inst. 582
18 - "Guide to the Selection of Backing Power," The Society of Naval Architects and Marine Engineers, The M9 Panel of the Ships Machinery Committee, New York, Technical & Research Bulletin 2-5, Dec 1957
19 - Hadler, J. B., and H. M. Cheng, "Analysis of Experimental Wake Data in Way of Propeller Plane of Single Screw and Twin Screw Ship Models," Transactions of The Society of Naval Architects and Marine Engineers, Vol. 73, 1965

20 - Hadler, J. B., C. J. Wilson, and A. L. Beal, "Ship Standardization Trial Performance and Correlation with Model Predictions," Transactions of The Society of Naval Architects and Marine Engineers, Vol. 70, 1962
21 - Hansen, E. Orm., "Thrust and Blade Spindle Torque Measurements of Five Controllable-Pitch Propeller Designs for MSO 421," NSRDC Rept 2325, Apr 1967
22 - "Helicopter Transient Performance with Free Turbine & Single Shaft Gas Turbine Engines," Inter-Controls, Inc., Rept CA-5120-R for Garrett Corp. Airesearch Mfg. Co., 14 Feb 1964
23 - Helmbold, H. B., "Beitrag zur Theorie der Nachstromschr Ingenieur-Archiv, Band II, daittes Heft, Sep 1921
24 - Hewins, E. F., H. J. Chase, and A. L. Ruiz, "The Backing Power of Geared-Turbine Driven Vessels," Transactions of The Society of Naval Architects and Marine Engineers, Vol. 58, 1950
25 - Horn, F., "Theories des Schiffes," Handbuck der Physica und Technischen Mechanik, Bank V., Lieferung 2, p. 657
26 - Jaeger, H. E., and M. Jourdain, "The Braking of Large Vessels," The Society of Naval Architects and Marine Engineers, No. 11, 18 June 1968
27 - Korvin-Kroukovsky, B. V., and Winnifred R. Jacobs, "Circumferentially Nonuniform Ship Propeller Inflow," I. S. P., Vol. 4, No. 38, Oct 1957
28 - Korvin-Kroukovsky, B. V., "On the Numerical Calculation of Wake Fraction and Thrust Deduction in a Propeller and a Hull Interaction," I. S. P., Vol. 1, No. 4, 1954
29 - Korvin-Kroukovsky, B. V., "Stern Propeller Interaction With A Streamline Body of Revolution," I. S. P., Vol. 3, No. 17, 1956
30 - Labberton and Marks, Marine Engineers Handbook, New York, McGraw-Hill Book Co., 1945
31 - Lewis, J. W., E. J. Lecourt, and F. W. Scoville, "Simulation of USCG Glacier," Phase I, U. S. Coast Guard Icebreaker Propulsion System Simulation, Sep 1967
32 - McLaughlin, P. W., "Hybrid Turbine Engine Simulation and Test Program (Hytest)," Pratt & Whitney Aircraft Co. Rept MR-1023, 30 June 1966
33 - Miniovich, I. Ya., "Investigation of Hydrodynamic Characteristics of Screw Propellers Under Conditions of Reversing and Calculation Methods for Backing of Ships," BUSHIPS Translation 697, translated by Royer and Roger, Inc., International Div., Washington, D. C., 1960
34 - Morgan, W. B., "Open Water Test Series of a Controllable Pitch Propeller with Varying Number of Blades," DTMB Rept 932, Nov 1954
35 - Nordstrom, H. F., "Screw Propeller Characteristics," Swedish State Tank Publication, No. 9, 1948
36 - O'Brien, T. P., The Design of Marine Screw Propellers, London, Hutchinson & Co., Ltd., 1962

37 - Peach, R. W., "A Method for Determining Acceleration of a Ship," International Shipbuilding Progress, Vol. 10, No. 106, June 1963
38 - Phelan, R. M., Dynamics of Machinery, New York, McGraw-Hill Book Co., 1967
39 - "Principles of Naval Architecture," The Society of Naval Architects and Marine Engineers, 1967
40 - Read, C. M. B., "The Control of Gas Turbines Driving Controllable-Pitch Propellers," Proceedings of the Ship Control Systems Symposium, Vol. 1, Annapolis, Md., 1966
41 - Rubis, C. J., and P. B. Perry, "A Quantitative Evaluation of the Control Complexities of Automated Ship Propulsion Systems," ANNA-DIV NSRDC Rept 2434, AD 825 452L, Dec 1967
42 - Rubis, C. J., P. B. Perry, and E. B. Richardson, "Automated COGAG Propulsion Plant Study," MEL Rept 291/66, AD 813 784, Mar 1967
43 - Saunders, Harold E., "The Action of Ship Propulsion Devices," Hydrodynamics in Ship Design, Vol. 1, Chapter 32, New York, The Society of Naval Architects and Marine Engineers, 1957
44 - Seward, H. L., Marine Engineering, Vol. 1, The Society of Naval Architects and Marine Engineers, 1962
45 - Surber, W. C., Jr., "An Investigation of the Flow in the Region of the Rudder of a Free Turning Model of a Multiscrew Ship," DTMB Rept 998, AD 086 820L, Oct 1955
46 - Troost, Ir. L., "Open Water Test Series with Modern Propeller Forms," North East Coast Institution of Engineers and Shipbuilders Transactions, Vol. 67, London, England, 1951

DISTRIBUTION LIST

NAVSHIPS (SHIPS 031) (J. H. Huth)
NAVSHIPS (SHIPS 2052) (2)
NAVSHIPS (SHIPS 03413) (2)
(R. R. Peterson)
NAVSHIPS (SHIPS 03414) (2)
(A. Chaikin)
NAVSHIPS (PMS 389-T11) (2)
(G. M. Boatwright)
NAVSHIPS (PMS 380) (2)
(M. L. Au)
NAVSHIPS (SHIPS 03415)
NAVSEC (SEC 6102C)
NAVSEC (SEC 6110) (2)
(M. Eckhart, Jr.)
NAVSEC (SEC 6140.01)
(L. Wechsler)
NAVSEC (SEC 6140B) (2)
(M. R. Hauschildt)
NAVSEC (SEC 6141) (H. W. Marron)
NAVSEC (SEC 6141) (G. Graves) (2)
NAVSEC (SEC 6144)
NAVSEC (SEC 6144G) (D. J. Berg) (2)
NAVSEC (SEC 6146) (2)
NAVSEC (SEC 6148)
NAVSEC (SEC 6152) (4)
NAVSEC (SEC 6165)
NAVSEC (SEC 6178B.04)
MSTS (M-4EX) (C. E. Hoch) Military Sea Trans Service Washington, D.C.
NAVSECPHILADIV (2)
NAVSECPHILADIV (Code 6734) (3)
NAVSECPHILADIV (Code 6770)
NSRDC (Code 01)
NSRDC (Code 042)
NSRDC (Code 520)
NSRDC (Code 522)
NSRDC (Code 526)
NSRDC (Code 527)
NSRDC (Code 530)
NSRDC (Code 587)
NSRDC (Code 850)
DDC (20)
MARAD (Code 833) Maritime Admin Dept of Commerce Washington, D.C.
(J. H. Lancaster)
MARAD (Code 813)
(T. J. Chwirut)
MARAD (Code 831)
(W. G. Bullock)
Engineering Dept., USNA
USCG Hdqtrs., Office of Engrg.
(J. W. Lewis)

A120
A620(4)
Files (2) PWK
Library
Book
Author (Rubis A621)(50) + extras

2/4 Rubis-Maker, GW

Security Classification — UNCLASSIFIED

DOCUMENT CONTROL DATA - R & D

(Security classification of title, body of abstract and indexing annotation must be entered when the overall report is classified)

1. ORIGINATING ACTIVITY *(Corporate author)*

Naval Ship Research and Development Laboratory
Annapolis, Maryland 21402

2a. REPORT SECURITY CLASSIFICATION

Unclassified

2b. GROUP

3. REPORT TITLE

Gas-Turbine Ship-Propulsion Dynamics

4. DESCRIPTIVE NOTES *(Type of report and inclusive dates)*

Independent Exploratory Development Report

5. AUTHOR(S) *(First name, middle initial, last name)*

C. J. Rubis and A. J. Moken

6. REPORT DATE	7a. TOTAL NO. OF PAGES	7b. NO. OF REFS
January 1969	129	46

8a. CONTRACT OR GRANT NO.

b. PROJECT NO. Z-F013 01 01
Task 11275
c. Assigt 62-139
d.

9a. ORIGINATOR'S REPORT NUMBER(S)

2846

9b. OTHER REPORT NO(S) *(Any other numbers that may be assigned this report)*

ELECLAB 213/68

10. DISTRIBUTION STATEMENT

Each transmittal of this document outside the Department of Defense must have prior approval of CO, NAVSHIPRANDLAB, Annapolis, Md. 21402

11. SUPPLEMENTARY NOTES

12. SPONSORING MILITARY ACTIVITY

NSRDL

13. ABSTRACT

This report is the first-phase analysis of the ship- and propulsion-plant dynamics for a vessel of the destroyer escort type. A combined gas turbine base and gas turbine boost single-screw propulsion plant of over 45,000 horsepower consisting of two FT4A-2 gas-turbine engines driving a reversing reduction gear with a water brake for dynamic braking was investigated. The analysis was conducted with an all digital simulation on an IBM System 360 computer. Quantitative results for all the major ship- and propulsion-plant parameters are given for the ship in a calm sea with no turning motions during acceleration, coast down, dynamic braking, and reversing under open-loop fuel-scheduled operation. These results are given for both the base- and base-plus-boost plant operating modes.

(Authors)

DD FORM 1 NOV 65 1473 (PAGE 1)

S/N 0101-807-6801

UNCLASSIFIED
Security Classification

14. KEY WORDS	LINK A		LINK B		LINK C	
	ROLE	WT	ROLE	WT	ROLE	WT
Propulsion plants						
Destroyer escorts						
Gas turbines						
Single screw						
Reversing reduction gears						
Water brake						
All digital simulation						
Acceleration						
Coast down						
Dynamic braking						
Reversing						
Boost plant						